NCTSPM

NATIONAL CENTER FOR TRANSPORTATION SYSTEMS PRODUCTIVITY AND MANAGEMENT

Evaluation of Anchor Bolt Clearance Discrepancies

Contract # DTRT12GUTC12 with USDOT Office of the Assistant Secretary for Research and Technology (OST-R)

Final Report

July 2016

Principal Investigator: Ian E. Hosch, Ph.D.

National Center for Transportation Systems Productivity and Management
O. Lamar Allen Sustainable Education Building
788 Atlantic Drive, Atlanta, GA 30332-0355
P: 404-894-2236 F: 404-894-2278
nctspm@ce.gatech.edu nctspm.gatech.edu

Georgia Institute of Technology | FIU Florida International University | UAB The University of Alabama at Birmingham | University of Central Florida

TABLE OF CONTENTS

LIST OF FIGURES

LIST OF TABLES

Executive Summary

A comprehensive study was conducted on mechanical analysis of stand-off anchor bolt connections with uneven stand-off distances. A new technique is introduced to calculate the resistive forces provided by each anchor bolt in the group in response to acting fatigue-level loads on the superstructure. The technique is able to accurately capture the resistive forces that are otherwise unaccounted for using current design and analysis methods, as well as codified provisions. The technique comprehensive, and is applicable for any stand-off anchor bolt connection with even and uneven stand-off distances, as well as differing anchor bolt size and spacing. The study evaluated connections with these conditions using the analytical technique and numerical finite element analysis, and further validated from experimental field data collected on a stand-off anchor bolt connection with uneven stand-off distances that was used to support a cantilever-type highway overhead sign support structure.

1 INTRODUCTION

1.1 Overview

The clearance distance (a.k.a. stand-off distance) of the anchor bolt for double-nut moment joint connections is the distance between the bottom of the leveling nut and the top of concrete foundation. The functionality of the anchor bolts is to translate the applied loads to the foundation. There are two types of anchor bolt connections that are used in sign and signal support structures. The first type is the base plate directly mounted to the concrete foundation surface. The second one is the double-nut moment joint, in which the anchors are attached to a stand-off base plate from the concrete surface with double nuts. Previous research has revealed that the anchor bolts stand-off distances have two uniformities: anchors with a uniform stand-off distance and with non-uniform stand-off distances. Figure 1.1-a) exhibits a double nut moment joint with anchors having a uniform stand-off distance. The uniform stand-off distance criterion is that the anchors are having the same stand-off distance. The schematic illustrated in **Error! Reference source not found.**-b) indicates the case of anchors with non-uniform stand-off distances. It can be observed from the figure that the inclination of the concrete surface imposes an irregular distribution of the anchor bolts stand-off distances. In other words, the anchor bolts are having diverse stand-off distances. This case is resulted from topographical limitations and leveling practices during construction.

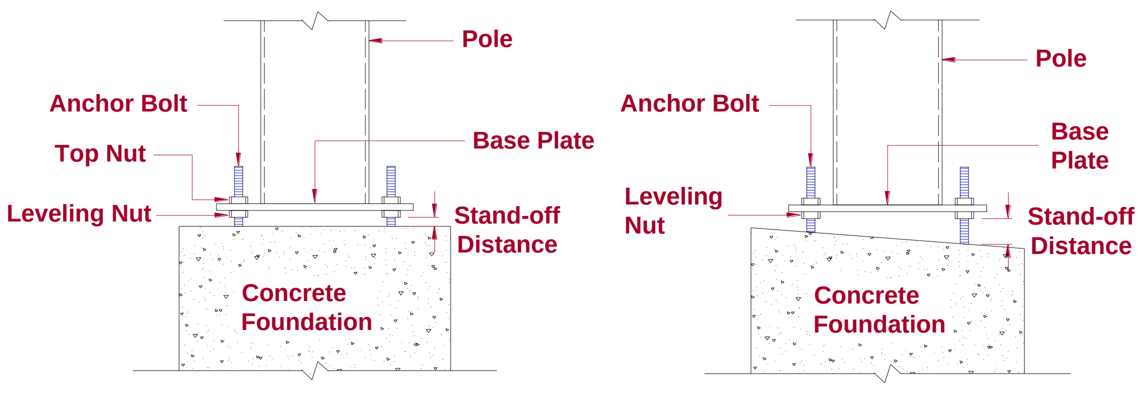

(a) **(b)**

Figure 1.1 Double-nut moment joint

The behavior of anchors with uniform stand-off distances has been the focus of the previous studies. The case of anchors with non-uniform stand-off distances was solely observed by ALDOT/UAB Project #930-680 in 2009, in which the research was focused to study the fatigue loads for overhead sign structures. The photo indicated in Figure 1.2 was captured from the project. The figure demonstrates the in-situ double-nut moment joint with anchors having non-uniform stand-off distances. It can be observed that the two anchor bolts at the left-bottom section have stand-off distances greater than the other anchors in the group.

Figure 1.2 Anchor bolts with non-uniform stand-off distances (Fouad et al. 2009)

1.2 Problem Statement

The results induced from the analysis of the data assembled from ALDOT/UAB Project #930-680 in 2009, have revealed the necessity to understand the behavior of anchors with non-uniform stand-off distances. The overhead sign structure was equipped by eight anchor bolts, each of which has an attached uniaxial strain gauge to measure the axial strain under service loading. The photo indicated in Figure 1.3 exhibits a close-up view of a uniaxial strain gauge attached to an anchor bolt within the group of anchors. The anchor bolts stand-off distances were ranged between 0.8125-in and 3.375-in.

Figure 1.3 Uniaxial strain gauge mounted on an anchor bolt (Fouad et al. 2009)

The strain data collected from the in-situ experimental work were analyzed by Hosch (2013). In general, the results showed a severe irregular stress distribution within the anchor group. This can be seen in Figure 1.4 that indicates the layout of the anchor bolts with respect to the stress distribution ranges, for wind loading measured normal to the face of the structure. The anchor group experienced stresses ranged between 12-Mpa (1.75-ksi) and approximately 90-Mpa (13-ksi). The highest stresses were found to be in anchors AB-7 and AB-8, in which those two anchors possess the highest stand-off distances.

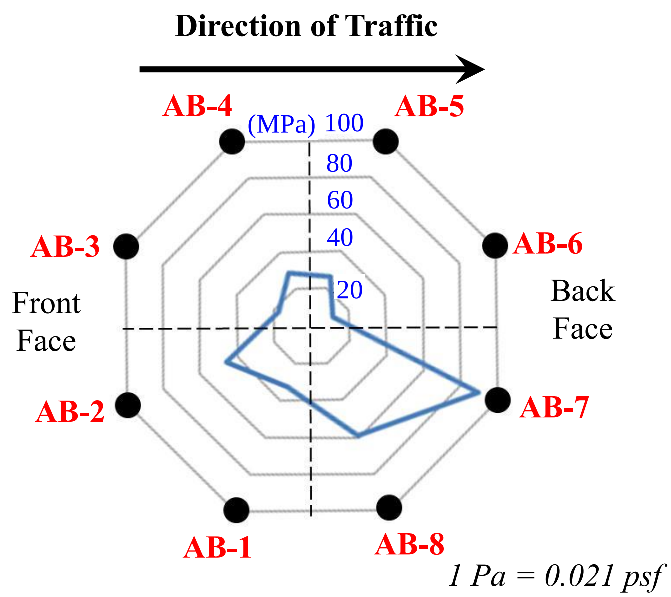

Figure 1.4 Anchors group orientation with respect to the stress ranges (Hosch 2013)

Figure 1.5 exhibits a comparison between the experimental stress ranges, constant amplitude fatigue limit (CAFL), and the fatigue stresses calculated using AASHTO *Standard Specifications for Structural Supports for Highway Signs, Luminaries, and Traffic Signals* (2013) [hereafter referred to as the *2013 Supports Specifications*]. The figure indicates that anchor bolts (AB-7 and AB-8) have stress ranges equal to 89.3-MPa (12.95-ksi) and 58.6-MPa (8.5-ksi), respectively. Those stresses were found to be higher than the constant amplitude fatigue limit (CAFL) of 48.3-MPa (7-ksi) that specified by the *2013 Supports Specifications*.

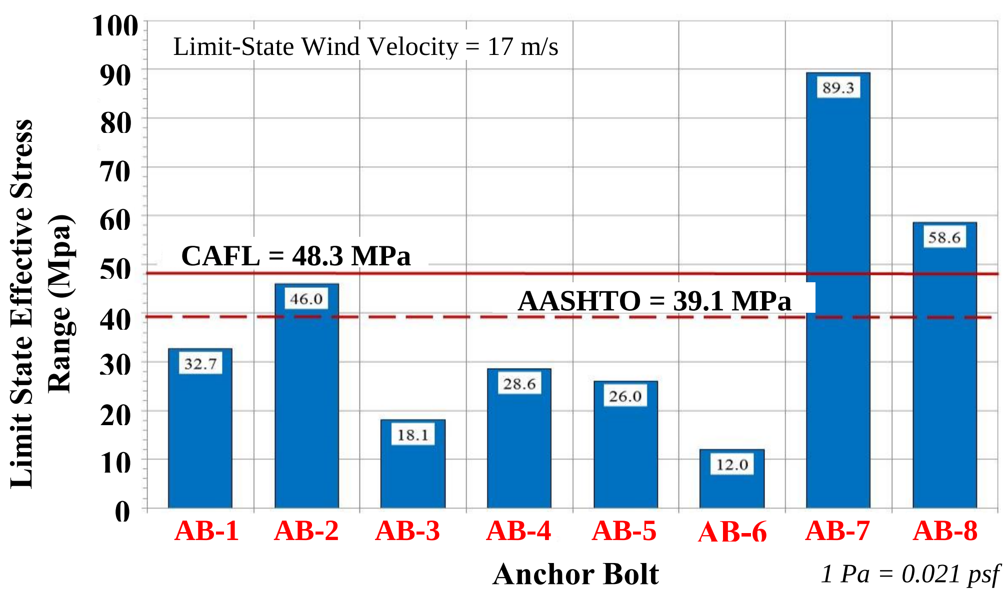

Figure 1.5 Comparison of fatigue stress ranges in anchor bolts (Hosch 2013)

It should be noted that the joint was originally designed for infinite life for fatigue. The results and discussion illustrated above indicate that the structure life would be finite. Such alteration may result in a premature fatigue failure, with other possibilities of much more severe consequences in the events of extreme wind. Therefore, this project was launched to investigate the behavior of load distribution on the anchor bolts with non-uniform stand-off distances.

1.3 Project Objectives

The main objective of this research is to investigate the effect of non-uniform stand-off distances on the stress distribution of the anchor bolts within the double-nut moment joint connection. Three specific objectives were considered to fulfill the main objective:

1. Perform analytical study to identify the mechanical relationships that govern the behavior of the connection with respect to non-uniform stand-off distances.

2. Perform numerical study using finite element analysis (FEA) to validate the developed mechanical relationships.

3. Propose design methodology applicable for evaluating the stresses on the anchor bolts with uniform and non-uniform stand-off distances.

1.4 Organization of the Report

This section provides the outlines of the report. A concise description of the work associated with each chapter will be expressed:

Chapter **2** **BACKGROUND**	• Provide a review of the previous work that is directly related to the scope of this study.
Chapter **3** **ANALYTICAL STUDY**	• A detail investigation of the development of the analytical relationships used to evaluate the staining actions on the anchor bolts with non-uniform stand-off distances.
Chapter **4** **NUMERICAL STUDY**	• A detail desccription of the DOE program. • Implement an FEA model using SAP2000 software. • Verify the numerical model then display the DOE program.

Chapter **6** **RESULTS AND DISCUSSION**	• A detailed analysis of the results induced from the analytical study and the numerical study.
Chapter **7** **DISCUSSIONS AND RECOMMENDATIONS**	• Provide a description of how the objectives were addressed throughout the study and a berif conclusion of the findings.
Chapter **8** **CONCLUSIONS AND FUTURE RESEARCH**	• A detailed illustration of the outcomes inferred from the discussion of results. • Propose future research ideas that promised to cover the aspects related to the overall subject of the report.
REFERENCES	• A list of the all cited references used through the entire the report.
APPENDICES	• A — Derivation of bending deflection for individual anchor bolt • B — Derivation of shear deflection for individual anchor bolt • C — Derivation of axial deflection for individual anchor bolt • D — Derivation of shear stresses on anchor bolts • E — Numerical model verification • F — Design example

2 BACKGROUND

In the double-nut moment joint, the load is transferred into the foundation through the threaded stand-off distance of the anchor bolts. The performance of anchor bolts to resist the applied forces (i.e., moment, shear, normal and torsion) is primarily dependent on proper installation. Previous research has investigated the effect of different loading conditions on the behavior of anchor bolts that have uniform stand-off distances. However, there currently are no studies in the literature that have investigated the behavior of anchor bolts with non-uniform stand-off distances. The following sections will address the previous research that directly related to the present study.

2.1 Construction Problems

The problems that may occur during the installation of anchor bolts can affect the performance of the structural supports, as well as the strength capacity. One of the construction problems that could occur at the site is the misalignment of anchor bolts (a.k.a. plumbing). It is specified in the *2013 Supports Specifications* that the vertical misalignment of anchor bolts should be less than 1:40. This limitation was derived from the research conducted with NCHRP Report 412 (Kaczinski et al. 1998). It was concluded that the increase in the bending stress range due to the misalignment of anchor bolts shall be neglected for vertical inclination up to 1:40.

Loosening nuts is another construction problem that affects the structural integrity of the base connection. Several studies have investigated the proper tightening procedure of nuts to prevent them from loosening. Tightening methods were investigated on large diameter anchor bolts applied in double-nut moment joints (James et al. 1996, Till and Lefke 1994). Garlich and Koonce (2011) emphasized the severity of loosening nuts and pointed to how prevalent this problem is within the United States. The axial load during tightening was measured in new anchor bolts during their installation on an existing pole (Hoisington et al. 2014). This project was launched as a response of observing several high mast poles with loosening nuts in Alaska. The measurements revealed that several anchors reached the yield stress during the tightening procedure.

Studies have shown that pretensioning of anchor bolts improves the performance of the connection under loading conditions (Garlich and Thorkildsen 2005). The pretensioning is only applied to the part of anchor between the two nuts. The turn-of-nut method is the tightening procedure that is used for pretensioning the anchors. The required torque can be calculated from Equation (**2-12-1**), which was provided by NCHRP Report 469 (Dexter and Ricker 2002).

$$T_v = 0.12\, d_p\, F \tag{2-1}$$

where:

T_v = verified torque (kip.in)
d_p = nominal diameter of the anchor bolt (in)

F = minimum installation pretension force in kips. F is equal to 50% of ASTM F1554 rod grade 36 and 60% of ASTM F1554 rod grade 55 and 105

The overview of the above construction problems was addressed to clarify the catastrophic consequences that may occur due to the in-situ conditions and human errors. If the misalignment of anchor bolts were not considered and investigated, the limitation of 1:40 would not be addressed. The required torque for proper tightening was determined because the problem of loosening nuts was observed and then investigated. This research reveals a new construction problem that was observed in the construction site, which occurred during the installation of the anchor bolts. The construction of the anchor bolts with non-uniform stand-off distances was evident to be severe in terms of fatigue (Hosch 2013). Therefore, it is important to understand the behavior of anchor bolts with non-uniform stand-off distances and produce recommendations that help to deal with this situation if un-avoidable.

2.2 Mechanics of Load Transfer

The loads are transferred to the anchor bolts in terms of direct shear, torsional moment, and bending moment. The stresses on the anchors corresponding to each load criteria are distributed according to mechanical relationships associated with the arrangement of the anchors. NCHRP Report 412 (Kaczinski, Dexter, and Dien 1998) provided Equations (**2-2**, **2-3**, and **2-4**) to calculate the axial stresses due to group bending moment. Equation (**2-2**) was also specified by *2013 Support Specifications* with adding the term of direct axial stress. Those equations shall be used to calculate the normal stresses on the anchor bolts with a uniform stand-off distance, when the anchors are having a stand-off distance lower than the anchor diameter, as indicated by *2013 Support Specifications*. If the anchors possess a stand-off distance more than the anchor diameter, a beam model should be used to account for the bending stresses. That model has anchors fixed at the bottom (connection between anchors and concrete surface) and free to translate but not to rotate at the top (connection between anchors and the bottom of the leveling nuts).

$$\sigma = \frac{M\,c}{I} \qquad \textbf{(2-2)}$$

$$I = \sum A_T \bar{c}^2 \qquad \textbf{(2-3)}$$

$$A_T = \frac{\pi}{4}\left[d_b - \frac{0.9743}{n}\right]^2 \qquad \textbf{(2-4)}$$

where:

σ = axial stress due to bending on the individual anchor

M = group moment

I = polar moment of inertia of the anchor group

c = distance between the centroid of the anchor group and the anchor under investigation in the direction of moment

A_T = net area of anchor bolt

$\overline{c}^2$ = the square distance of the centroid of the anchor group to the anchors in the direction of mement
d_p = diameter of anchor bolt (in)
n = number of threads per inch

Cook and Bobo (2001) proposed design guidelines to calculate the thickness of the base plate and the required area of steel anchor bolts. The equations were derived based on the experimental program performed in the project as well the results of the previous works. Equations (**2-5** and **2-6**) compute the base plate thickness and the anchor bolt area. In addition, Cook has presented Equation (**2-7**) to determine the axial load on the anchor bolt due to group bending moment

$$t = \sqrt{\frac{M_u(r_b - r_p)}{\emptyset\, F_y\, r_b\, r_p}} \tag{2-5}$$

$$A_{se} = \frac{2\, M_u}{\emptyset\, F_u\, n\, r_b} \tag{2-6}$$

$$P = \frac{2\, M}{n\, r} \tag{2-7}$$

where:

t = design plate thickness
φ = reduction factor equals 0.9
M_u = factored moment
r_b = distance between the c.g of the plate to the centerline of anchor group
r_p = outside radius of the post
F_y = plate yield stress
A_{se} = effective area of the bolt that equals 0.75 gross area of the bolt
n = number of anchors
f_u = plate ultimate stress
P = unfactored axial force on the anchor due to moment group
M = unfactored moment group
r = distance between the c.g of the anchor group to the bolt under investigation

Equation (**2-8**) is expressed in the *2013 Support Specifications* to calculate the shear forces due to torsion. The total shear force is the shear force due to torsion plus the shear force due to direct shear.

$$F = \frac{T.r}{J} \tag{2-8}$$

where:

F	=	shear force due to torsion
T	=	torsional moment
r	=	distance between the c.g. of the anchor group to the outmost anchor
J	=	polar moment of inertia of the group of anchors

The shear forces due to torsion can also be expressed in the form of forces in x and y directions, as shown in Figure 2.1. The figure illustrates the directions of shear forces, as well as the measuring of the horizontal and vertical dimensions. Equations (**2-9** and **2-10**) were specified by McCormac and Csernak (2012) to calculate the horizontal and vertical shear forces due to torsion, respectively. Those equations are applicable for anchors with a uniform stand-off distance.

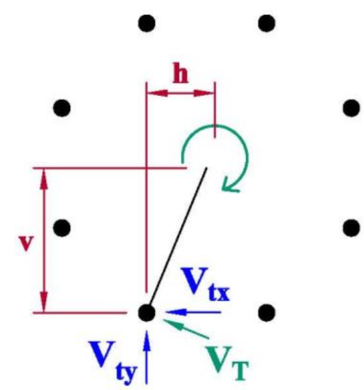

Figure 2.1 Shear forces due to torsional moment

$$H = \frac{M.v}{\sum d^2} \tag{2-9}$$

$$V = \frac{M.h}{\sum d^2} \tag{2-10}$$

where:

H	=	horizontal shear force due to torsion on each anchor
V	=	vertical shear force due to torsion on each anchor
v	=	vertical distance between the c.g. of the group of anchors to the anchor under investigation
h	=	horizontal distance between the c.g. of the group of anchors to the anchor under investigation

$\sum d^2 = \sum v^2 + \sum h^2$

McBride et al. (2014) performed an experimental program to study the reduction in the shear strength of anchor bolts associated with the change in the uniform stand-off distance. Three loading conditions were investigated: direct shear, torsion, and torsion. Several factors were considered including stand-off distance, grouted and un-grouted stand-off base plate, and base plate mounted in the concrete surface. The author concluded that the shear strength of anchor bolts is inversely proportional to the increase of uniform stand-off distance.

McBride also established a design approach to determine the tension and shear stresses terms in Equation (**2-11**), specified by *2013 Support Specifications*. Those terms are expressed in Equations (**2-12** to **2-16**).

$$\left(\frac{f_{t,1} + f_{t,2}}{F_t}\right)^2 + \left(\frac{f_v}{F_v}\right)^2 \leq 1 \tag{2-11}$$

$$f_{t,1} = \frac{M_{group}}{S_{group}} + \frac{N_{group}}{n\, A_{net}} \tag{2-12}$$

$$S_{group} = \frac{n\, r_{group}}{2} \tag{2-13}$$

$$m_{bolt} = \frac{V_{bolt}\, L_{LN}}{2} \tag{2-14}$$

$$V_{bolt} = \frac{V_{group}}{n} + \frac{T_{group}}{n\, r_{group}} \tag{2-15}$$

$$f_v = \frac{V_{bolt}}{A_{net}} \tag{2-16}$$

where:

$f_{t,1}$	=	tensile stress on the individual anchor due to the group moment
$f_{t,2}$	=	tensile stress on the individual anchor due to the bending moment on the stand-off distance
f_v	=	shear stress
F_t	=	allowable tension stresses
F_v	=	allowable shear stresses
n	=	number of anchor bolts
r	=	radius of anchor group
V_{bolt}	=	total shear on anchor
m_{bolt}	=	bending moment due to V_{bolt}
L_{LN}	=	stand-off distance
T_{group}	=	torsional moment
A_{net}	=	net area of the bolt

2.3 Standard Comparisons

The *2013 Support Specifications* is the only standard found in the literature that provides design guidance for anchor bolts with uniform stand-off distance. Equations (**2-**

17and **2-18**) are used to compute the allowable tension and compression stresses on anchor bolts. In the case of combined shear and tension or combined shear and compression on the individual anchor bolt, the conditions in Equations (**2-19** and **2-20**) shall be satisfied.

$$F_t = 0.5\, F_y \qquad \textbf{(2-17)}$$

$$F_t = 0.5\, F_y \qquad \textbf{(2-18)}$$

$$\left(\frac{f_v}{F_v}\right)^2 + \left(\frac{f_t}{F_t}\right)^2 \leq 1 \qquad \textbf{(2-19)}$$

$$\left(\frac{f_v}{F_v}\right)^2 + \left(\frac{f_c}{F_c}\right)^2 \leq 1 \qquad \textbf{(2-20)}$$

where:

F_t = allowable tension stress
F_c = allowable compression stress
F_y = yield stress
f_v = applied shear stress on the individual anchor
f_t = applied tension stress on the individual anchor
f_c = applied compression stress on the individual anchor

It has been observed in AISC Steel Design Guide 1 (Fisher and Kloiber 2006, *Appendix A*) that it is recommended to use Equation (**2-21**) to calculate the compression limit for anchor bolts in double-nut moment joints.

$$R_c = F_y\, A_g \qquad \textbf{(2-21)}$$

where:

R_c = compressive strength of anchor
F_y = yield stress
A_g = gross area of anchor bolt

It should be noted that the *2013 Support Specifications* and the AISC Steel Design Guide 1 specified the compression strength limit-state equation to be valid for anchor bolts with uniform stand-off distance not greater than four times the anchor bolt diameter. If the stand-off distance exceeded that limit, buckling of anchors shall be considered.

2.4 Grout

The presence of grout underneath the base plate is a matter of argument. Some researches recommended the presence of grout (Cook et al. 2000, Cook and Bobo 2001) because it protects the base plate as well as the anchors from corrosion. In addition, the performance of the base connection can be improved by placing the grout pads along with the base plate stiffeners. The investigation conducted by McBride et al. (2014) showed a significant increase in the shear capacity due to the installation of the grout pads.

Other opinions oppose the installation of grout pads in the double-nut moment joints (Garlich and Thorkildsen 2005, Dexter and Ricker 2002). Non-shrink grout may crack, and moisture will be trapped inside the gout exposing the anchor bolts to corrode. Also, the presence of grout will prevent the inspection of the leveling nuts tightening.

The consideration of grout was addressed in two different standards. It was specified by *2013 Support Specifications* that the presence of grout will not be considered in the calculations of the load capacity of the connection. However, the American Concrete Institute in 2011 (ACI 318-11) specified that the presence of grout reduces the shear capacity of anchor bolts by 20%.

In review of the relevant studies on grout placement, the presence of grout will not be included in this present investigation.

2.5 Previous Research Related to Double-Nut Moment Joints

Limited studies were observed in the literature on anchor bolts with stand-off distances subjected to different loading conditions. Lin et al. (2011) performed experimental tests to study the shear behavior on the individual stand-off anchor bolts. The experimental program included double shear tests on threaded anchor bolts with different uniform stand-off distances. The anchor bolts were divided into two groups that differ in their end conditions. The end conditions of the first group were fixed, whereas end rotations were permitted in the second group. The results showed that the magnitude of the uniform stand-off distance has a potential effect on the strength of the connection. The shear capacity of the connection becomes weaker with the increase in the uniform stand-off distance. In addition, restraining the end rotations recorded lower strength as compared to permitting rotation at the end conditions.

Lin also conducted a numerical study using the ABAQUS finite element analysis software to investigate the shear capacity of individual anchor bolts with stand-off distances. The 3-D quadratic hybrid element was used to model the anchors to ensure a good level of accuracy. The anchor bolt model was divided into three zones. Two zones were located at the top and bottom ends of the anchor bolt to represent the area between the two nuts. A middle zone of the anchor bolt was modeled to represent the stand-off distance. It was modeled with nonlinear material, while the two ends zones were modeled with elastic elements to reduce the stress concentration. The author studied three end conditions: fixed at both ends, limited ends rotations, and the bottom end is fixed and top end is free to transmit laterally. It was noticed that the rotation of the end conditions had an effect on the shear capacity of anchor bolts. For free rotation end conditions, the anchor bolts with shorter stand-off distances recorded the highest increase in shear capacity. Also, the decrease in the shear capacity for anchor bolts with larger stand-off distance (more than three times the anchor bolt diameter) was not high. For specimens with fixed end conditions, the mode of failure of the anchor bolts changed with the increasing stand-off distances. Shear failure was noticed for anchor bolts with stand-off distance equal to 0.2

times the diameter of the anchor bolt (d_a), while bending deformations and strain hardening modes were found in stand-off distances equal 2 times da and 4 times d_a, respectively. The main outcome of the above experimental and numerical investigations was the production of an equation to calculate the shear capacity of the individual anchor bolt with a stand-off distance. The determination of shear capacity proceeds according to the proposed terms in Equation (**2-22**).

$$V_{se} = f_{ya}A_{se,v}sin(\beta) + \frac{f_{ya}cos(\beta)}{\frac{1}{0.9A_{se,v}} + \frac{1}{3.4S}} \quad \textbf{(2-22)}$$

where:

V_{se}	=	shear capacity
f_{ya}	=	yield stress
$A_{se,v}$	=	effective cross sectional area of anchor bolt
S	=	=section modulus with the consideration of the presence of threads
β	=	rotation angle between the deformed position and the anchor vertical axis

Liu (2014) investigated the bending behavior of anchor bolts with excessive uniform stand-off distances. A numerical study was conducted using RISA-3D 9.1 finite element analysis software to simulate the individual anchor bolt as well as the anchor group. The finite element models were conducted to test the beam model identified by *2013 Support Specifications*, which recommended including bending stresses when the uniform stand-off distance is more than one anchor bolt diameter. The Liu's beam model consisted of free anchor bolts to displace laterally with no rotation at the top (anchor bolt/base plate connection) and fixed at the bottom (anchor bolt/concrete connection). The parameters included in Liu's study of the anchor bolt group are the thickness of base plate, stand-off distance, and number of anchor bolts. It was concluded that the beam model provided by the *2013 Support Specifications* to determine the bending stresses on the individual anchor bolts is accurate. In case of the anchor group, the author stated that the shear forces generated from torsion created significant bending stresses even if the stand-off distance is less than one anchor bolt diameter.

Liu also provided design strength limit-states to account for the effect of bending stresses due to direct shear and torsion. The author proposed two assumptions to derive the strength limit-state equations. The first assumption is that every point on the cross-section of the anchor bolt will reach the yield stress. The second assumption is that the cross-section of the anchor bolt is divided into two areas to sustain the axial load and moment. Three limit-state equations were provided by the author. Equation (**2-23**) describes the axial load and bending on individual anchor bolts. Equation (**2-24**) describes the axial load, shear, and bending on individual anchor bolt. Finally, Equation (**2-25**) describes the moment and torsion on an anchor bolt group.

$$\varphi F_y \geq f_t + f_b/3 \quad \textbf{(2-23)}$$

$$\varphi R_n \geq P_u + A\, f_b/3 \quad \textbf{(2-24)}$$

$$\varphi M_n \geq M_u + f_b\, Z_g/3 \quad \textbf{(2-25)}$$

where:

φ	=	resistance factor
F_y	=	yield stress
f_t	=	factored axial stress due to dead load
f_b	=	factored bending stress due to wind loading
R_n	=	combined compression or tension with shear
P_u	=	factored axial load due to bending and dead load
A	=	area of the bolt
M_n	=	moment resistance of the group of anchors
M_u	=	group moment
Z_g	=	section modulus of the entire group about the major axis

Scheer et al. (1987) investigated the behavior of anchor bolts under the effect of static bending stress, and developed a design code equation for anchors that have a stand-off distance. The original source of this report is not available as it originally made and published in German language. The findings of this report were cited in Eligehausen et al. (2006). The moment capacity of the threaded bolt as mentioned by the author is expressed in Equation 31. The derived equation corresponded to a failure criterion of the anchor bolt at a rotation angle (β) of 10˚. The shear capacity for anchor bolts with stand-off distances was also expressed by the author in terms of moment capacity, stand-off distance, and the criteria of the end condition between the anchor and the base plate. Equations (**2-26** and **2-27**) exhibit the calculations of moment and shear capacities for the individual anchor bolt with a stand-off distance, respectively.

$$M_{u,s} = 1.7\, W_{el}\, F_y \quad \textbf{(2-26)}$$

$$V_{u,s} = \frac{\alpha_m\, M_{u,s}}{l} \quad \textbf{(2-27)}$$

where:

$M_{u,s}$	=	moment capacity
$V_{u,s}$	=	shear capacity
W_{el}	=	section modulus corresponds to the threaded area
F_y	=	yield stress
α_m	=	1 — for the non-restrained or restrained end rotation with the base plate 2 — for restrained end rotation with the base plate
l	=	stand-off distance

3 ANALYTICAL STUDY

The second moment of inertia of shear walls provides the stiffness required to resist the lateral loads such as wind and seismic loads. The distribution of lateral loads is based on the inertia of shear walls, in the direction of the lateral load. Walls with high inertia can sustain more loads, and therefore they tend to have more reinforcement. This brief overview might not be directly related to the present investigation, but the concept of load distribution can help deriving the design equations. In double-nut moment joints, the anchors are having the same size and spacing, but they may differ in the stand-off distances. Therefore, the resistance of anchors is not governed by their inertia only, as in shear walls, instead it is governed by the stiffness, in which stiffness combines all the pre-mentioned factors. The derivation of stiffness for the individual anchor bolt is addressed in the following section.

3.1 Stiffness of the Individual Anchor Bolts

The anchor bolts within a double-nut moment joint, are characterized by their short height. As a result, they have bending, axial, and considerable shear deflections. The boundary conditions represent one of the major factors that control the deflection. The boundary conditions of an individual anchor bolt are pre-identified in *2013 Support Specifications*. The anchor bolts are fixed at the bottom (connection between the anchors and the concrete foundation) and free to translate but not to rotate at the top (connection between the anchor and the nuts). The following sections include: deriving of bending and shear deflections, and addressing the axial deflection equation. Those equations will also be verified for the individual anchors with stand-off distances, using numerical analysis by SAP2000.

3.1.1 Deflection due to Bending

The deflection due to bending was derived using the integration method. The schematic illustrated in Figure 3.1 exhibits the deflection shape due to bending. The shown straining actions were established according to *2013 Support Specifications* boundary conditions.

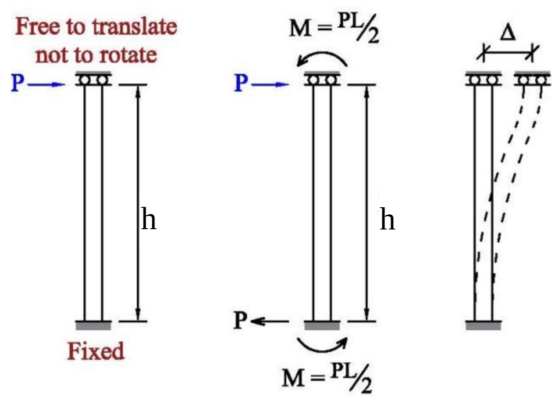

Figure 3.1 Deflection of the individual anchor bolt due to moment

The steps adopted to determine the deflection due to bending are detailed in *Appendix A*. The outcome of those steps is Equation (**3-1**), in which it determines the deflection on the individual anchor bolt due to bending.

$$\Delta_b = \frac{Ph^3}{12EI} \qquad \textbf{(3-1)}$$

where:

Δ_b	=	deflection of the individual anchor due to bending
P	=	lateral load
h	=	stand-off distance
E	=	modulus of elasticity of the anchor
I	=	anchor second moment of inertia

3.1.2 Deflection due to Shear

The stand-off distance of an anchor is considered the major factor that determines the significance of shear deflection. The deflection due to bending is normally considered more critical than shear deflection. However, for very short anchors, the effect of shear deflection becomes more critical (Blodgett 1966, Pope 1997). The shear deflection of anchors with h/d (stand-off distance / anchor diameter) ≥ 10 can be neglected; however, for $h/d < 3$, which is the case of very short anchors, the shear deflection can't be ignored (Richards 2012). The derivation of the shear deflection equation is indicated in *Appendix B*. The deflection equation is indicated in Equation (**3-2**). The shear expressed in this equation is calculated with assuming that the shear is uniformly distributed over the cross section. However, the actual shear stress is distributed over the effective shear area, not on the whole cross sectional area. Therefore, Equation (**3-2**) is multiplied by a factor (k), which is called the shear correction factor to compensate the error occurred in the pre-mentioned assumption. The magnitude of (k) for solid circular cross section is equal to 10/9 (Amany and Pasini 2009, ANSYS@ Element Reference, Release 12.1).

$$\delta_s = k\frac{Ph}{GA} \qquad \textbf{(3-2)}$$

where:

δ_s	=	deflection of the individual anchor due to shear
P	=	lateral load
h	=	stand-off distance
G	=	modulus of rigidity of the anchor
A	=	anchor cross sectional area
k	=	correction factor = 10/9

3.1.3 Total Lateral Deflection

The lateral load (P) indicated in sections [3.1.1 and 3.1.2] is the force on the individual anchor that causes shear and bending deflections. Therefore, the total deflection would be the summation of shear and bending deflections. Equation (**3-3**) determines the total deflection on the individual anchor bolt with a stand-off distance (h) due to lateral loading. It should be noted that in case of sign and signal structures, the total lateral deflection is resulted from the lateral forces due to direct shear and torsional moment.

$$\Delta_l = \frac{Ph^3}{12EI} + \frac{10Ph}{9GA} \tag{3-3}$$

where:

Δ_l	=	total deflection of the individual anchor due to lateral loading
P	=	lateral load
h	=	stand-off distance
E	=	modulus of elasticity of the anchor
G	=	modulus of rigidity of the anchor
I	=	anchor second moment of inertia
A	=	anchor cross sectional area

3.1.4 Axial Deflection

The anchor bolts with stand-off distances; whether uniform or non-uniform, have axial loading due to the own weight of the structure and the moment group. The derivation of the axial deflection is indicated in *Appendix C*. Equation (**3-4**) was adopted to determine the axial deflection of the individual anchors with a stand-off distance.

$$\Delta_a = \frac{Ph}{EA} \tag{3-4}$$

where:

Δ_a	=	axial deflection of the individual anchor
P	=	axial load
h	=	stand-off distance
E	=	modulus of elasticity of the anchor
A	=	anchor cross sectional area

3.1.5 Verification of the Derived Bending, Shear, and Axial Deflections

A finite element model was conducted using SAP2000 program to verify the derived deflection equations The schematic shown in Figure 3.2 demonstrates the beam element that used in SAP2000, to simulate the individual anchor bolt with a stand-off distance. The anchors are having the same boundary conditions specified by *2013 Support Specifications*. The anchors were constructed with a circular cross section of 1.5 in diameter and a stand-off distance (*h*) that is varied from 1.2-in to 6-in, with increments of 0.2-in. The ratios of *h/d* (anchor stand-off distance / anchor diameter) are ranged between 0.8 and 4. The reason for not exceeding the ratio more than 4 is that *2013 Support Specifications* has specified to include buckling deformations in the calculations when the anchor length exceeds four times the anchor diameter.

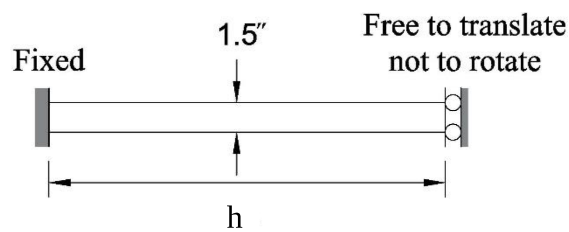

Figure 3.2 Layout of the anchor modeled in SAP2000

A number of 25 anchors were constructed on SAP2000. Two cases were studied: the first case was to apply a lateral force of 1-kip at the end that is free to transmit with no rotation, to determine the bending and shear deflections. The second one was to apply an axial force of 1-kip at the same preceding position, to determine the axial deflection. The same model was used for both cases. Figures (3.3 and 3.4) show a snap shoot from SAP2000 that demonstrates the lateral and axial loading on anchors, respectively.

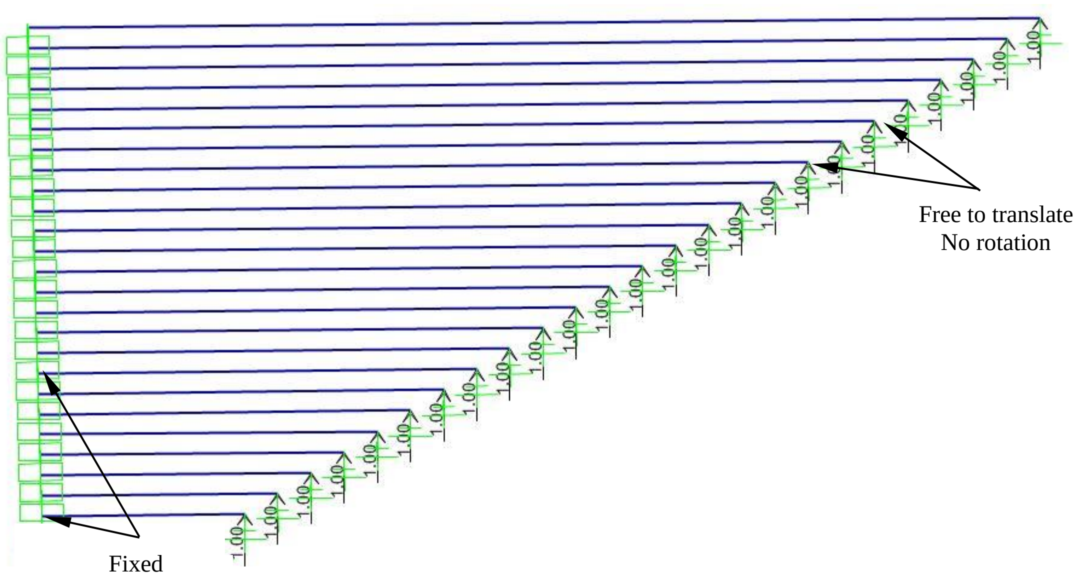

Figure 3.3 Application of lateral loads on the anchors

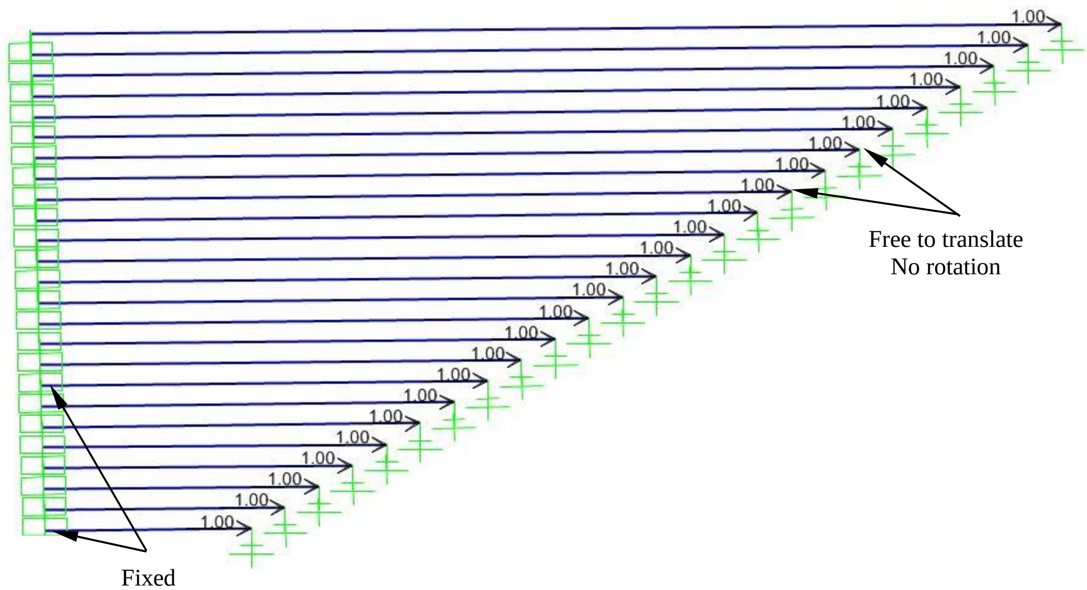

Figure 3.4 Application of axial loads on the anchors

Results and Analysis

The results exhibit in Table 3.1 represents a comparison between the numerical and analytical deflections for lateral and axial loading. It can be noticed that the results are almost identical, in which the max percentage of differences was found to be equal to 0.273% for vertical and 0.068% for axial. This means that the derived deflection equations are accurate for individual anchors with stand-off distances.

Table 3.1 Comparison between numerical and analytical deflections

h-in	*h/d*	Vertical			Axial		
		$\Delta_{Numerical}$, in	Analytical Δ_t, in	% of difference	$\Delta_{Numerical}$, in	Analytical Δ_a, in	% of difference
1.2	0.8	8.74E-05	8.73E-05	0.059	2.34E-05	2.34E-05	0.025
1.4	0.93	1.10E-04	1.10E-04	0.068	2.73E-05	2.73E-05	0.031
1.6	1.07	1.37E-04	1.37E-04	0.010	3.12E-05	3.12E-05	0.036
1.8	1.2	1.69E-04	1.68E-04	0.007	3.51E-05	3.51E-05	0.011
2	1.33	2.05E-04	2.05E-04	0.007	3.90E-05	3.90E-05	0.017
2.2	1.47	2.47E-04	2.47E-04	0.027	4.29E-05	4.29E-05	0.021
2.4	1.6	2.95E-04	2.95E-04	0.004	4.68E-05	4.68E-05	0.025
2.6	1.73	3.49E-04	3.49E-04	0.000	5.07E-05	5.07E-05	0.028
2.8	1.87	4.11E-04	4.11E-04	0.007	5.46E-05	5.46E-05	0.031
3	2	4.81E-04	4.81E-04	0.006	5.85E-05	5.85E-05	0.017
3.2	2.13	5.59E-04	5.59E-04	0.010	6.24E-05	6.24E-05	0.020
3.4	2.27	6.45E-04	6.45E-04	0.010	6.63E-05	6.63E-05	0.023

h-in	*h/d*	**Vertical**			**Axial**		
		$\Delta_{Numerical}$, in	Analytical Δ_t, in	% of difference	$\Delta_{Numerical}$, in	Analytical Δ_a, in	% of difference
3.6	2.4	7.42E-04	7.42E-04	0.014	7.02E-05	7.02E-05	0.025
3.8	2.53	8.48E-04	8.48E-04	0.016	7.41E-05	7.42E-05	0.027
4	2.67	9.65E-04	9.65E-04	0.012	7.80E-05	7.81E-05	0.017
4.2	2.8	1.09E-03	1.09E-03	0.228	8.19E-05	8.20E-05	0.019
4.4	2.93	1.23E-03	1.23E-03	0.165	8.58E-05	8.59E-05	0.021
4.6	3.07	1.38E-03	1.38E-03	0.273	8.97E-05	8.98E-05	0.023
4.8	3.2	1.55E-03	1.55E-03	0.111	9.36E-05	9.37E-05	0.025
5	3.33	1.73E-03	1.73E-03	0.225	9.75E-05	9.76E-05	0.027
5.2	3.47	1.92E-03	1.92E-03	0.113	1.01E-04	1.01E-04	0.068
5.4	3.6	2.12E-03	2.12E-03	0.187	1.05E-04	1.05E-04	0.068
5.6	3.73	2.34E-03	2.35E-03	0.217	1.09E-04	1.09E-04	0.068
5.8	3.87	2.58E-03	2.58E-03	0.068	1.13E-04	1.13E-04	0.020
6	4	2.83E-03	2.83E-03	0.160	1.17E-04	1.17E-04	0.018

The section herein was adopted to comprehend the significance of shear deflection to the bending deflection. The analytical analysis indicated in Table 3.1 was extended to include anchors with stand-off distances lower than 1.2 in and more than 6 in. The *h/d* ratios that used in this analysis was ranged between 0.13 and 10. Figure 3.5 shows a comparison between bending deflections and shear deflections, with respect to the increase in the stand-off distance (*h*). As shown in the figure, the rate of the increase in bending deflection with respect to the stand-off distance is much higher compared to the rate of increase in shear deflection. The relationship provided in Figure 3.6 illustrates the degradation in the significance of the shear deflection with respect to the ratio of the change in stand-off distance with the diameter of 1.5-in. It can be noticed that the percentage of shear deflection to total lateral deflection is very high for very short anchors. However, this percentage is rapidly decrease with the increase of *h/d* ratio. At *h/d* equal to 10, the percentage of δ_s/Δ_t is equal to 2.1%, which indicates that shear deflection can be ignored. However, the percentage corresponded to the ratio of *h/d* < 3 is ranged between 35.1% and 99.2%, which emphasis the significance of shear deflection at low *h/d* levels. The results expressed in this section are complied with the limitations specified by (Richards 2012) that mentioned in section [3.1.2].

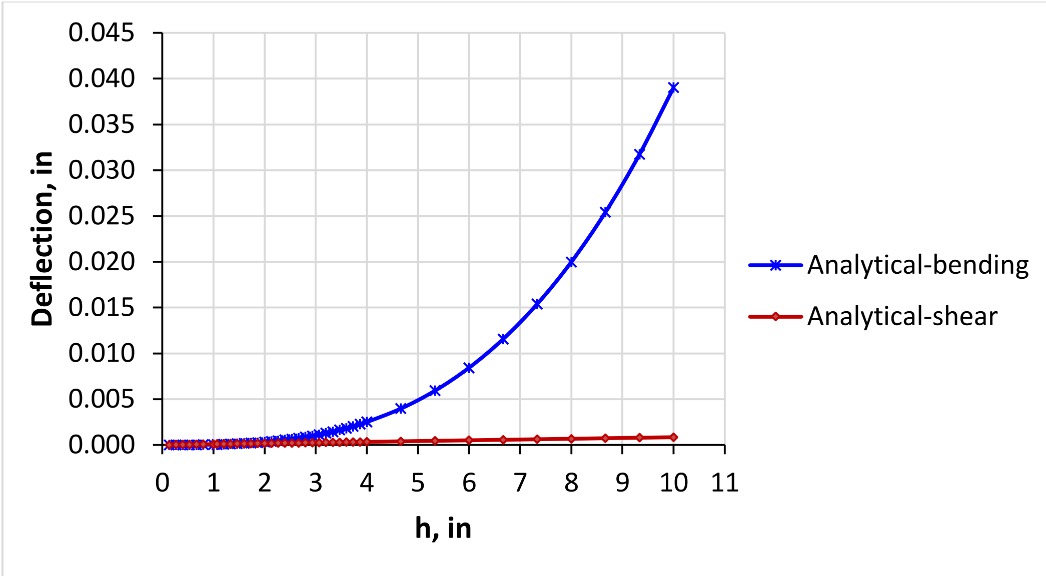

Figure 3.5 Comparison between bending and shear deflections

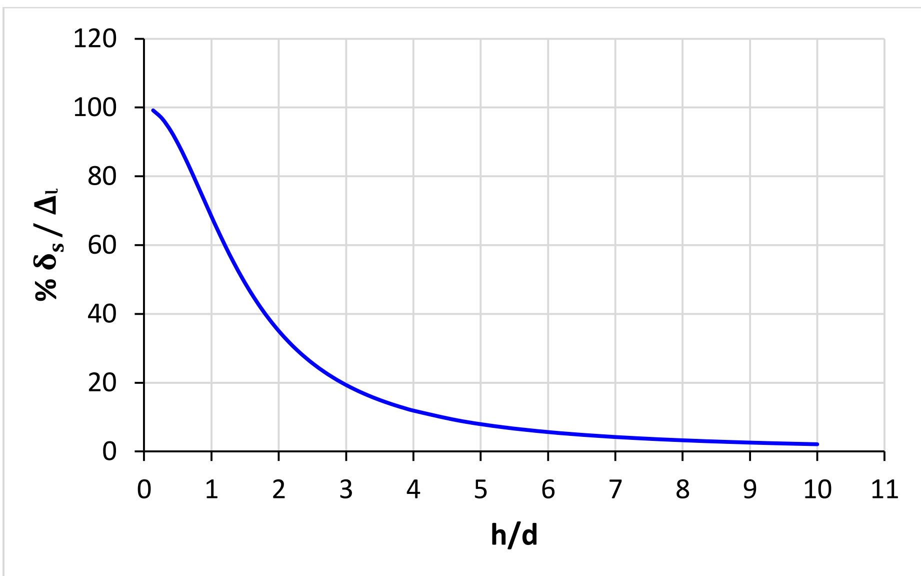

Figure 3.6 Relation between *h/d* and the percentage of shear deflection

3.1.6 Evaluation of Stiffness Equations

The lateral stiffness of the anchor bolts with stand-off distances is the stiffness adopted to resist the lateral loading that induces bending and shear deflections, in the direction perpendicular to the longitudinal axis of the anchor. The lateral stiffness equation is developed using the following procedure.

$$P = K_l \, \Delta_l = K_l \left(\frac{Ph^3}{12EI} + \frac{10Ph}{9GA} \right) \quad \textbf{(3-5)}$$

$$K_l = \left(\frac{h^3}{12EI} + \frac{10h}{9GA}\right)^{-1} \quad \textbf{(3-6)}$$

where:

K_l	=	stiffness of anchors with stand-off distances due to lateral loading
P	=	lateral load
h	=	stand-off distance
E	=	modulus of elasticity of the anchor
G	=	modulus of rigidity of the anchor
I	=	anchor second moment of inertia
A	=	anchor cross sectional area

The axial stiffness of the anchor bolts with stand-off distances is the stiffness adopted to resist the axial loading that induces axial deflection, in the direction of the longitudinal axis of the anchor. The axial stiffness equation is developed using the following procedure.

$$P = K_a \, \Delta_a = K_a \left(\frac{Ph}{EA}\right) \quad \textbf{(3-7)}$$

$$K_a = \frac{EA}{h} \quad \textbf{(3-8)}$$

where:

K_a	=	stiffness of anchors with stand-off distances due to axial loading
P	=	axial load
h	=	stand-off distance
E	=	modulus of elasticity of the anchor
A	=	anchor cross sectional area

3.2 Center of Rigidity (C.R.)

The anchor bolts and the base plate are connected using nuts and washers, therefore they behave as a rigid body. When a force is applied on the centroid of anchors, the anchor group will react as a rigid body to resist this force. The center of rigidity (C.R.) for anchor group can be defined as the center of the stiffness or resistance within the group. The anchor bolts have a C.R. that might or might not coincide with their centroid. When the lateral loads are applied on the center of rigidity of anchors, the anchor group will tend to translate with no rotation. In case of that the C.R. is not coinciding with the centroid of anchors, the lateral loads applied on the centroid will tend to translate and rotate the anchor group.

In double-nut moment joints, the anchors with uniform stand-off distances are having the same area, spacing, and stand-off distances. Therefore, the location of the center of rigidity shall be at the same location of the center of gravity. The anchors with non-uniform stand-off distances are having the same area and spacing, but they differ in the stand-off distance. That difference will create a change in the stiffness of anchors, in a way that the anchors with high stand-off distances tend to have lower stiffness and vice versa. This can be explained by the fact that the lateral stiffness of anchors is inversely proportional to the stand-off distance. As a result, the center of rigidity will shift towards the anchors that have the lower stand-off distances.

Figure 3.7 indicates the layout of anchor bolts with their distances towards the center of rigidity. The number of anchors indicated in the figure was randomly selected to represent the anchor group. The determination of the center of rigidity for anchor bolts with stand-off distances was developed using the following procedure.

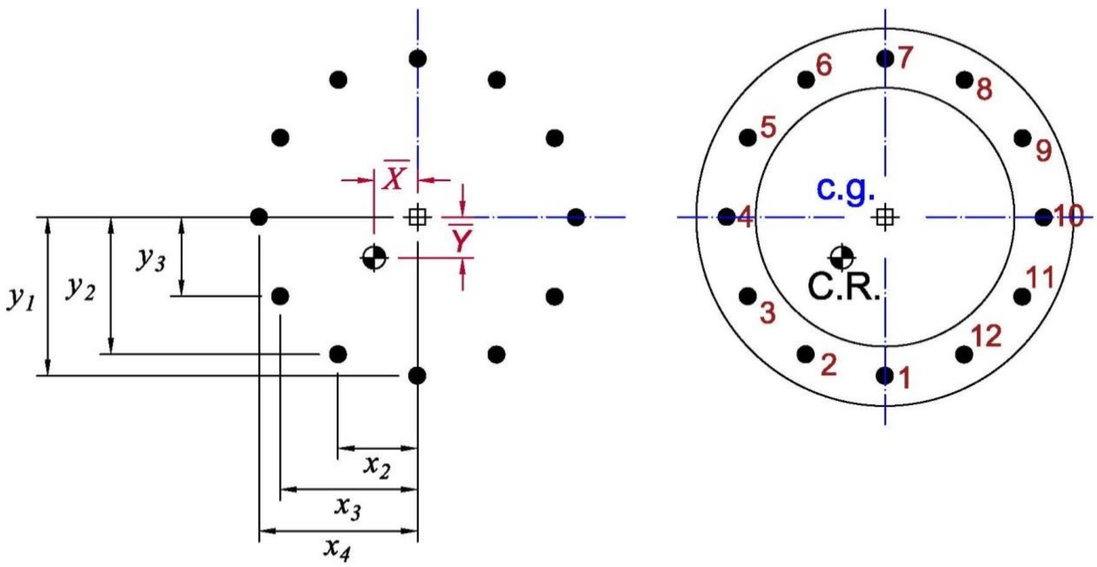

Figure 3.7 Determination of center of rigidity

By taking the summation of moment rigidity about *y*-axis:

$$\bar{X} \sum_{i=1}^{n} K_i = K_1\, x_1 + K_2\, x_2 + K_3\, x_3 + K_4\, x_4 + \cdots\cdots + K_n\, x_n \qquad \textbf{(3-9)}$$

$$\bar{X} \sum_{i=1}^{n} K_i = \sum_{i=1}^{n} K_i\, x_i \qquad \textbf{(3-10)}$$

$$\bar{X} = \frac{\sum_{i=1}^{n} K_i\, x_i}{\sum_{i=1}^{n} K_i} \qquad \textbf{(3-11)}$$

The equation resulted from taking the summation of moment rigidity about *x*-axis is as follows:

$$\bar{Y} = \frac{\sum_{i=1}^{n} K_i \, y_i}{\sum_{i=1}^{n} K_i} \tag{3-12}$$

The group of anchors within the double-nut moment joints expose to two types of deformations: lateral and axial. The stiffness due to lateral and axial loading can be determined using the pre-mentioned equations (**3-6** and **3-8**), respectively. The impact of that is the formation of two center of rigidities: lateral center of rigidity and axial center of rigidity. Equations (**3-13** and **3-14**) represent the lateral center of rigidity, whereas Equations (**3-15** and **Error! Reference source not found.**) represent the axial center of rigidity. The employment of those centers is distinct from each other, in which the function of the lateral center of rigidity is to obtain the shear forces due to direct shear loading and torsion, whereas the axial center of rigidity will be utilized for obtaining the axial forces on anchors due to moment group and the structure own weight. The determination of those forces is presented in the following sections.

$$\bar{X}_l = \frac{\sum_{i=1}^{n} K_{li} \, x_i}{\sum_{i=1}^{n} K_{li}} \tag{3-13}$$

$$\bar{Y}_l = \frac{\sum_{i=1}^{n} K_{li} \, y_i}{\sum_{i=1}^{n} K_{li}} \tag{3-14}$$

$$\bar{X}_a = \frac{\sum_{i=1}^{n} K_{ai} \, x_i}{\sum_{i=1}^{n} K_{ai}} \tag{3-15}$$

$$\bar{Y}_a = \frac{\sum_{i=1}^{n} K_{ai} \, y_i}{\sum_{i=1}^{n} K_{ai}} \tag{3-16}$$

where:

$\bar{X}_l$	=	*x*-coordinate of the center of rigidity due to lateral loading
$\bar{X}_a$	=	*x*-coordinate of the center of rigidity due to axial loading
$\bar{Y}_l$	=	*y*-coordinate of the center of rigidity due to lateral loading
$\bar{Y}_a$	=	*y*-coordinate of the center of rigidity due to axial loading
K_{li}	=	stiffness of anchor *i* due to lateral loading
K_{ai}	=	stiffness of anchor *i* due to axial loading
x_i	=	*x*-coordinate of anchor *i*
y_i	=	*y*-coordinate of anchor *i*
n	=	number of anchor bolts

3.3 Shear Forces on the Anchor Bolts due to Direct Shear Loading

As mentioned previously, the stiffness of an anchor is inversely proportional to the stand-off distance. When the anchors have a uniform distribution of stand-off distances, each of them would have the same stiffness. Therefore, the C.R. will coincide with the center of gravity. The consequence is that the shear forces will be distributed equally on the anchor bolts. That case doesn't comply with the case of anchors with non-uniform stand-off distances, in which each anchor has a different stand-off distance. The result is the mismatch of the center of rigidity with the center of gravity. That will lead to the unequal distribution of shear forces on the anchor bolts. The reason for that is the un-uniformity of the anchor bolts stiffness, in which the anchors with high stiffness among the group would carry more loads. Therefore, the shear forces would be transmitted to the anchors according to the lateral stiffness of the individual anchor bolt. The following procedure was performed to develop the shear forces on anchors with non-uniform stand-off distances.

For anchors with a uniform stand-off distance, Figure 3.8

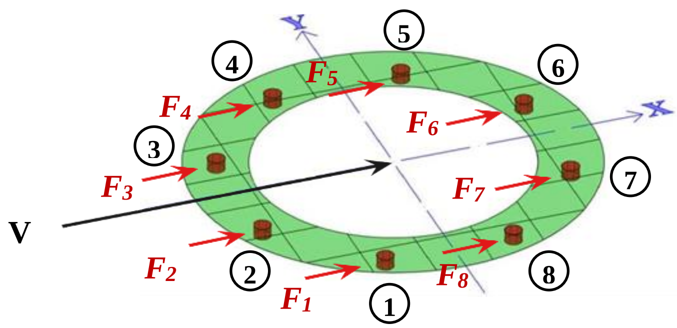

Figure 3.8 Anchors with a uniform stand-off distance

Alternative 1:

The characteristics of anchors with a uniform stand-off distance are: they have the same area, spacing, and stand-off distance. Therefore, the shear force will be uniformly distributed on the anchor bolts. The following equation shall be used to determine the shear force on the individual anchor bolt within the group.

$$F_1 = F_2 = F_3 = \cdots = F_n = \frac{V}{n} \qquad \textbf{(3-17)}$$

Alternative 2:

Since the anchors have the same characteristics, they would have the same stiffness.

$$Anchor\ lateral\ stiffness: K_{l1} = K_{l2} = K_{l3} = K_{l4} = \cdots = K_{ln} \qquad \textbf{(3-18)}$$

Distribution Factor C_{1i}: is the factor that determines the shear force share for each individual anchor bolt within the group

$C_{1i} = anchor\ i\ stiffness/summation\ of\ anchors\ stiffness$

$$C_{1i} = \frac{K_{li}}{\sum_{i=1}^{n} K_{li}} \quad \textbf{(3-19)}$$

By substituting Equation (**3-18**) in Equation (**3-19**):

$$C_{1i} = \frac{K_l}{n\,K_l} = \frac{1}{n} \qquad where: n\ is\ the\ number\ of\ anchor\ bolts \quad \textbf{(3-20)}$$

$$Shear\ on\ individual\ anchor\ (F_{1i}) = C_{1i}\,V \quad \textbf{(3-21)}$$

By substituting Equation (**3-20**) in Equation (**3-21**):

$$F_{1i} = \frac{V}{n} \quad \textbf{(3-22)}$$

It can be noticed from the above derivations that they led to the same equation. Therefore, alternative 2 will be adopted to derive the general equations that can be used to determine the shear forces on the anchors with non-uniform stand-off distances due to direct shear loading. Alternative 1 will not be used because one of its characteristics is not complied with the case of anchors with non-uniform stand-off distances. That characteristic is the inequality of the stand-off distances in the case of anchors having non-uniform stand-off distances.

For anchors with non-uniform stand-off distances, Figure 3.9

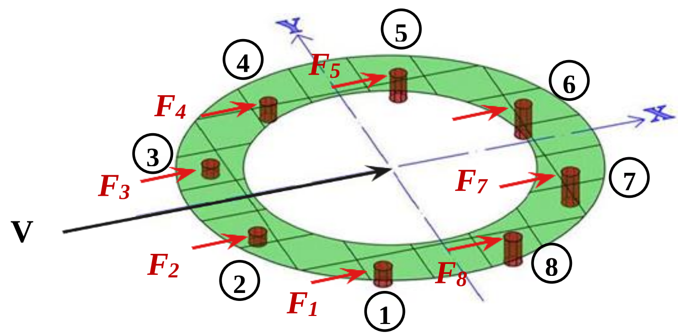

Figure 3.9 Anchors with non-uniform stand-off distances

By recalling Equation (**3-19**), illustrated above in Alternative 2:

$$C_{1i} = \frac{K_{li}}{\sum_{i=1}^{n} K_{li}} \quad \textbf{(3-19)}$$

The above equation will not transformed to any form because the anchors stiffness are not equal.

By recalling Equation (**3-21**), illustrated above in Alternative 2:

$$F_{1i} = C_{1i}\, V \tag{3-21}$$

By substituting equation (**3-19**) in Equation (**3-21**), the shear forces on the anchors with non-uniform stand-off distances can be calculated from the following equation.

$$F_{1i} = V \frac{K_{li}}{\sum_{i=1}^{n} K_{li}} \tag{3-23}$$

From the previous derivations and discussions, the general equations that adopted to calculate the shear forces due to direct shear loading on the anchors with uniform and non-uniform stand-off distances are presented below.

$$F_{1xi} = V_x \frac{K_{li}}{\sum_{i=1}^{n} K_{li}} \tag{3-24}$$

$$F_{1yi} = V_y \frac{K_{li}}{\sum_{i=1}^{n} K_{li}} \tag{3-25}$$

where:

F_{1xi}	=	shear force on anchor *i* in *x*-direction due to direct shear loading
F_{1yi}	=	shear force on anchor *i* in *y*-direction due to direct shear loading
V_x	=	direct shear loading in *x*-direction
V_y	=	direct shear loading in *y*-direction
K_{li}	=	stiffness of anchor *i* due to lateral loading

3.4 Induced Torsional Moment on the Anchor Bolts due to Direct Shear Loading

The center of rigidity is shifted from the anchors' centroid due to the non-uniformity of the stand-off distances within the anchor group. Whether the anchors stand-off distances are uniform, or non-uniform, the induced wind loads will be applied on the center of the base plate, i.e. centroid of anchors. Among those loads are the direct shear loading in x and y directions. Figure 3.10 exhibits the direct shear loading in the directions of *x* and *y*, applied on the centroid of anchors with non-uniform stand-off distances. The figure also indicates that the anchors are having an additional torsional moment, due to the translation of the center of rigidity from the location of the center of gravity. That additional torsion would not be created in case of anchors with uniform stand-off distances.

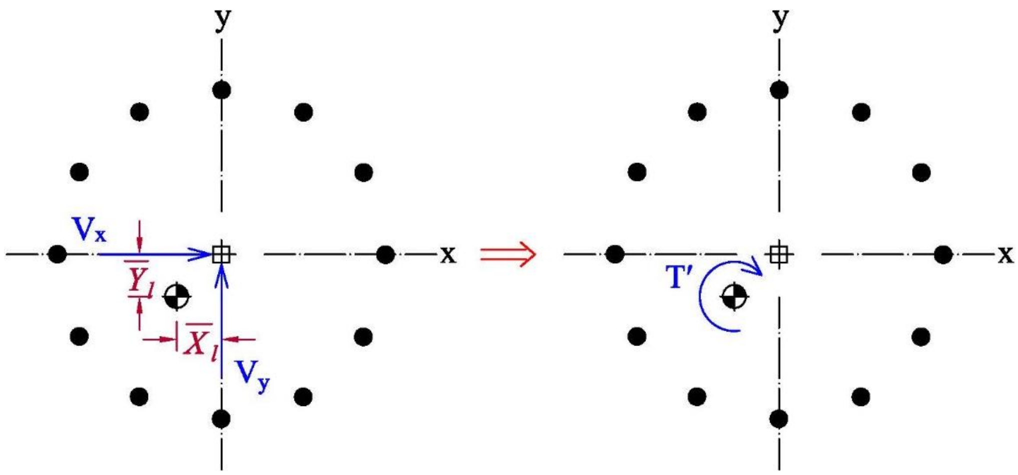

Figure 3.10 Torsional moment due to direct shear loading

The following procedure was adopted to derive the equation that calculates the induced torsion due to direct shear loading.

By taking the moment about the center of rigidity:

$$\sum M_{@C.R.} = T' \pm V_x \bar{X}_l \pm V_y \bar{Y}_l = 0 \quad \textbf{(3-26)}$$

The equation below can be used to calculate the additional torsion due to direct shear loading.

$$T' = \pm V_x \bar{X}_l \pm V_y \bar{Y}_l \quad \textbf{(3-27)}$$

where:

T'	=	shear force on anchor *i* in *x*-direction due to direct shear loading
V_x	=	direct shear loading in *x*-direction
V_y	=	direct shear loading in *y*-direction
$\bar{X}_l$	=	*x*-coordinate of the center of rigidity due to lateral loading
$\bar{Y}_l$	=	*y*-coordinate of the center of rigidity due to lateral loading

3.5 Shear Forces due to Pure Torsion and the Induced Torsion from Direct Shear Loading

The torsional moment is conveyed to the anchor bolts in following manner. The wind loads applied on the cantilever arm, induces a torsional moment on the base plate. That torsional moment will then be transferred to the anchor bolts with shear forces. The fixation of anchors with the base plate through nuts and washers, makes the joint performs as a rigid body. The uniformity of the stand-off distances determine the magnitude of the shear forces that each anchor should carry. The anchors with a uniform stand-off distance are having even distribution of shear forces. However, the shear forces are not equally distrusted for anchors with non-uniform stand-off distances.

The concept of the equations presented in this section is came from the equations that used to distribute the lateral loads in the design of buildings under wind and seismic loads. In case of buildings, the loads are distributed with respect to the inertia of shear walls. However, in case of sign structures, the inertia of anchors is equal because they have the same size, therefore the stiffness is the governed factor that determines the magnitude of the shear force on each anchor due to torsion. The following procedure was developed to determine the equations that can be used to calculate the shear forces due to torsion.

For anchors with a uniform stand-off distance, Figure 3.11

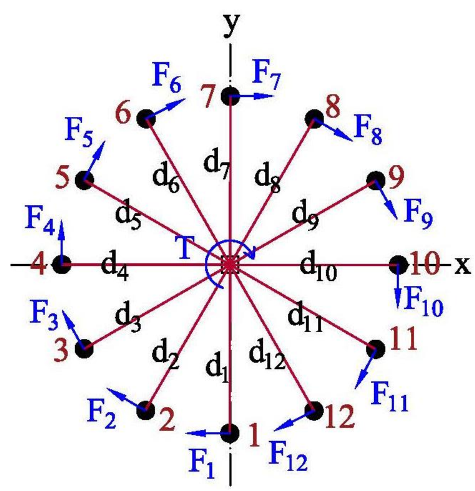

Figure 3.11 Distribution of shear forces due to torsion for anchors with a uniform stand-off distance

$$\frac{F_1}{K_{l1}\, d_1} = \frac{F_2}{K_{l2}\, d_2} = \frac{F_3}{K_{l3}\, d_3} = \cdots = \frac{F_n}{K_{ln}\, d_n} \qquad \textbf{(3-28)}$$

In steel design, particularly in the design of connections under eccentric loads, the above equation is used to develop the equation that calculates the shear forces on bolts due to torsion, but without the stiffness term (McCormac and Csernak 2012). In the procedure herein, the stiffness term is included to account for the difference in the stand-off distances, if occurred. However, if the stand-off distances are the same, the stiffness terms will cancel each other and the end result of the equation will be the same. The addition of stiffness was come from the assumption that the anchors are in the elastic zone, and there is a directly proportional relationship between the anchor deformation and the distance between the c.g. of the base plate and the anchor. The stiffness term in the above equation is came from that concept, in which the anchor deformation is the product of the lateral force divided by the stiffness. Therefore, the inclusion of stiffness in the equation is more generic to account for all the aspects that may change the behavior of the connection. The above equation is transformed into the form below.

$$\frac{F_1}{d_1} = \frac{F_2}{d_2} = \frac{F_3}{d_3} = \cdots = \frac{F_n}{d_n} \tag{3-29}$$

$$\frac{F_1}{d_1} = \frac{F_2}{d_2} \Longrightarrow F_2 = \frac{F_1\, d_2}{d_1} \quad , \quad \frac{F_1}{d_1} = \frac{F_3}{d_3} \Longrightarrow F_3 = \frac{F_1\, d_3}{d_1} \cdots F_n = \frac{F_1\, d_n}{d_1} \tag{3-30}$$

The torsional moment in the equation below is resulted from the pure torsion due to wind loads and the induced torsion from the direct shear loading. The summation is algebraic depends on the direction of the induced torsion.

$$T = \sum_{i=1}^{n} F_i\, d_i = F_1\, d_1 + F_2\, d_2 + F_3\, d_3 + \cdots + F_n\, d_n \tag{3-31}$$

By substituting Equation (**3-30**) in Equation (**3-31**):

$$T = F_1\, d_1 \frac{d_1}{d_1} + \frac{F_1\, d_2}{d_1}\, d_2 + \frac{F_1\, d_3}{d_1}\, d_3 + \cdots + \frac{F_1\, d_n}{d_1}\, d_n \tag{3-32}$$

$$T = \frac{F_1}{d_1}[d_1^2 + d_2^2 + d_3^2 + \cdots + d_n^2] = \frac{F_1}{d_1} \sum_{i=1}^{n} d_i^2 \tag{3-33}$$

$$d_i^2 = x_i^2 + y_i^2 \tag{3-34}$$

Since the distance between the centroid of anchors to the anchors is the same, the shear forces will be distributed equally. By substituting Equation (**3-34**) in Equation (**3-33**):

$$F_{Ri} = \frac{T\, d}{\sum_{i=1}^{n}(x_i^2 + y_i^2)} \tag{3-35}$$

The above derivations are led to the following equation, which comply with the equation specified by *2013 Support Specifications* to calculate the shear forces due to torsion for anchors with a uniform stand-off distance.

$$F_R = \frac{T\, d}{J} \tag{3-36}$$

where:

F_R = shear force due to torsion
T = torsional moment
d = distance between the c.g. of the anchor group to the outmost anchor
J = polar moment of inertia of the anchor group

For anchors with non-uniform stand-off distances, Figure 3.12

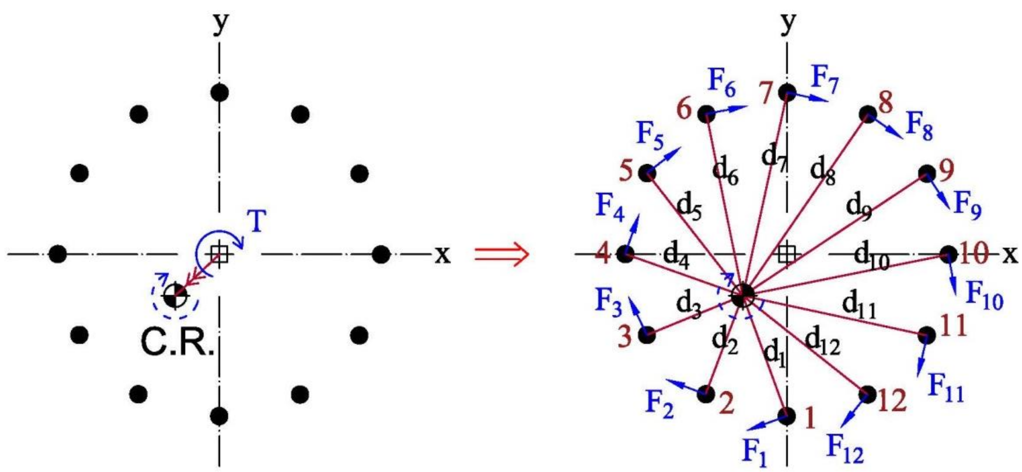

Figure 3.12 Distribution of shear forces due to torsion for anchors with non-uniform stand-off distances

By recalling Equation (**3-28**):

$$\frac{F_1}{K_{l1}\,d_1} = \frac{F_2}{K_{l2}\,d_2} = \frac{F_3}{K_{l3}\,d_3} = \cdots = \frac{F_n}{K_{ln}\,d_n} \tag{3-28}$$

The stiffness for the above equation will not cancel each other as in the case of anchors with a uniform stand-off distance. The reason for that is the irregularity of the stand-off distances that led to the change in anchors stiffness.

$$\frac{F_1}{K_{l1}\,d_1} = \frac{F_2}{K_{l2}\,d_2} \Longrightarrow F_2 = \frac{K_{l2}\,F_1\,d_2}{K_{l1}\,d_1} \;\cdots\; \frac{F_1}{K_{l1}\,d_1} = \frac{F_n}{K_{ln}\,d_n} \Longrightarrow F_n = \frac{K_{ln}\,F_1\,d_n}{K_{l1}\,d_1} \tag{3-37}$$

By recalling Equation (**3-31**):

$$T = \sum_{i=1}^{n} F_i\,d_i = F_1\,d_1 + F_2\,d_2 + F_3\,d_3 + \cdots + F_n\,d_n \tag{3-31}$$

By substituting Equation (**3-37**) in Equation (**3-31**):

$$T = F_1\,d_1\,\frac{K_{l1}\,d_1}{K_{l1}\,d_1} + \frac{K_{l2}\,F_1\,d_2}{K_{l1}\,d_1}\,d_2 + \cdots + \frac{K_{ln}\,F_1\,d_n}{K_{l1}\,d_1}\,d_n \tag{3-38}$$

$$T = \frac{F_1}{K_{l1}\,d_1}\left[K_{l1}\,d_1^2 + K_{l2}\,d_2^2 + \cdots + K_{ln}\,d_n^2\right] = \frac{F_1}{K_{l1}\,d_1}\sum_{i=1}^{n} K_{li}\,d_i^2 \tag{3-39}$$

$$F_1 = T\frac{K_{l1}\, d_1}{\sum_{i=1}^{n} K_{li}\, d_i^2} \quad , \quad F_2 = T\frac{K_{l2}\, d_2}{\sum_{i=1}^{n} K_{li}\, d_i^2} \cdots\cdots\cdots \tag{3-40}$$

By recalling Equation (**3-34**):

$$d_i^2 = x_i^2 + y_i^2 \tag{3-34}$$

By substituting Equation (**3-34**) in Equation (**3-40**):

$$F_i = T\frac{K_{li}\, d_i}{\sum_{i=1}^{n} K_{li}\, (x_i^2 + y_i^2)} \tag{3-41}$$

From the previous derivations and discussions, the general equations that adopted to calculate the shear forces due to torsion on the anchors with uniform and non-uniform stand-off distances are presented below.

$$F_{2xi} = T\frac{K_{li}\, y_i}{\sum_{i=1}^{n} K_{li}\, (x_i^2 + y_i^2)} \tag{3-42}$$

$$F_{2yi} = T\frac{K_{li}\, x_i}{\sum_{i=1}^{n} K_{li}\, (x_i^2 + y_i^2)} \tag{3-43}$$

where:

F_{2xi} = shear force on anchor *i* in *x*-direction due to torsion
F_{2yi} = shear force on anchor *i* in *y*-direction due to torsion
T = torsional moment pure torsion and direct shear loading
K_{li} = stiffness of anchor *i* due to lateral loading
x_i = distance between anchor *i* and the c.r. due to bending and shear in *x*-direction
y_i = distance between anchor *i* and the c.r. due to bending and shear in *y*-direction

3.6 Group Moment Induced from the Shear forces on Anchors due to Direct Shear Loading and Torsion

In order to understand how the direct shear loading will result in a group bending moment on the anchor bolts, an example of a single story building will be used for clarification. Figure 3.13 shows the layout of a steel structure that comprised of one story. As shown in the figure, the building is consisted of a steel deck rested on four steel columns. A load *F* is applied horizontally at the mid height of the story building. It can be noticed that the load is equally distributed on the steel columns, with no additional bending moment because the load is applied at the c.g of columns. If the load is shifted upwards to be applied at the centerline of the steel deck, as illustrated in Figure 3.14, the load will create an additional group moment. This moment is equal to the shear load *F* multiplied by the distance between the centerline of the steel deck to the mid height of columns. It should be noticed that all columns are having the same height, so the group moment will be equally distributed on the top of columns.

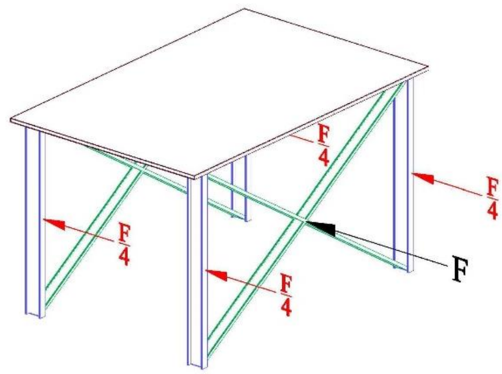

Figure 3.13 Single story steel building with a load at the middle height

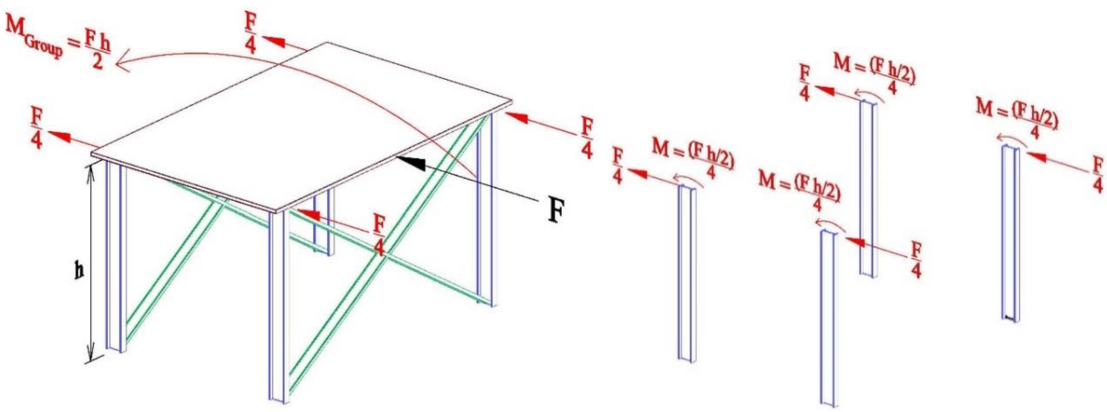

Figure 3.14 Single story steel building with a load on the steel deck

The case described in Figure 3.14 is similar to the case of anchor bolts with a uniform stand-off distance. The load is applied on the centerline of the base plate that is connected to the anchor bolts with the uniform stand-off distance. For sign and signal structure, the following equation can be used to determine the moment group of anchors with a uniform stand-off distance.

$$\left(M_{Group}\right)_{1x} = V_y \, h/2 \tag{3-44}$$

$$\left(M_{Group}\right)_{1y} = V_x \, h/2 \tag{3-45}$$

where:

$(M_{Group})_{1x}$ = group moment about x-axis due to direct shear loading in y-direction
$(M_{Group})_{1y}$ = group moment about y-axis due to direct shear loading in x-direction
V_x = direct shear loading in x-direction

V_y	=	direct shear loading in *y*-direction
h	=	stand-off distance

It should be noted that the shear forces applied on the anchor group are due to direct shear loading and torsion. In case of anchors with a uniform stand-off distance, the anchors are having the same stand-off distance, therefore the summation of moments on the anchors within the group due to torsion would be zero. The shear forces due to direct shear loading would be the forces that produce the group moment. That is the reason that the above equations are having the direct shear loading only.

The procedure indicated below is another generic alternative, to determine the moment group of anchors with a uniform stand-off distance. Figure 3.15 (a and b) shows the summation of shear forces due to direct shear loading and torsion, respectively. Those forces were indicated in sections [3.3 and 3.5]. To determine the bending moments on the individual anchors within the group, the beam model specified by *2013 Support Specifications* will be used for calculations. That model considers the connection between the anchors and concrete foundation to be fixed, and the anchors/leveling-nuts connection to be free to transmit without rotation. It was also specified that the beam model should be used when the anchors uniform stand-off distance is more than the anchor diameter. That condition will not be considered in the present study for accuracy. With the conditions of: torsion induces a summation of forces in *x* and *y* directions equal to zero (Figure 3.15-b), and the stand-off distances are equal; the summation of the induced moment on the anchor group due to torsion would be zero. That context was mentioned in the preceding paragraph, but it is recalled herein because this discussing alternative approach will be used for anchors with non-uniform stand-off distances, and the moment due to torsion at that case will be considered. The subsequent procedure will exclude the torsion from calculations.

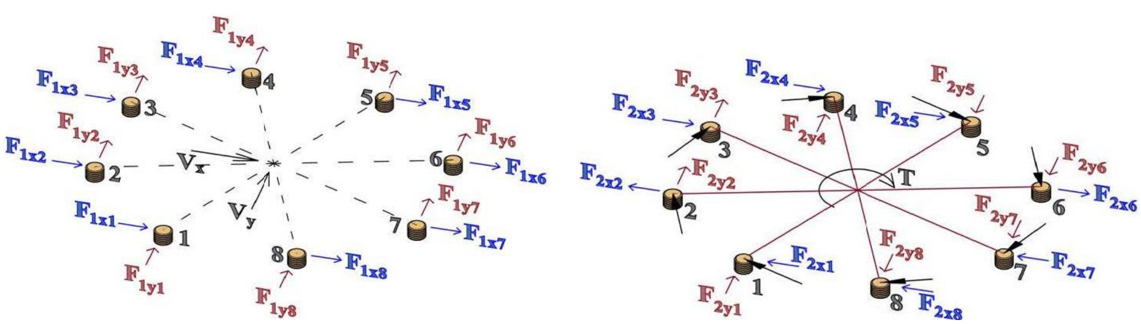

(a) **(b)**

Figure 3.15 Shear forces due to direct shear loading and torsion for anchors with a uniform stand-off distances

The schematic shown in Figure 3.16 indicates the moments on the individual anchor bolts, at the anchors/concrete-foundation connection, induced from the shear forces due to direct shear loading, about *x* and *y* axes. The algebraic summation of those moments will result in the moment group about each direction. This procedure was conducted to obtain the moment group on anchors with a uniform stand-off distance, and compare the moment equations with those indicated in Equations (**3-44** and **3-45**). If complied, that alternative procedure will be used to determine the group moment for anchors with non-uniform stand-off distances.

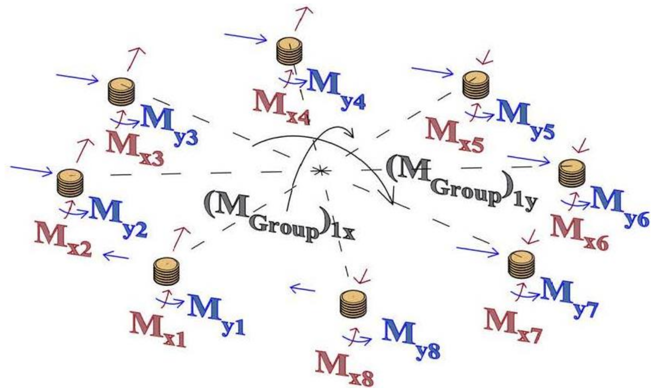

Figure 3.16 Moment group on anchors with a uniform stand-off distance

Consider that the anchors in the above figure have a uniform stand-off distance of *h*-in. The determination of the moment group will be performed about *x*-axis only, and the terms of the end result equation will be converted to comply with the moment group about *y*-axis.

$$M_{x1} = \frac{F_{1y1}\,h}{2}\,, M_{x2} = \frac{F_{1y2}\,h}{2} \cdots M_{xn} = \frac{F_{1yn}\,h}{2} \quad \textbf{(3-46)}$$

$$\sum_{i=1}^{n} M_{xi} = \frac{h}{2}\sum_{i=1}^{n} F_{1yi} = \frac{h}{2}\,V_y \quad \textbf{(3-47)}$$

Equation (**3-47**) will be transformed into the following:

$$\sum_{i=1}^{n} M_{xi} = \left(M_{Group}\right)_{1x} = V_y\,\frac{h}{2} \quad \textbf{(3-48)}$$

For moment group about *y*-axis:

$$\sum_{i=1}^{n} M_{yi} = \left(M_{Group}\right)_{1y} = V_x\,\frac{h}{2} \quad \textbf{(3-49)}$$

Equations (**3-48** and **3-49**) are complied with Equations (**3-44** and **3-45**). It can be inferred from these results that the alternative procedure used to determine the moment group for anchors with a uniform stand-off distance is correct. That procedure will be used to determine the moment group due to shear forces for anchors with non-uniform stand-off distances. The figure below shows the moment group for anchors with non-uniform stand-off distances.

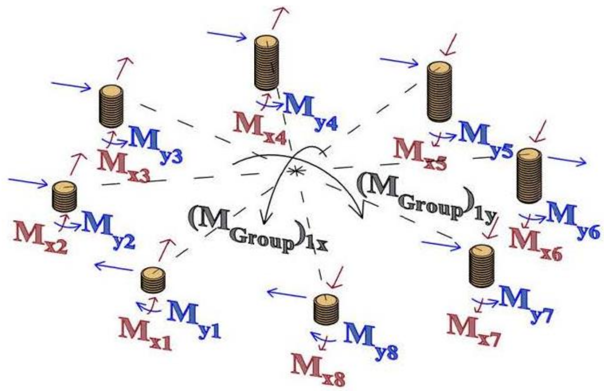

Figure 3.17 Moment group on anchors with non-uniform stand-off distances

Since the anchors are having unequal stand-off distances, the shear forces due to torsion will be considered in the calculations. The next procedure was adopted to develop the equations that calculate the moment group about *x* and *y* axes, for anchors with non-uniform stand-off distances.

$$M_{x1} = \frac{(F_{1y1} \pm F_{2y1})\, h_1}{2}, M_{x2} = \frac{(F_{1y2} \pm F_{2y2})\, h_2}{2} \cdots M_{xn} = \frac{(F_{1yn} \pm F_{2yn})\, h_n}{2} \qquad \textbf{(3-50)}$$

$$\sum_{i=1}^{n} M_{xi} = \frac{1}{2}\sum_{i=1}^{n}(F_{1yi} \pm F_{2yi})\, h_i = \sum_{i=1}^{n} F_{lyi}\frac{h_i}{2} \qquad \textbf{(3-51)}$$

The moment group equations due to shear forces:

$$(M_{Group})_{1x} = \sum_{i=1}^{n} F_{lyi}\frac{h_i}{2} \qquad \textbf{(3-52)}$$

$$(M_{Group})_{1y} = \sum_{i=1}^{n} F_{lxi}\frac{h_i}{2} \qquad \textbf{(3-53)}$$

where:

$(M_{Group})_{1x}$	=	group moment about *x*-axis due to direct shear loading in *y*-direction
$(M_{Group})_{1y}$	=	group moment about *y*-axis due to direct shear loading in *x*-direction
F_{lxi}	=	total lateral force on anchor *i* in *x*-direction due to direct shear loading and torsion
F_{lyi}	=	total lateral force on anchor *i* in *y*-direction due to direct shear loading and torsion
h_i	=	stand-off distance of anchor *i*

3.7 Axial forces on Anchor bolts due to the Total Own Weight of the Structure

The total own weight of the structure is applied on the centroid of anchor bolts. For anchors with a uniform stand-off distance, the axial forces induced from the own weight will be distributed equally on the anchor bolts. The reason for that is the compliance of the center of gravity with the center of rigidity. The following equation can be used to calculate the shear forces on the anchors having a uniform stand-off distance:

$$N_{1i} = \frac{N_{o.w}}{n} \tag{3-54}$$

where:

N_{1i} = axial force on anchor *i* due to the total own weigh of the structure
$N_{o.w}$ = total own weight of the structure
n = number of anchors

In case of anchors with non-uniform stand-off distances, the total own weight of the structure will induce axial forces, as well as group moments. The procedure of the determination of axial forces is the same as that adopted to determine the shear forces on the anchor bolts due to direct shear loading, section [3.3]. The forces were distributed according to the lateral stiffness of anchors, see equations (3-24 and 3-25). Those equations were recalled below for demonstration.

$$F_{1xi} = V_x \frac{K_{li}}{\sum_{i=1}^{n} K_{li}} \tag{3-24}$$

$$F_{1yi} = V_y \frac{K_{li}}{\sum_{i=1}^{n} K_{li}} \tag{3-25}$$

The distribution of axial forces was performed to comply with the equations above with a difference that the adopted stiffness would be the axial stiffness. The equations illustrated below can be used to calculate the axial forces due to the total own weight, on the anchors with uniform and non-uniform stand-off distance.

$$N_{1i} = N_{o.w} \frac{K_{ai}}{\sum_{i=1}^{n} K_{ai}} \tag{3-55}$$

where:

N_{1i} = axial force on anchor *i* due to the total own weigh of the structure
$N_{o.w}$ = total own weight of the structure
K_{ai} = axial stiffness of anchor *i*

The determination of the group moment due to the total own weight will be performed in the next section.

3.8 Moment Group on the Anchor Bolts due to the Total Own Weight of the Structure

This section is applicable only for anchors with non-uniform stand-off distances. Since the total own weight is applied on the c.g. of anchor group, and the C.R. is shifted from the c.g.; moment groups will be generated about *x* and *y* axes. The following procedure was adopted to determine the moment groups on the anchors having non-uniform stand-off distances.

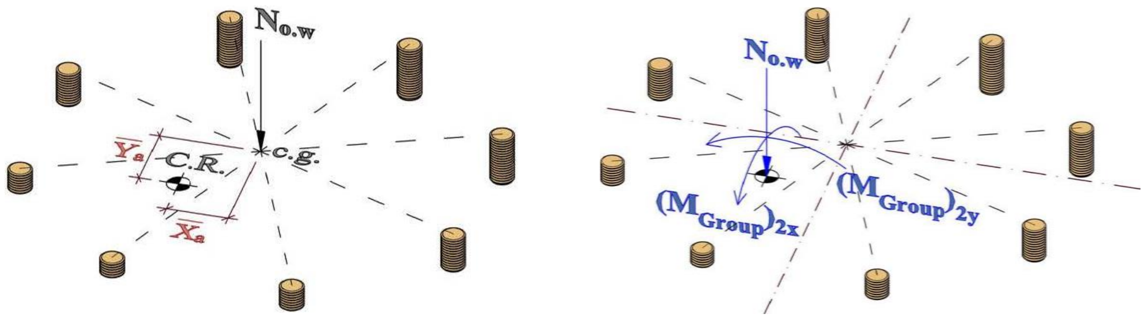

Figure 3.18 Moment group due to the own weight of the structure

By taking the moment about the center of rigidity:

$$\sum M_{x@C.R.} = \left(M_{Group}\right)_{x1} \pm N_{o.w}\,\bar{Y}_a = 0 \quad \textbf{(3-56)}$$

$$\sum M_{y@C.R.} = \left(M_{Group}\right)_{y1} \pm N_{o.w}\,\bar{X}_a = 0 \quad \textbf{(3-57)}$$

The equation below can be used to calculate the moment groups about *x* and *y* axes due to the own weight, with the addition of the weight of arms and attachments, if applicable.

$$\left(M_{Group}\right)_{2x} = \pm\, N_{o.w} \cdot \bar{Y} \pm (M_{Arms+attachments})_x \quad \textbf{(3-58)}$$

$$\left(M_{Group}\right)_{2y} = \pm\, N_{o.w} \cdot \bar{X} \pm (M_{Arms+attachments})_y \quad \textbf{(3-59)}$$

where:

$(M_{Group})_{2x}$	=	group moment about *x*-axis due to the total own weight of the structure
$(M_{Group})_{2y}$	=	group moment about *y*-axis due to the total own weight of the structure
$(M_{Arms+Attachments})_x$		group moment about x-axis due to arms and attachments, if applicable
$(M_{Arms+Attachments})_y$		group moment about *y*-axis due to arms and attachments, if applicable
$N_{o.w}$	=	total own weight of the structure
$\bar{X}_{\iota}$	=	*x*-coordinate of the center of rigidity due to axial loading

$\bar{Y}_i$ = y-coordinate of the center of rigidity due to axial loading

3.9 Axial Forces on the Anchor Bolts due to Group Bending Moment

This section is dedicated to determine the axial forces due to group moment induced from wind loading, for anchors with uniform and non-uniform stand-off distances. The concept of deriving the shear forces due to torsion, in section [3.5], is used to determine the axial forces due to group moment. The concept is based on assumption that the anchor deformation is directly proportional to the distance between the c.g. of the anchor group and the anchors, with the consideration of that the anchors and the base plate are a rigid system. The derivation procedure is as follows:

For anchors with a uniform stand-off distance, Figure 3.19*:*

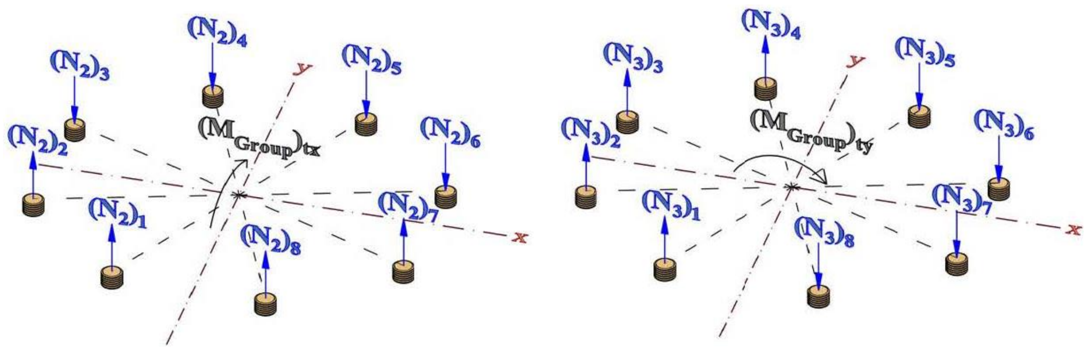

Figure 3.19 Axial forces due to group moments for anchors with a uniform stand-off distance

The following procedure is performed for the moment group due to wind loading about x-axis:

$$\frac{N_1}{K_{a1}\,y_1} = \frac{N_2}{K_{a2}\,y_2} = \frac{N_3}{K_{a3}\,y_3} = \cdots = \frac{N_n}{K_{an}\,y_n} \quad \textbf{(3-60)}$$

All the anchors are having the same stiffness because they have equal stand-off distances. The above equation will be transformed to:

$$\frac{N_1}{y_1} = \frac{N_2}{y_2} = \frac{N_3}{y_3} = \cdots = \frac{N_n}{y_n} \quad \textbf{(3-61)}$$

$$\frac{N_1}{y_1} = \frac{N_2}{y_2} \Rightarrow N_2 = \frac{N_1\,y_2}{y_1} \quad , \quad \frac{N_1}{y_1} = \frac{N_3}{y_3} \Rightarrow N_3 = \frac{N_1\,y_3}{y_1} \cdots N_n = \frac{N_1\,y_n}{y_1} \quad \textbf{(3-62)}$$

$$M_x = \sum_{i=1}^{n} N_i\,y_i = N_1\,y_1 + N_2\,y_2 + N_3\,y_3 + \cdots + N_n\,y_n \quad \textbf{(3-63)}$$

By substituting Equation (**3-62**) in Equation (**3-63**):

$$M_x = N_1\, y_1 \frac{y_1}{y_1} + \frac{N_1\, y_2}{y_1}\, y_2 + \frac{N_1\, y_3}{y_1}\, y_3 + \cdots + \frac{N_1\, y_n}{y_1}\, y_n \quad \textbf{(3-64)}$$

$$M_x = \frac{N_1}{y_1}\left[y_1^2 + y_2^2 + y_3^2 + \cdots + y_n^2\right] = \frac{N_1}{y_1}\sum_{i=1}^{n} y_i^2 \quad \textbf{(3-65)}$$

$$N_1 = \frac{M_x\, y_1}{\sum_{i=1}^{n} y_i^2} \quad \textbf{(3-66)}$$

The following general equations can be used to determine the axial forces due to the total moment group due to: direct shear forces (section 3.6), total own weight (section 3.8), and wind loading.

$$N_{2i} = \left(M_{Group}\right)_{tx} \frac{y_i}{\sum_{i=1}^{n} y_i^2} \quad \textbf{(3-67)}$$

$$N_{3i} = \left(M_{Group}\right)_{ty} \frac{x_i}{\sum_{i=1}^{n} x_i^2} \quad \textbf{(3-68)}$$

where:

N_{2i}	=	total axial force on anchor *i* due to group bending moments about *x*-axis
N_{3i}	=	total axial force on anchor *i* due to group bending moments about *y*-axis
$(M_{Group})_{tx}$	=	total group moment about *x*-axis due to wind loading in *y*-direction, direct shear forces, and total own weight
$(M_{Group})_{ty}$	=	total group moment about *y*-axis due to wind loading in *x*-direction, direct shear forces, and total own weight
x_i	=	distance between anchor *i* and the c.g. of anchor group in *x*-direction
y_i	=	distance between anchor *i* and the c.g. of anchor group in *y*-direction

For anchors with non-uniform stand-off distances, Figure 3.20

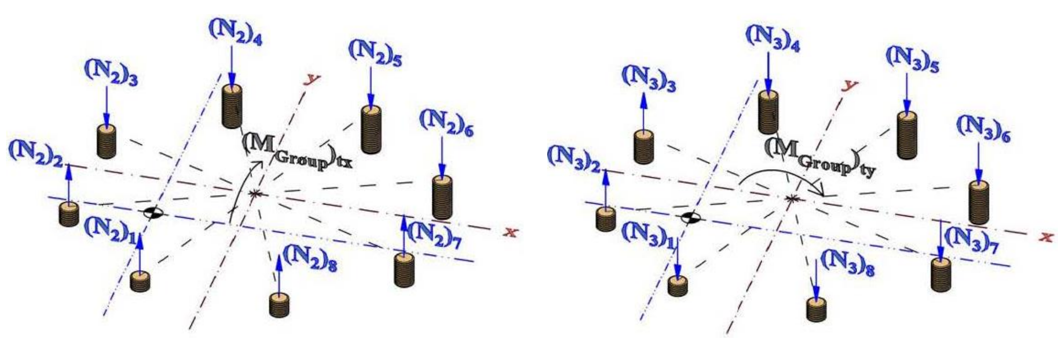

Figure 3.20 Axial forces due to group moments for anchors with non-uniform stand-off distances

The following procedure is performed for the moment group due to wind loading about x-axis. By recalling Equation (**3-60**):

$$\frac{N_1}{K_{a1}\, y_1} = \frac{N_2}{K_{a2}\, y_2} = \frac{N_3}{K_{a3}\, y_3} = \cdots = \frac{N_n}{K_{an}\, y_n} \tag{3-60}$$

Since the anchors are having non-uniform stand-off distances, the stiffness will not be the same. Figure 3.21 demonstrates the distances x_i and y_i that measured from the anchor to the c.r. in x and y directions, respectively.

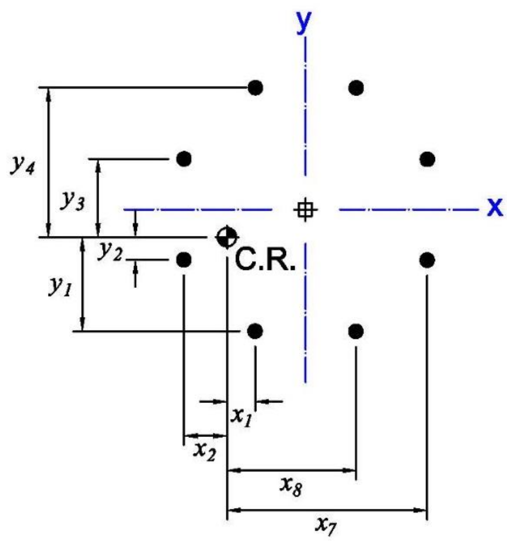

Figure 3.21 Measurements of x_i and y_i

$$\frac{N_1}{K_{a1}\, y_1} = \frac{N_2}{K_{a2}\, y_2} \Longrightarrow N_2 = \frac{K_{a2}\, N_1\, y_2}{K_{a1}\, y_1} \cdots N_n = \frac{K_{an}\, N_1\, y_n}{K_{a1}\, y_1} \tag{3-69}$$

By recalling Equation (**3-63**):

$$M_x = \sum_{i=1}^{n} N_i\, y_i = N_1\, y_1 + N_2\, y_2 + N_3\, y_3 + \cdots + N_n\, y_n \tag{3-63}$$

By substituting Equation (**3-69**) in Equation (**3-63**):

$$M_x = N_1\, y_1 \frac{K_{a1}\, y_1}{K_{a1}\, y_1} + \frac{K_{a2}\, N_1\, y_2}{K_{a1}\, y_1}\, y_2 + \cdots + \frac{K_{an}\, N_1\, y_n}{K_{a1}\, y_1}\, y_n \tag{3-70}$$

$$M_x = \frac{N_1}{K_{a1}\, y_1}\left[K_{a1}\, y_1^2 + K_{a2}\, y_2^2 + K_{a3}\, y_3^2 + \cdots + K_{an}\, y_n^2\right] = \frac{N_1}{K_{a1}\, y_1}\sum_{i=1}^{n} K_{ai}\, y_i^2 \tag{3-71}$$

$$N_1 = \frac{M_x \, K_{a1} \, y_1}{\sum_{i=1}^{n} K_{ai} \, y_i^2} \quad \textbf{(3-72)}$$

The following general equations can be used to determine the axial forces due to the total moment group due to: direct shear forces (section 3.6), total own weight (section 3.8), and wind loading. Those equations can be used to determine the axial forces for anchors with uniform and non-uniform stand-off distances.

$$N_{2i} = \left(M_{Group}\right)_{tx} \frac{K_{ai} \, y_i}{\sum_{i=1}^{n} K_{ai} \, y_i^2} \quad \textbf{(3-73)}$$

$$N_{3i} = \left(M_{Group}\right)_{ty} \frac{K_{ai} \, x_i}{\sum_{i=1}^{n} K_{ai} \, x_i^2} \quad \textbf{(3-74)}$$

where:

N_{2i}	=	total axial force on anchor *i* due to group bending moments about *x*-axis
N_{3i}	=	total axial force on anchor *i* due to group bending moments about *y*-axis
$(M_{Group})_{tx}$	=	total group moment about *x*-axis due to wind loading in *y*-direction, direct shear forces, and total own weight
$(M_{Group})_{ty}$	=	total group moment about *y*-axis due to wind loading in *x*-direction, direct shear forces, and total own weight
K_a	=	stiffness of anchor *i* due to axial loading
x_i	=	distance between anchor *i* and the c.g. of anchor group in *x*-direction
y_i	=	distance between anchor *i* and the c.g. of anchor group in *y*-direction

3.10 Combined Loading on the Anchor Bolts

The calculations of stresses on the anchors with uniform and uniform stand-off distances are summarized in the following steps:

1. Determination of shear forces due to: pure torsion, direct shear loading, and induced torsion from direct shear loading.

$$F_{txi} = \pm F_{1xi} \pm F_{2xi} \quad \textbf{(3-75)}$$

$$F_{tyi} = \pm F_{1yi} \pm F_{2yi} \quad \textbf{(3-76)}$$

where:

F_{txi}	=	total shear forces on anchor *i* in *x*-direction
F_{tyi}	=	total shear forces on anchor *i* in *y*-direction
F_{1xi}	=	shear force on anchor *i* in *x*-direction due to direct shear loading, section [3.3]
F_{1yi}	=	shear force on anchor *i* in *y*-direction due to direct shear loading, section [3.3]
F_{2xi}	=	shear force on anchor *i* in *x*-direction due to torsion, section [3.5]

F_{2yi} = shear force on anchor *i* in *y*-direction due to torsion, section [3.5]

2. Determination of axial forces resulted from total own weight of the structure, and the moment group induced from: direct shear forces, total own weight of the structure, and wind loads.

$$N_{ti} = \pm N_{1i} \pm N_{2i} \pm N_{3i} \quad \textbf{(3-77)}$$

where:

N_{ti} = total axial force on anchor *i*
N_{1i} = axial force on anchor *i* due to the total own weigh of the structure
N_{2i} = total axial force on anchor *i* due to group bending moments about *x*-axis (total own weight, wind loading, and direct shear forces in *y*-direction)
N_{3i} = total axial force on anchor *i* due to group bending moments about *y*-axis (total own weight, wind loading, and direct shear forces in *x*-direction)

3. Determination of axial stresses due to the loads developed in steps 1 and 2.

$$\sigma_{Ni} = \pm \frac{N_{ti}}{A} \pm \frac{M_{xi} \cdot r}{I} \pm \frac{M_{yi} \cdot r}{I} \quad \textbf{(3-78)}$$

$$M_{xi} = \frac{F_{tyi} \cdot h}{2} \quad \textbf{(3-79)}$$

$$M_{yi} = \frac{F_{txi} \cdot h}{2} \quad \textbf{(3-80)}$$

where:

σ_{Ni} = total normal stress on anchor *i*
N_{ti} = total axial force on anchor *i*
M_{xi} = total moment on anchor *i* about *x*-axis due to total shear forces
M_{yi} = total moment on anchor *i* about *y*-axis due to total shear forces
F_{txi} = total shear forces on anchor *i* in *x*-direction
F_{tyi} = total shear forces on anchor *i* in *y*-direction
h = stand-off distance of anchor *i*
A = cross sectional area of the anchor bolt
r = radius of the anchor bolt
I = second moment of inertia of the anchor bolt

4. Determination of shear stresses due to the loads developed in steps 1 and 2.

The derivation of the following equation is detailed in *Appendix D*.

$$\tau_i = \frac{16}{3\pi d^2} F_{Ri} \quad \textbf{(3-81)}$$

$$F_{Ri} = \sqrt{(F_{txi})^2 + (F_{tyi})^2} \quad \textbf{(3-82)}$$

where:

τ_i = total shear stress on anchor *i*
F_{Ri} = resultant shear force on anchor *i*
F_{txi} = total shear forces on anchor *i* in *x*-direction
F_{tyi} = total shear forces on anchor *i* in *y*-direction
d = diameter of the anchor bolt

4 NUMERICAL STUDY

The main objective of the numerical study is to validate the developed analytical equations, which used to determine the straining actions and stresses on the anchor bolts with uniform and non-uniform stand-off distances. A numerical analysis using the SAP2000 finite element analysis software package was used for modeling. The design of experiment is consisted of four cases varied in the angle of the concrete surface: 0˚, 2˚, 4˚, and 5˚. The case of angle 0˚ represents the anchor bolts with a uniform stand-off distance. Angles: 2˚, 4˚, and 5˚, represent the case of anchor bolts with non-uniform stand-off distances. Table 4.1 exhibits the details of the design of experiment related to the numerical study. The table indicates that the uniform stand-off distance has brought to change to represent the excessive and non-excessive uniformity cases, it which the uniform stand-off distances are ranged between 0.75-in and 3-in. It can also be seen from the table that the lowest anchor bolt stand-off distance for angles: 2˚, 4˚, and 5˚, is 1-in, which is lower than the anchor bolt diameter. The reason for that is to configure if there are limitations for the developed analytical equations, which related to the change of the percentages of the excessive to non-excessive stand-off distances.

Table 4.1 Design of experiment for the numerical study

Angle (α˚)	Diameter of Anchor (d_o), in.	Uniform Stand-off Distance	Excessive Uniform Stand-off Distance	Non-Uniform Stand-off Distances
0	1.5	$0.5d_o$ = 0.75 in.	2 in.	—
		d_o = 1.5 in.	3 in.	
2	1.5	—	—	$d_{o(min)}$ = 1 in.
4	1.5	—	—	$d_{o(min)}$ = 1 in.
5	2	—	—	$d_{o(min)}$ = 1 in.

4.1 Design of Specimens

The double-nut moment joint that used in the numerical study, is equipped with eight anchor bolts attached to a base plate with a thickness of 1.25 in. The schematic shown in Figure 4.1 demonstrates the cross sectional dimensions of the specimens. As shown in the figure, the anchor bolts are having the same spacing, and the dimensions of the inner and outer diameter of the base plate are 24 in and 35 in, respectively. It can also be seen that the diameter of the anchor bolts circle is equal to 30 in. It should be noted that the specimens were modeled without the presence of pole. The absence of pole will not influence on the final results, since the scope of this analysis is to quantify the straining actions on the anchor bolts.

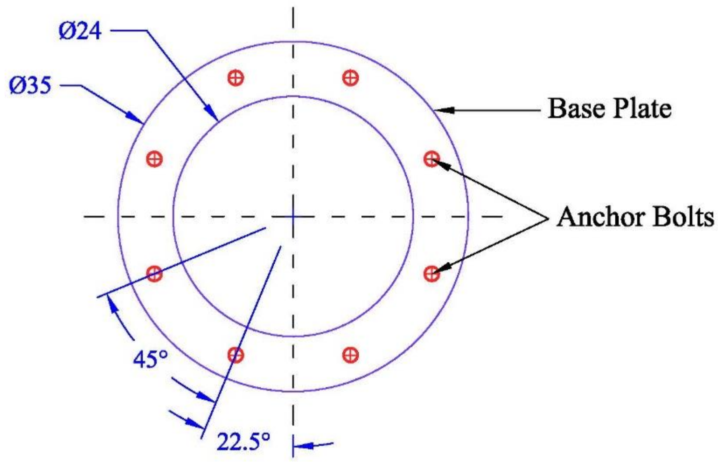

Figure 4.1 Layout of the double-nut moment joint

The schematics shown in figures (4.2, 4.3, 4.4, and 4.5) illustrate the anchor bolts stand-off distances with respect to the angles of the concrete surface (α°). As shown in Figure 4.2, the anchor bolts are having a uniform stand-off distance (ℓ) that, according to the design of experiment, is ranged between 0.75-in and 3-in, with a diameter of 1.5-in. The stand-off distances of the anchor bolts shown in Figure 4.3, corresponded to $\alpha = 2^{\circ}$ in $+x$-direction, are ranged between 1-in and 1.9679-in. This angle is tended to provide a fifty-fifty mixture between the excessive and non-excessive stand-off distances. In case of $\alpha = 4^{\circ}$ in $+x$-direction, indicated in Figure 4.4, the anchor bolts stand-off distances are ranged between 1-in and 2.9381-in. This angle is attributed to increase the percentage of excessive stand-off distances to 75%, and decrease the percentage of non-excessive stand-off distances to 25%. Figure 4.5 provides the distribution of anchor bolts stand-off distances with respect to $\alpha = 5^{\circ}$. The figure exhibits that the angle was carried out along the line that passes through anchor #1 and #5. The stand-off distances are ranged between 1-in and 3.6247-in, which consequent a percentage of excessive stand-off distances of 62.5%, and 37.5% for non-excessive stand-off distances. There are two distinct criteria that distinguish the joint with angle 5˚ from the other considered angles. The first criterion is that the joint with an angle 5˚ has anchor bolts with a diameter of 2-in, whereas the other joints have 1.5-in. The second criterion is that the concrete surface is inclined in $+xy$-direction in case of $\alpha = 5^{\circ}$, whereas the direction is in $+x$-direction for the other two angles. Those changes were aimed to increase the level of discrepancy in the direction of loading.

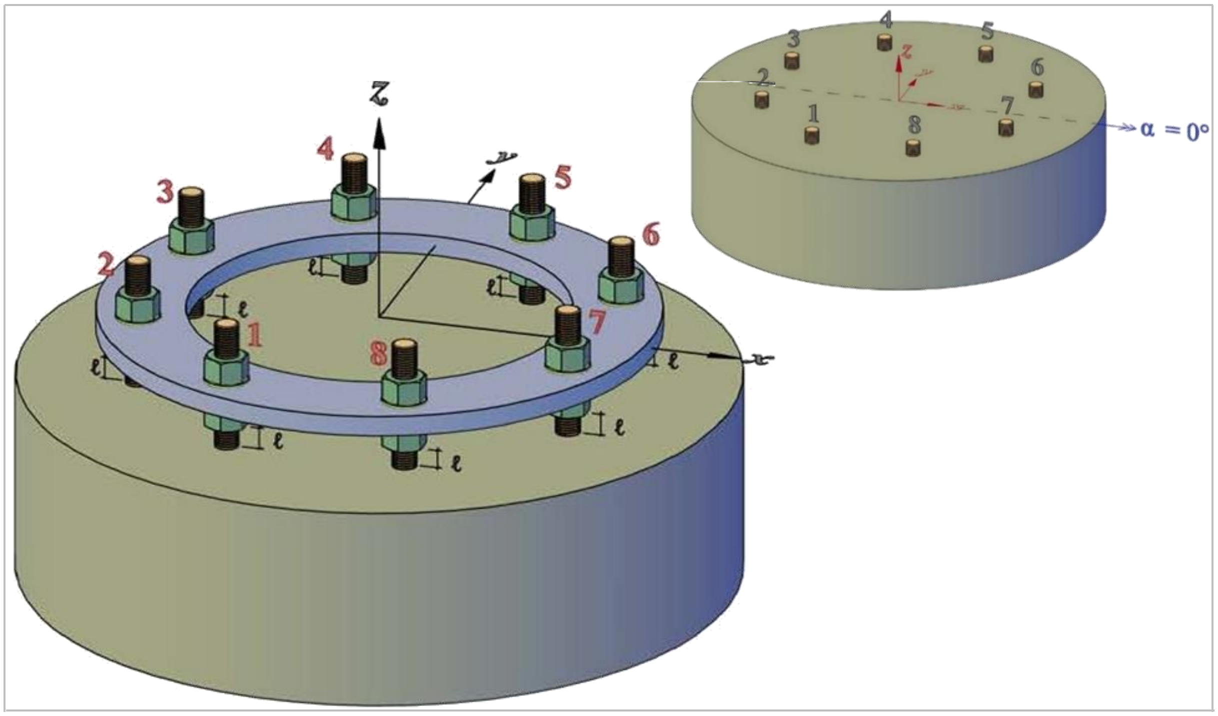

Figure 4.2 Distribution of anchor bolts stand-off distances with α = 0∘

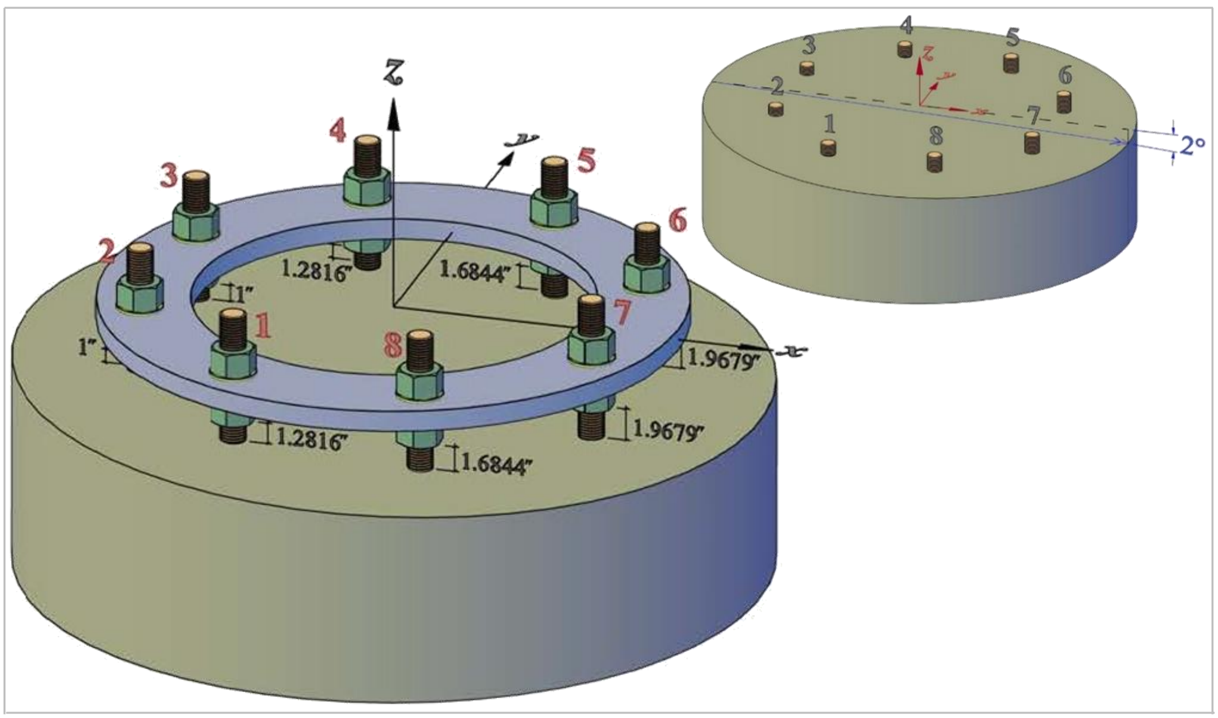

Figure 4.3 Distribution of anchor bolts stand-off distances with α = 2∘ in +*x*-direction

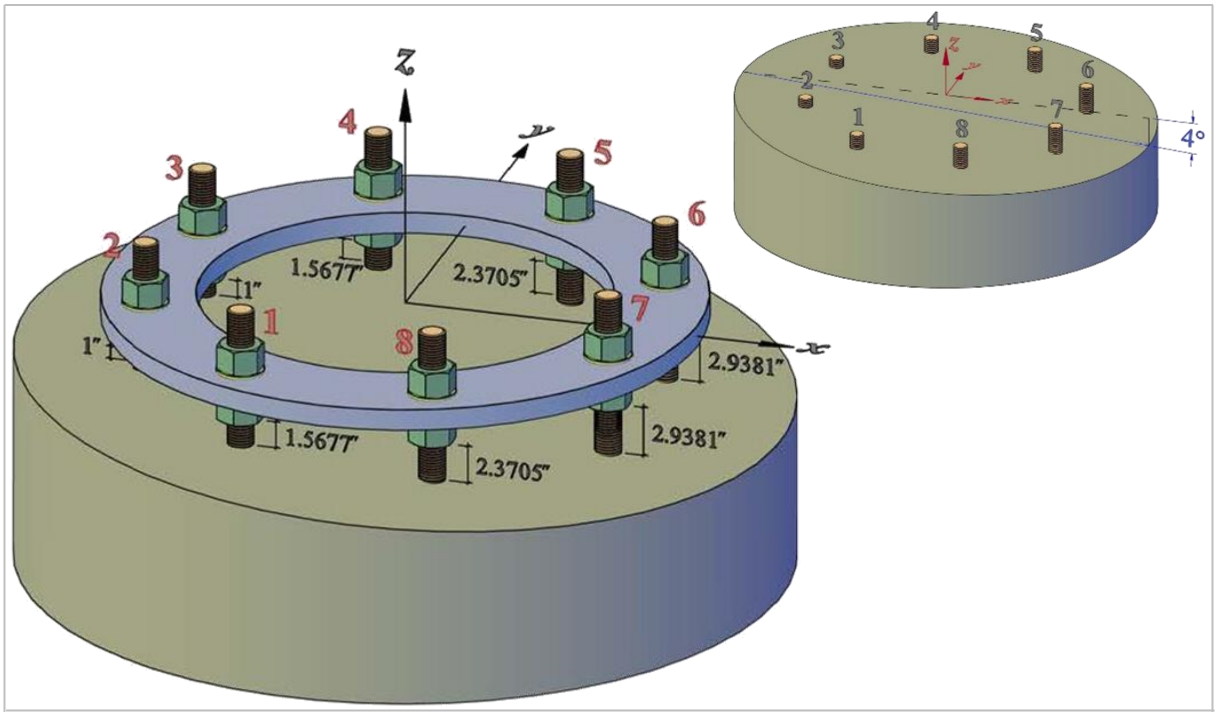

Figure 4.4 Distribution of anchor bolts stand-off distances with α = 4° in +*x*-direction

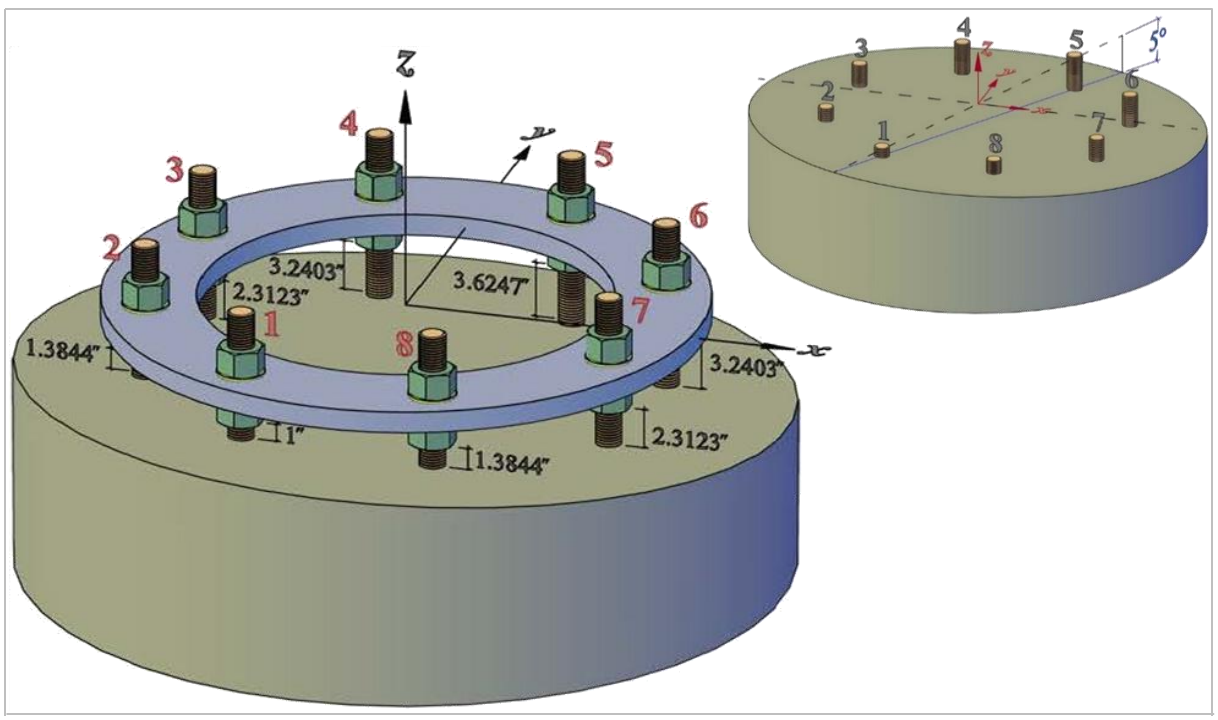

Figure 4.5 Distribution of anchor bolts stand-off distances with α = 5° in +*xy*-direction

4.2 Modeling and Boundary Conditions

The element types used to model the joint were frame elements for anchors and shell elements for the base plate. This study is focused on the anchor bolts; therefore the presence of pole as well as the nuts and washers were neglected. The presence of threads was also not considered because the area taken in the analysis was the gross area. Therefore, the final results will not be influenced by the absence of threads. A close up of the components of a real double-nut moment joint is illustrated in Figure 4.6. As shown in the figure, the anchor bolts are connected to the base plate by two nuts and two washers. The forces induced from wind loading are applied on the anchor bolt at the section beneath the bottom of the leveling nut. The figure also shows an extruded view from SAP2000, that exhibit the connection between the anchor bolt and the base plate in modeling. The anchor bolt is directly connected to the base plate, and the stand-off distance is measured from the centerline of the base plate to the fixed node.

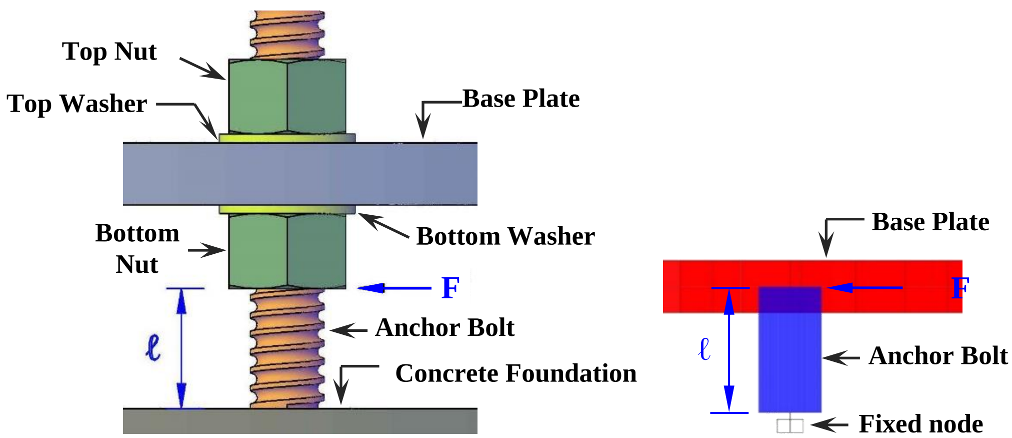

Figure 4.6 Real joint versus simulated joint

The boundary conditions for the anchor bolts were considered to be completely fixed at the bottom (connection between the anchors and the concrete surface), and full body constraint at the top (connection between the anchor and the base plate). Figure 4.7 shows a snap shot from SAP2000 that demonstrates the boundary conditions of the connection. The figure indicates that the loads were applied at the center of the base plate. Those loads should be transferred to the anchors; therefore a point was inserted at the center of the base plate. The anchor bolts are connected to that point through full body constraint. The criterion of the full body constraint is that the connected joints are translating and rotating as a rigid body.

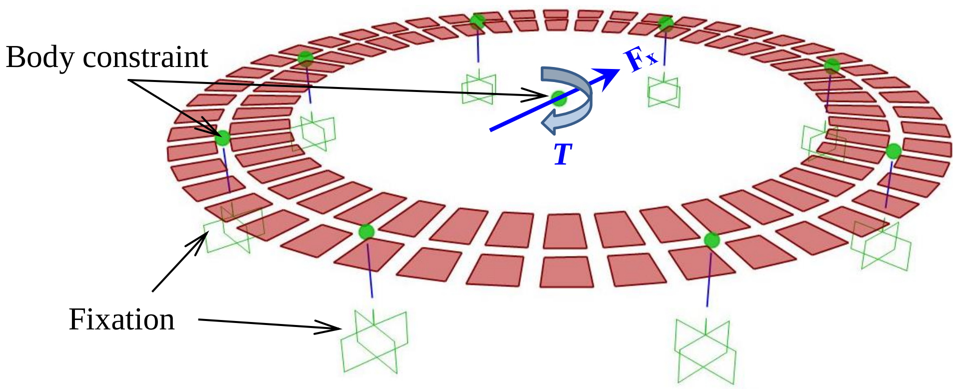

Figure 4.7 Boundary conditions of the connection

4.3 Loading Conditions

The dimensions of the overhead cantilevered sign structure investigated by Hosch (Hosch 2013) was used to determine the applied loads on the joint under investigation. The sign is consisted of a pole with a height of 26.75 ft and a truss arm with a length of 32 ft. The induced loads due to a force of 0.75 kip in *x* and *y* directions are: torsion (T) = 0.75*x*32*x*12 = 288 kip.in, $M_x = M_y$ = 0.75*x*26.75*x*12 = 240.75 kip.in, and $V_x = V_y$ = 0.75 kip. Figure 4.8 shows the directions of the applied loads on the c.g of the base plate. Those loads will be used, in the following section, to verify the boundary conditions and structural elements specified in the numerical model.

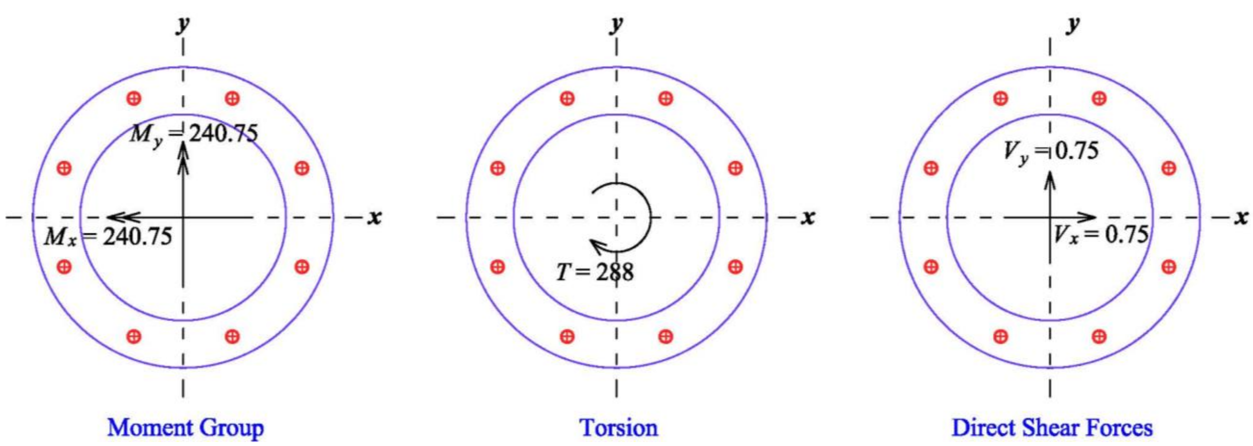

Figure 4.8 Application of load on SAP2000 Model

4.4 Verifying the Numerical Model

Before applying the design of experiment table illustrated at the beginning of this chapter, the numerical model should first be verified. The aim of this section is to verify the boundary conditions and the structural elements in the numerical model. The numerical model was intended to be verified using equations both; validated experimentally and specified in *2013 Supports Specifications*. Those equations are limited to anchors with a uniform strand-off distance.

2013 Supports Specifications specified to Equation (**2-2**) to determine the axial stresses due to moment group. This equation has been proved experimentally by NCHRP Report 412 (Kaczinski, Dexter, and Dien 1998). *2013 Supports Specifications* also specified Equation (**2-8**) to calculate the resultant shear forces due to torsion. Those equations were listed in the background section in this report, but they repeated herein for demonstration.

$$\sigma = \frac{M\ c}{I} \tag{2-2}$$

where:

σ = axial stress due to bending on the individual anchor
M = group moment
I = polar moment of inertia of the anchor group
c = distance between the centroid of the anchor group and the anchor under investigation in the direction of moment

$$F = \frac{T.r}{J} \tag{2-8}$$

where:

F = shear force due to torsion
T = torsional moment
r = distance between the c.g. of the anchor group to the outmost anchor
J = polar moment of inertia of the group of anchors

The schematic exhibited in Figure 4.1 was adopted in the numerical model, with the following characteristics: (1) the diameter of anchors is 1.5-in; and (2) the uniform stand-off distance is 1-in. The considered forces are specified in the previous section [4.3]. Those forces were applied at the center of the base plate.

2013 Supports Specifications specified that, if the anchor bolts are having a uniform stand-off distance less than the anchor bolt diameter, the bending stresses shall be ignored. For accuracy purposes, the bending stresses were considered in the analysis of the joint under investigation. The boundary conditions of the anchor bolts are: fixed at the bottom, and full body constraint at the top. Those boundaries are promised to simulate the beam model specified by *2013 Supports Specifications*. The beam model criterion is that the anchors are permit to translate but not to rotate. To recap, the considered boundary conditions and the selected structural elements were being tested, to verify the numerical model.

Results and discussion

The results illustrated in Table 4.2 represent a comparison between the straining actions induced from the analytical and numerical analysis. As shown in the table, the forces induced from the analytical Equations (**2-2** and **2-8**), are identical with those from the numerical model. The numerical results exhibited in Table 4.2 are given in Figure 4.9. The figure demonstrates the shear forces on each anchor bolt, in *x* and *y* directions, as well as the axial force. The details of the analytical equations are provided in the *Appendix E* section.

Table 4.2 Comparison between analytical and numerical straining actions

Anchor #	[1]$(F_x)_{AN}$	[2]$(F_x)_{NU}$	[3]$(F_y)_{AN}$	[4]$(F_y)_{NU}$	[5]$(N)_{AN}$	[6]$(N)_{NU}$
1	-2.12	-2.12	1.01	1.01	5.24	5.24
2	-0.82	-0.82	2.31	2.31	5.24	5.24
3	1.01	1.01	2.31	2.31	2.17	2.17
4	2.31	2.31	1.01	1.01	-2.17	-2.17
5	2.31	2.31	-0.82	-0.82	-5.24	-5.24
6	1.01	1.01	-2.12	-2.12	-5.24	-5.24
7	-0.82	-0.82	-2.12	-2.12	-2.17	-2.17
8	-2.12	-2.12	-0.82	-0.82	2.17	2.17

[1]$(F_x)_{AN}$: analytical shear force in *x*-direction
[2]$(F_x)_{NU}$: numerical shear force in *x*-direction
[3]$(F_y)_{AN}$: analytical shear force in *y*-direction
[4]$(F_y)_{NU}$: numerical shear force in *y*-direction
[5]$(N)_{AN}$: analytical axial force
[6]$(N)_{NU}$: numerical axial force

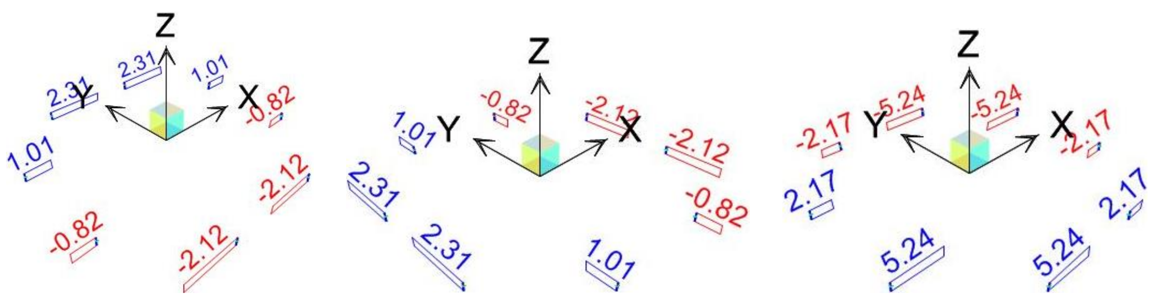

Shear in *x*-direction Shear in *y*-direction Axial force

Figure 4.9 Numerical straining actions

Table 4.3 shows a comparison between the numerical and analytical normal stresses on each anchor within the group. The results indicated in the table confirm that the boundary conditions and element types, specified in the numerical model, are correct, in which the analytical and numerical stresses are almost identical. The highest percentage of difference with respect to the analytical stress is equal to 3.91%. Figure 4.10 displays the numerical stresses that indicated in Table 4.3. As inferred from the above discussed results, the numerical model is verified and can be used to validate the developed analytical equations.

Table 4.3 Comparison between analytical and numerical stresses

Anchor #	* $(\sigma_N)_{AN}$	** $(\sigma_N)_{NU}$	%
1	7.70	7.69	0.11
2	7.70	7.69	0.11
3	6.24	6.46	3.46
4	6.24	-6.46	3.46
5	7.70	-7.69	0.11
6	7.70	-7.69	0.11
7	5.68	-5.90	3.91
8	5.68	5.90	3.91

*$(\sigma_N)_{AN}$: analytical normal stress
**$(\sigma_N)_{NU}$: numerical normal stress

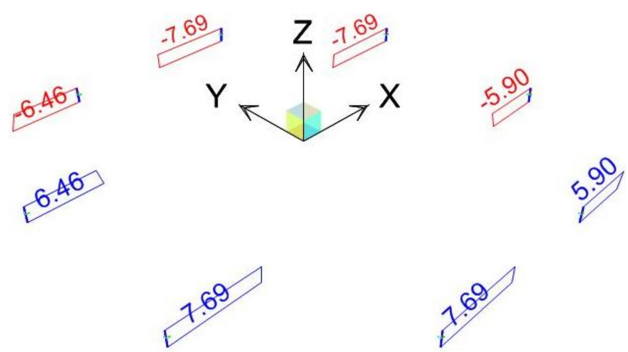

Figure 4.10 Numerical stresses

5 RESULTS AND DISCUSSION

In Chapter 4, the structural elements and boundary conditions developed in the numerical model was verified. The numerical model will then be used to validate the developed analytical equations in Chapter 3. The design of experiment expressed in table 4.1 was used to validate the analytical equations. The cases indicated in that table were subjected to the loads established in the section [4.3] in Chapter 4. The schematic displayed in Figure 5.1 represents an example of a joint that modeled on SAP2000, with the pre-calculated loads that applied on the center of the base plate. The results induced from the numerical analysis are compared to their correspondence from the developed analytical equations. The compatibility of the analytical results with the numerical results will determine the reliability of the analytical equations.

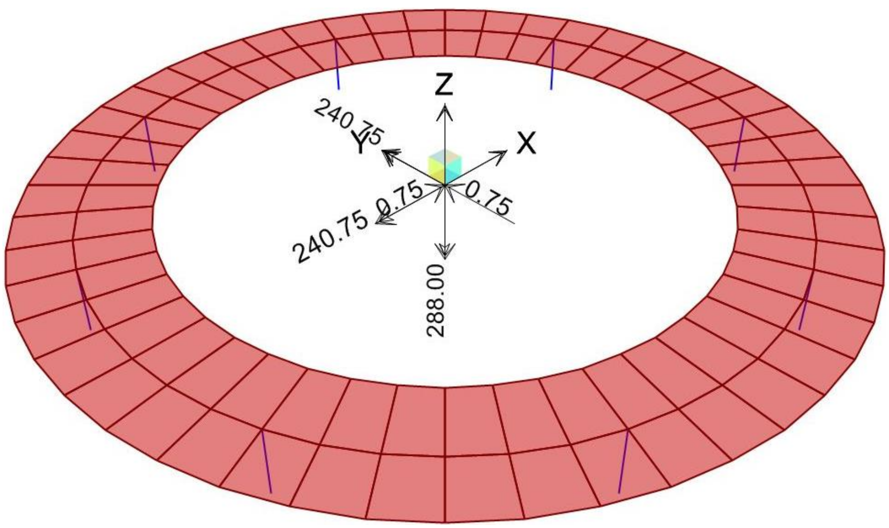

Figure 5.1 Example of a joint with the applied loads

5.1 Induced Forces from the Analytical and Numerical Analysis

Two different sets of variables: anchor bolts with a uniform stand-off distance and non-uniform stand-off distances. The findings associated with each variable will be discussed in the following sections.

5.1.1 Forces on Anchors having a Uniform Stand-off Distance

A series of uniform stand-off distances ranged between 0.75-in and 3-in were investigated to test the developed analytical equations under induced wind loads. Figure 5.2 demonstrates the staining actions on the anchor bolts with a stand-off distance equals to 1-in. This figure is a representative of all the other uniform stand-off distances. It was found that all the uniform stand-off distances were given the same straining actions. This can be explained by the compatibility of the center of rigidity with the center of gravity. Hence, the anchor bolts that having any level of uniform stand-off distance will result in the same straining actions. It should be noted that the shear forces are applied on the anchor at the section below the leveling nut, as illustrated previously in Figure 4.6 in Chapter 4, whereas the forced applied axially are distributed on the entire stand-off distance. The figure indicates that the developed analytical equations provided shear and axial forces that complied with their correspondence numerical forces. This means that the analytical equations adopted to calculate the straining actions are accurate and valid to design the anchor bolts with uniform stand-off distance.

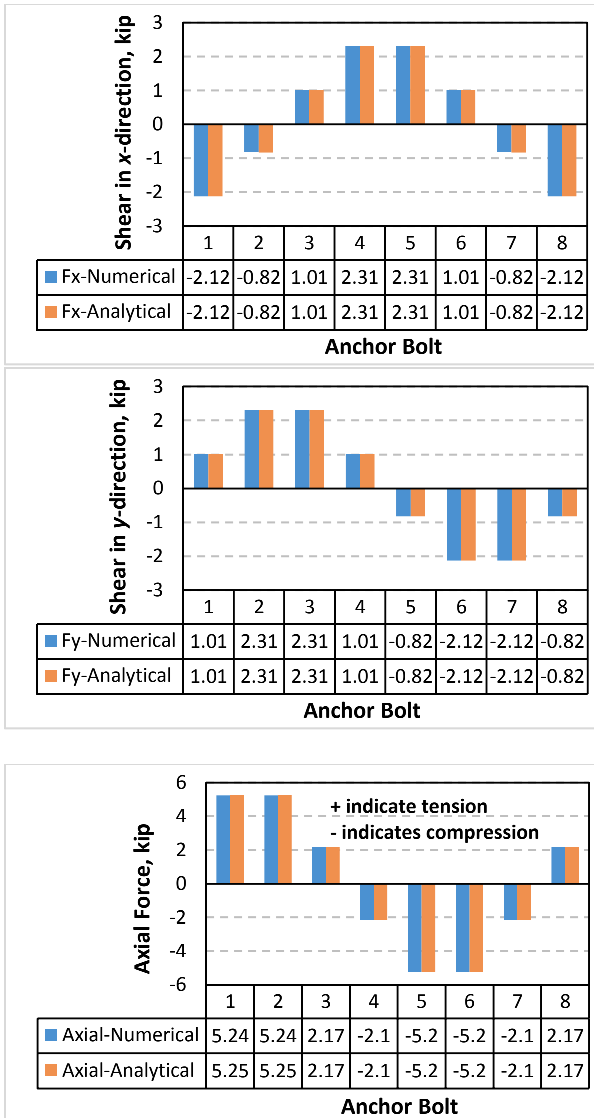

Figure 5.2 Comparison between analytical and numerical forces for uniform stand-off distance of 1-in

5.1.2 Forces on Anchors having Non-uniform Stand-off Distances

Figure 5.3 exhibits a comparison between the straining actions induced numerically, and analytically for anchors with non-uniform stand-off distances. The figure is divided into three groups, in each of which three bar charts were drawn to represent the shear forces in x and y directions, and the axial forces. The groups are differing in the angle of inclination (α˚). Three angles were studied: 2˚, 4˚, and 5˚. The figure indicates an obvious compatibility between the straining actions obtained by applying the developed analytical equations, and their correspondence from the numerical analysis. It is worth mentioning to observe that the anchors that possess the lowest stand-off distances have the highest forces and vice versa. This can be explained by their closeness to the center of rigidity, in which the anchors are adapted to carry more forces when they near the center of rigidity. The above results and discussions have revealed the validity of adopting the developed analytical equations to calculate the straining actions on the anchor bolts having uniform and non-uniform stand-off distances.

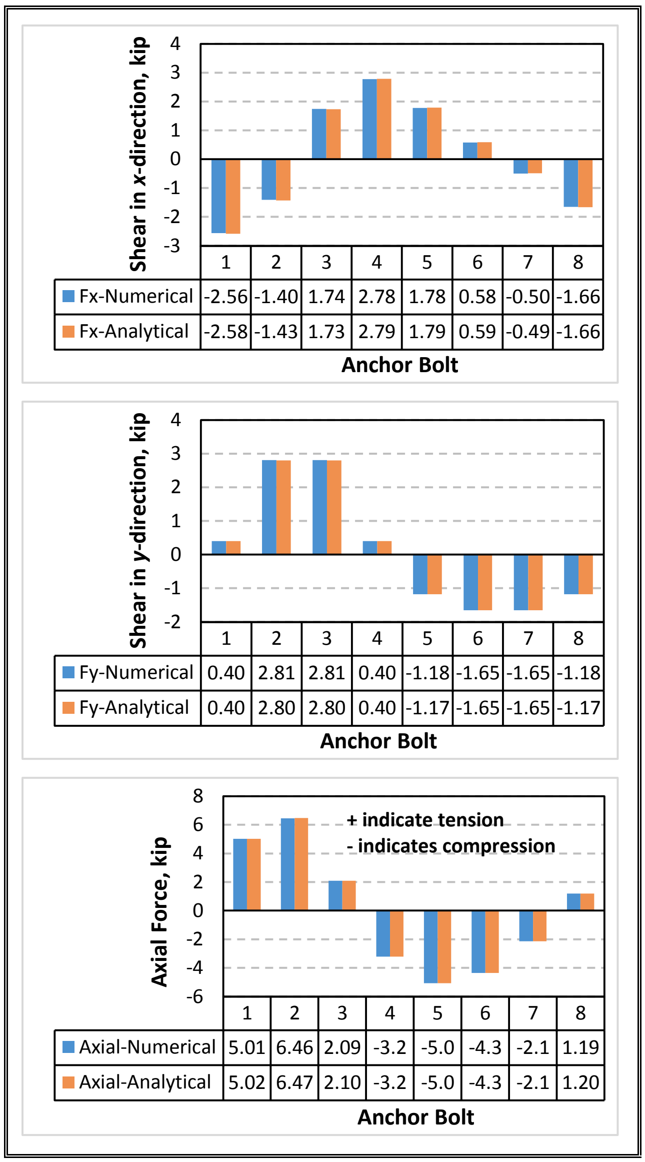

Inclination angle — α = 2˚

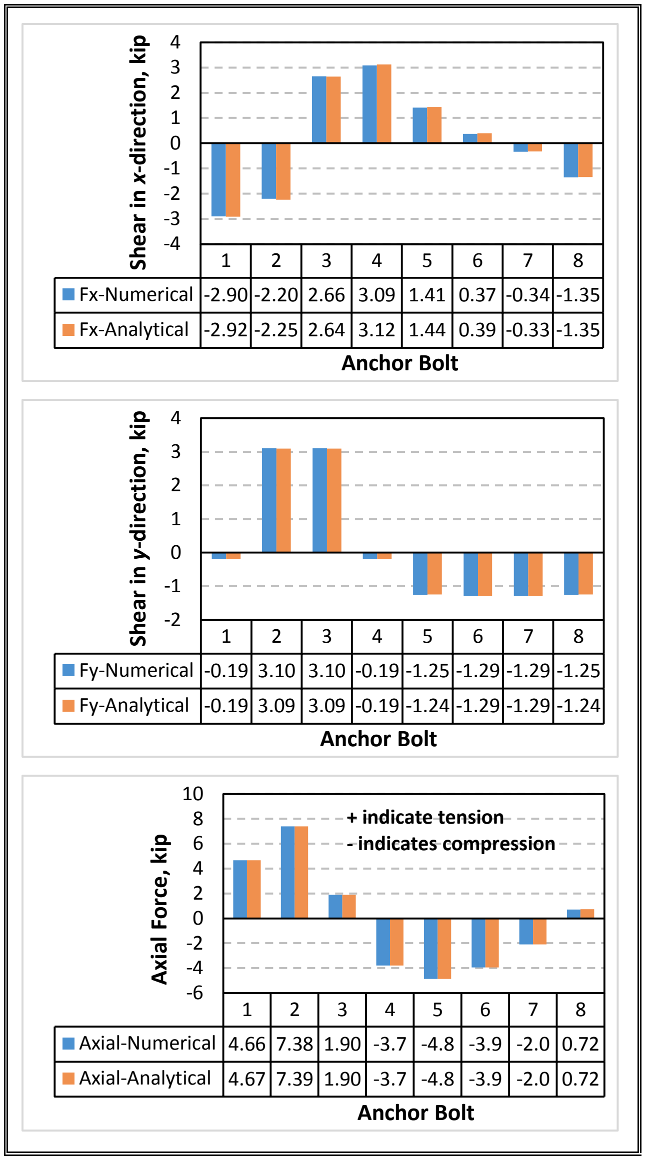

Inclination angle — α = 4°

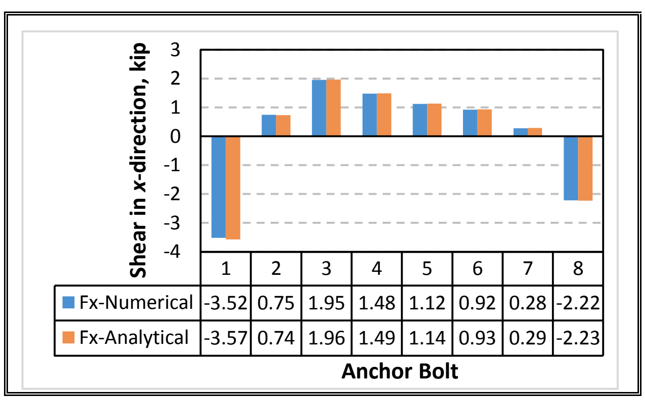

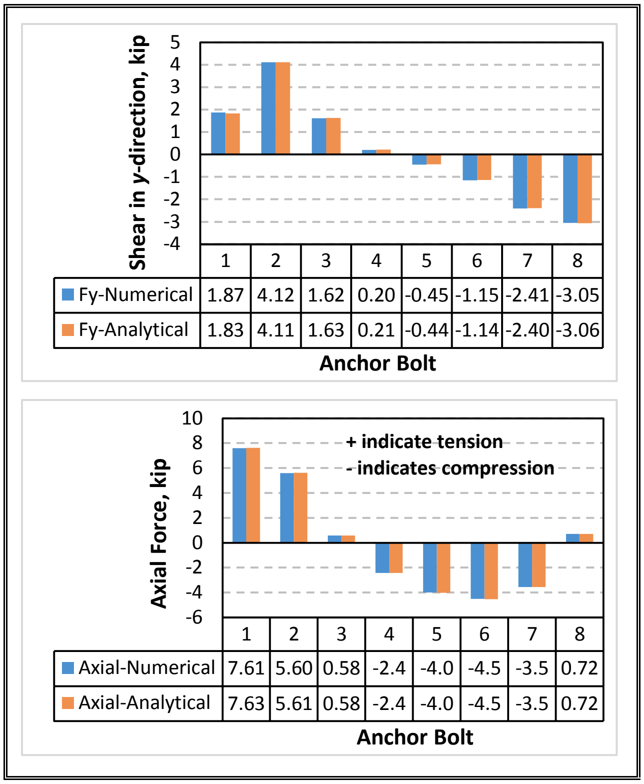

Inclination angle — α = 5˚

Figure 5.3 Comparison between analytical and numerical forces for anchor bolts with non-uniform stand-off distance

5.2 Induced Stresses from the Analytical and Numerical Analysis

The analysis discussed in the previous sections has confirmed the eligibility of the developed analytical equations, to obtain the straining actions on the anchor bolts with uniform and non-uniform stand-off distances. The determination of stresses was the step that followed by the calculation of straining actions. The analytical and numerical forces expressed in section [5.1] were transformed into normal stresses and compared, to confirm the accuracy of the developed analytical equations. In order to determine the maximum normal stress for each anchor: (1) combine the bending stresses due to shear forces in *x* and *y* directions, regardless of the sign; (2) add the absolutes of the summation of bending stresses and axial stress to obtain the maximum normal stress; and (3) the determination of whether the anchor has a compression or tension stress, can be configured from the sign of the axial force.

5.2.1 Stresses on Anchors having a Uniform Stand-off Distance

The discussion herein this section was adopted to confirm the approach used to determine the normal stresses. A comparison between the numerical and analytical normal stresses was dedicated to validate the analytical approach. The comparison indicated in Figure 5.4 concerns the case of anchor bolts with uniform stand-off distances. The figure is dissected into four bar charts, each of which has a uniform stand-off distance. It can be indicated that the stresses are increasing with the increase of the stand-off distance. The figure also shows that the numerical and analytical normal stresses are compatible. This means that the analytical approach is applicable to determine the normal stresses on the anchor bolts with uniform stand-off distances.

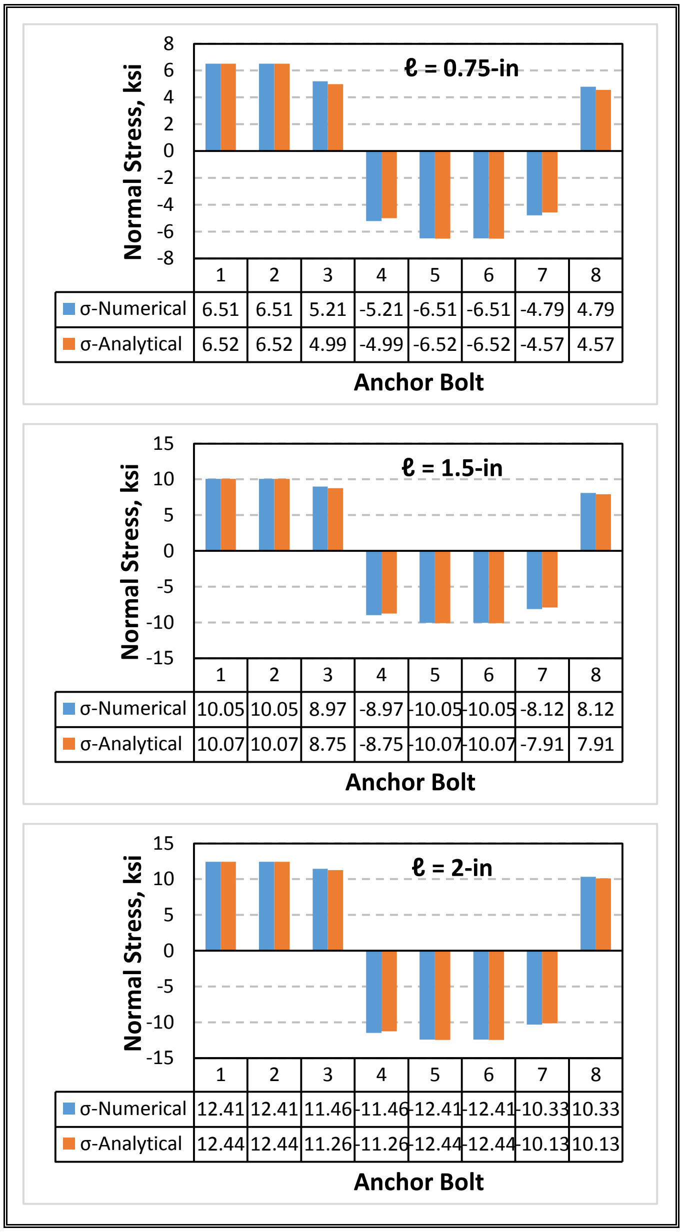

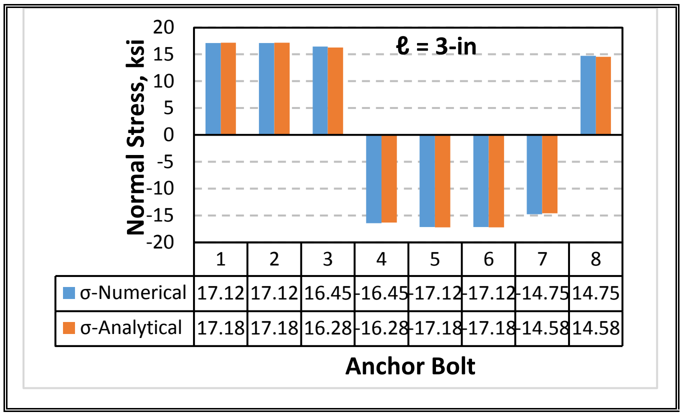

Figure 5.4 Comparison between numerical and analytical normal stresses for anchor bolts with a uniform stand-off distance

5.2.2 Stresses on Anchors having Non-uniform Stand-off Distances

The investigation was extended to analyze the normal stresses for the case of anchors with non-uniform stand-off distances. **Error! Reference source not found.** exhibits a comparison between the normal stresses induced from the analytical approach and the numerical analysis, for different inclination angles. The table shows that the normal stresses, for the anchor group having α = 5˚, were lower than those in the other two angles. The reason is that the diameter of the anchor group with angle equal to 5˚ is 2-in, whereas the diameter is 1.5-in for the other two angles. In case of angle 2˚, the highest percentage of difference was observed in anchor #3 with a magnitude of 4.3%. Similarly, the highest percentage of difference was recorded in the same anchor with 4.61%, in the case of α = 4˚. Anchor #2 was observed to have the highest percentage of difference of 5.12%, for α = 5˚. As also noticed in the table, the highest percentages of differences were not observed for the anchors having the highest stresses. The recorded percentages of difference for those anchors were ranged between 0.36% and 0.69%.

Table 5.1 Numerical and analytical stresses for anchors with non-uniform stand-off distances

Anchor #	$\alpha = 2^\circ$			$\alpha = 4^\circ$			$\alpha = 5^\circ$		
	*$(\sigma_N)_{AN}$	**$(\sigma_N)_{NU}$	%	$(\sigma_N)_{AN}$	$(\sigma_N)_{NU}$	%	$(\sigma_N)_{AN}$	$(\sigma_N)_{NU}$	%
1	8.60	8.56	0.44	9.98	10.19	2.12	5.69	5.69	0.05
2	10.05	10.01	0.36	12.24	12.18	0.49	5.52	5.8	5.12
3	8.03	8.37	4.30	9.73	10.18	4.61	5.51	5.64	2.27
4	-7.99	-8.21	2.82	-9.96	-9.9	0.59	-4.67	-4.69	0.40
5	-10.42	-10.37	0.43	-12.35	-12.26	0.69	-5.34	-5.33	0.20
6	-9.12	-9.08	0.42	-9.69	-9.62	0.71	-6.07	-6.06	0.11
7	-7.56	-7.75	2.56	-8.37	-8.58	2.49	-4.95	-4.95	0.03
8	7.88	8.07	2.45	9.67	9.87	2.10	4.53	4.76	5.11

*$(\sigma_N)_{AN}$: analytical shear force in *x*-direction
**$(\sigma_N)_{NU}$: numerical shear force in *x*-direction

The recap of the above discussed sections is that the developed analytical procedure, adopted to calculate the staining actions and stresses is valid to design the anchor bolts with uniform and non-uniform stand-off distances.

5.3 Design Example

This section is dedicated to detail the design steps using the developed analytical equations for anchor bolts having non-uniform stand-off distances. The joint adopted in this example is very similar to the joint investigated by Hosch (2013). The joint represents a case within the design of experiment discussed in Chapter 4. The angle used in this design example is equal to 5˚.

Two design approaches will be displayed. The first approach would be using the developed analytical equations to calculate the stresses. The second one is to calculate the stresses using the equations specified by *2013 Supports Specifications*. The results accompanying the two approaches will be compared to evaluate the standpoint of using *2013 Supports Specifications* equations in the design of anchor bolts with non-uniform stand-off distances. The design details are expressed in *Appendix F*.

Figure 5.5 shows a comparison between the normal stresses calculated using the two design approaches: developed analytical equations and *2013 Supports Specifications*. It can be noticed that there is a severe difference between the stresses calculated using the analytical approach and their correspondence designed by *2013 Supports Specifications*. The highest recorded normal stress using the developed analytical equations was equal to 6.07 ksi, whereas a stress of 8.9 ksi was recorded using *2013 Supports Specifications* equations. This means that the percentage of increase in stresses using *2013 Supports Specifications* equations has reached 46.6%, with respect to the analytical equations.

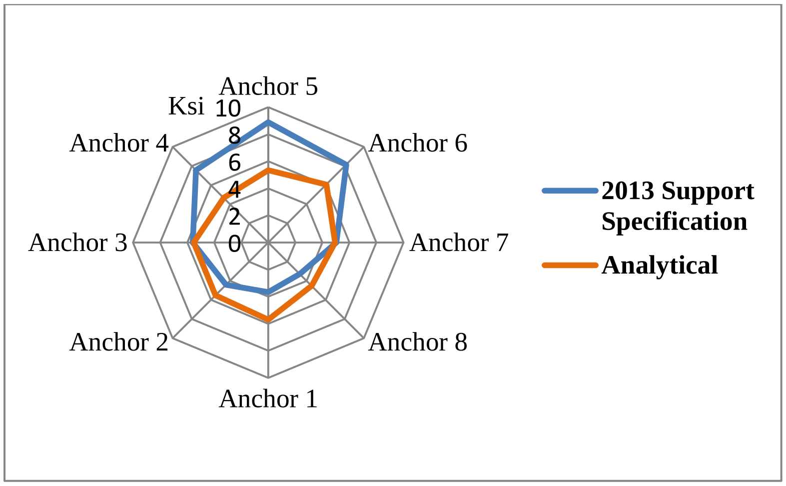

Figure 5.5 Comparison between uniform and non-uniform normal stresses

Figure 5.6 shows a comparison between the shear stresses determined using the developed analytical equations and *2013 Supports Specifications*. It can be noticed that there is a uniform distribution of shear stresses calculated using *2013 Supports Specifications.* The reason is that the equations used to determine the straining actions do not rely on the stand-off distance. On the other hand, the shear stresses calculated using the analytical equations have irregular distribution because of the inclusion of the stand-off distance term in the design equations. The figure also indicates that the highest shear stress determined using the analytical equations was equal to 1.63 ksi, whereas a shear of 1.07 ksi was calculated using *2013 Supports Specifications*.

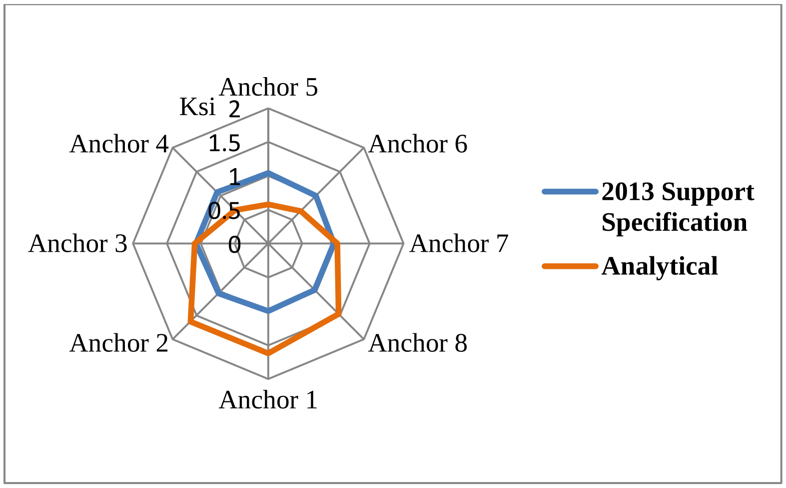

Figure 5.6 Comparison between uniform and non-uniform shear stresses

It can be concluded from the above results and discussions that using *2013 Supports Specifications* equations for the design of anchor bolts with non-uniform stand-off distances is not accurate and uneconomic.

6 DISCUSSIONS AND RECOMMENDATIONS

The main objective of this project is to investigate the effect of non-uniform stand-off distances on the stress distribution of the anchor bolts within the double-nut moment joint connection. Three specific objectives are specified. Specific objective #1 is: perform analytical study to identify the mechanical relationships that govern the behavior of the connection with respect to non-uniform stand-off distances. The analytical study was based on idea of how the lateral loads are distributed on shear walls as a result of wind and seismic loads. It was found that the key factor that determines how the loads are distributed on the anchors with uniform or non-uniform stand-off distances is the stiffness. The distribution of lateral loads on the anchor bolts is governed by the lateral stiffness that deduced from the bending and shear deflections. On the other hand, the distribution of axial forces is governed by the axial stiffness that deduced from the axial deflection. It was found that the lateral loads on anchors induce: direct shear forces, torsion due to direct shear forces (in case of anchors with non-uniform stand-off distances), and torsion due to wind loading. The axial loads on anchors are come from: the own weight of the structure and the group of moments induced from: direct shear forces, total own weight of the structure (in case of anchors with non-uniform stand-off distances), and wind loads.

The second specific objective is: perform numerical study using finite element analysis (FEA) to validate the developed mechanical relationships. A numerical analysis using the SAP2000 finite element analysis software package was used for modeling. The design of experiment is consisted of four cases varied in the angle of the concrete surface: 0˚, 2˚, 4˚, and 5˚. The case of angle 0˚ represents the anchor bolts with a uniform stand-off distance. Angles: 2˚, 4˚, and 5˚, represent the case of anchor bolts with non-uniform stand-off distances. The element types used to model the joint were frame elements for anchors and shell elements for the base plate. The boundary conditions for the anchor bolts were considered to be completely fixed at the bottom (anchors/concrete surface), and full body constraint at the top (anchors/the base plate). It was found that the stresses calculated using the developed analytical equations are compatible with their correspondence induced from the numerical model. This means that the analytical equations are valid to be used to calculate the stresses on anchor bolts with uniform or non-uniform stand-off distances. The third specific objective is: propose design methodology applicable for evaluating the stresses on the anchor bolts with uniform and non-uniform stand-off distances. The design methodology can be concluded in determining the straining actions due to lateral loads and axial loads on anchors, then transform those forces into stresses. The stresses should be compared to the limitations specified by *2013 Supports Specifications*.

7 CONCLUSIONS AND FUTURE RESEARCH

The results and discussions implemented in this report have revealed the following design equations, the used to determine the loads on the anchors with uniform and non-uniform stand-off distances.

- Stiffness of anchor bolts:

$$K_l = \left(\frac{h^3}{12EI} + \frac{10h}{9GA}\right)^{-1} \quad \textbf{(3-6)}$$

$$K_a = \frac{EA}{h} \quad \textbf{(3-8)}$$

where:

K_l	=	stiffness of anchors with stand-off distances due to lateral loading
K_a	=	stiffness of anchors with stand-off distances due to axial loading
P	=	lateral load
h	=	stand-off distance
E	=	modulus of elasticity of the anchor
G	=	modulus of rigidity of the anchor
I	=	anchor second moment of inertia
A	=	anchor cross sectional area

Center of rigidity:

$$\bar{X}_l = \frac{\sum_{i=1}^{n} K_{li}\, x_i}{\sum_{i=1}^{n} K_{li}} \quad \textbf{(3-13)}$$

$$\bar{Y}_l = \frac{\sum_{i=1}^{n} K_{li}\, y_i}{\sum_{i=1}^{n} K_{li}} \quad \textbf{(3-14)}$$

$$\bar{X}_a = \frac{\sum_{i=1}^{n} K_{ai}\, x_i}{\sum_{i=1}^{n} K_{ai}} \quad \textbf{(3-15)}$$

$$\bar{Y}_a = \frac{\sum_{i=1}^{n} K_{ai}\, y_i}{\sum_{i=1}^{n} K_{ai}} \quad \textbf{(3-16)}$$

where:

$\bar{X}_l$	=	*x*-coordinate of the center of rigidity due to lateral loading
$\bar{X}_a$	=	*x*-coordinate of the center of rigidity due to axial loading
$\bar{Y}_l$	=	*y*-coordinate of the center of rigidity due to lateral loading
$\bar{Y}_a$	=	*y*-coordinate of the center of rigidity due to axial loading

K_{li} = stiffness of anchor *i* due to lateral loading
K_{ai} = stiffness of anchor *i* due to axial loading
x_i = *x*-coordinate of anchor *i*
y_i = *y*-coordinate of anchor *i*
n = number of anchor bolts

- Shear forces due to direct shear loading:

$$F_{1xi} = V_x \frac{K_{li}}{\sum_{i=1}^{n} K_{li}} \quad \textbf{(3-24)}$$

$$F_{1yi} = V_y \frac{K_{li}}{\sum_{i=1}^{n} K_{li}} \quad \textbf{(3-25)}$$

where:

F_{1xi} = shear force on anchor *i* in *x*-direction due to direct shear loading
F_{1yi} = shear force on anchor *i* in *y*-direction due to direct shear loading
V_x = direct shear loading in *x*-direction
V_y = direct shear loading in *y*-direction
K_{li} = stiffness of anchor *i* due to lateral loading

- Torsion due to direct shear forces:

$$T' = \pm V_x \bar{X}_l \pm V_y \bar{Y}_l \quad \textbf{(3-27)}$$

where:

T' = shear force on anchor *i* in *x*-direction due to direct shear loading
V_x = direct shear loading in *x*-direction
V_y = direct shear loading in *y*-direction
$\bar{X}_l$ = *x*-coordinate of the center of rigidity due to lateral loading
$\bar{Y}_l$ = *y*-coordinate of the center of rigidity due to lateral loading

- Shear forces due to torsion:

$$F_{2xi} = T \frac{K_{li}\, y_i}{\sum_{i=1}^{n} K_{li}\,(x_i^2 + y_i^2)} \quad \textbf{(3-42)}$$

$$F_{2yi} = T \frac{K_{li}\, x_i}{\sum_{i=1}^{n} K_{li}\,(x_i^2 + y_i^2)} \quad \textbf{(3-43)}$$

where:

F_{2xi} = shear force on anchor *i* in *x*-direction due to torsion

F_{2yi} = shear force on anchor *i* in *y*-direction due to torsion
T = torsional moment pure torsion and direct shear loading
K_{li} = stiffness of anchor *i* due to lateral loading
x_i = distance between anchor *i* and the c.r. due to bending and shear in *x*-direction
y_i = distance between anchor *i* and the c.r. due to bending and shear in *y*-direction

- Moment group due to direct shear loading:

$$\left(M_{Group}\right)_{1x} = \sum_{i=1}^{n} F_{lyi}\,\frac{h_i}{2} \tag{3-52}$$

$$\left(M_{Group}\right)_{1y} = \sum_{i=1}^{n} F_{lxi}\,\frac{h_i}{2} \tag{3-53}$$

where:

$(M_{Group})_{1x}$ = group moment about *x*-axis due to direct shear loading in *y*-direction
$(M_{Group})_{1y}$ = group moment about *y*-axis due to direct shear loading in *x*-direction
F_{lxi} = total lateral force on anchor *i* in *x*-direction due to direct shear loading and torsion
F_{lyi} = total lateral force on anchor *i* in *y*-direction due to direct shear loading and torsion
h_i = stand-off distance of anchor *i*

- Axial forces due to the structure own weight:

$$N_{1i} = N_{o.w}\,\frac{K_{ai}}{\sum_{i=1}^{n} K_{ai}} \tag{3-55}$$

where:

N_{1i} = axial force on anchor *i* due to the total own weigh of the structure
$N_{o.w}$ = total own weight of the structure
K_{ai} = axial stiffness of anchor *i*

- Moment group due to the structure own weight (for the case of anchors with non-uniform stand-off distances):

$$\left(M_{Group}\right)_{2x} = \pm\, N_{o.w} \cdot \bar{Y} \pm \left(M_{Arms+attachments}\right)_x \tag{3-58}$$

$$\left(M_{Group}\right)_{2y} = \pm\, N_{o.w} \cdot \bar{X} \pm \left(M_{Arms+attachments}\right)_y \tag{3-59}$$

where:

$(M_{Group})_{2x}$	=	group moment about x-axis due to the total own weight of the structure
$(M_{Group})_{2y}$	=	group moment about y-axis due to the total own weight of the structure
$(M_{Arms+Attachments})_x$		group moment about x-axis due to arms and attachments, if applicable
$(M_{Arms+Attachments})_y$		group moment about y-axis due to arms and attachments, if applicable
$N_{o.w}$	=	total own weight of the structure
$\bar{X}_\imath$	=	x-coordinate of the center of rigidity due to axial loading
$\bar{Y}_\imath$	=	y-coordinate of the center of rigidity due to axial loading

- Axial forces due to moment groups:

$$N_{2i} = \left(M_{Group}\right)_{tx} \frac{K_{ai}\ y_i}{\sum_{i=1}^{n} K_{ai}\ y_i^2} \tag{3-83}$$

$$N_{3i} = \left(M_{Group}\right)_{ty} \frac{K_{ai}\ x_i}{\sum_{i=1}^{n} K_{ai}\ x_i^2} \tag{3-84}$$

where:

N_{2i}	=	total axial force on anchor i due to group bending moments about x-axis
N_{3i}	=	total axial force on anchor i due to group bending moments about y-axis
$(M_{Group})_{tx}$	=	total group moment about x-axis due to wind loading in y-direction, direct shear forces, and total own weight
$(M_{Group})_{ty}$	=	total group moment about y-axis due to wind loading in x-direction, direct shear forces, and total own weight
x_i	=	distance between anchor i and the c.g. of anchor group in x-direction
y_i	=	distance between anchor i and the c.g. of anchor group in y-direction

- Normal stresses:

$$\sigma_{Ni} = \pm \frac{N_{ti}}{A} \pm \frac{M_{xi} \cdot r}{I} \pm \frac{M_{yi} \cdot r}{I} \tag{3-78}$$

$$M_{xi} = \frac{F_{tyi} \cdot h}{2} \tag{3-79}$$

$$M_{iy} = \frac{F_{txi} \cdot h}{2} \tag{3-80}$$

where:

σ_{Ni} = total normal stress on anchor *i*
N_{ti} = total axial force on anchor *i*
M_{xi} = total moment on anchor *i* about *x*-axis due to total shear forces
M_{yi} = total moment on anchor *i* about *y*-axis due to total shear forces
F_{txi} = total shear forces on anchor *i* in *x*-direction
F_{tyi} = total shear forces on anchor *i* in *y*-direction
h = stand-off distance of anchor *i*
A = cross sectional area of the anchor bolt
r = radius of the anchor bolt
I = second moment of inertia of the anchor bolt

- Shear stresses:

$$\tau_i = \frac{16}{3\pi d^2} F_{Ri} \qquad \textbf{(3-81)}$$

$$F_{Ri} = \sqrt{(F_{txi})^2 + \left(F_{tyi}\right)^2} \qquad \textbf{(3-82)}$$

where:

τ_i = total shear stress on anchor *i*
F_{Ri} = resultant shear force on anchor *i*
F_{txi} = total shear forces on anchor *i* in *x*-direction
F_{tyi} = total shear forces on anchor *i* in *y*-direction
d = diameter of the anchor bolt

REFERENCES

Amany, A., and Pasini, D. (2009). "Material and shape selection for stiff beams under non-uniform flexure." *Materials and Design* 30 (4), 1110-1117.

American Association of State Highway and Transportation Officials (AASHTO), (2013). "Standard specifications for structural supports for highway signs, luminaires and traffic signals." 6th Ed., AASHTO, Washington, D.C.

American Concrete Institute (ACI), (2011). "Building code requirements for structural concrete and commentary." ACI 318-11, Farmington Hills, MI.

ANSYS, Inc. Release 12.1, Nov. 2009. "Element reference." Accessed Accessed May 21, 2015. http://orange.engr.ucdavis.edu/Documentation12.1/121/ans_elem.pdf.

Blodgett, Omer W. (1966). *Design of welded structures.*, *James F. Lincoln Arc Welding Foundation*.

Cook, Ronald A., and Bobo, Brandon J., (2001), "Design guidelines for annular base plates." FDOT Report BC354-04, Florida Department of Transportation, Tallahassee, FL.

Cook, Ronald A., Tia, Mang, Fischer, Kevin B., and Darku, Daniel D., (2000), "Use of grout pads for sign and lighting structures." Report No. BB-512, Engineering and Industrial Experiment Station, University of Florida, Gainesville, Florida.

Dexter, R. J., and Ricker, M. J., (2002), "Fatigue-resistant design of cantilevered signal, sign, and light supports." NCHRP Report 469, Transportation Research Board, National Research Council, Washington, D.C.

Eligehausen, Rolf, Mallée, Rainer, and Silva, John F. (2006). *Anchorage in concrete construction*: John Wiley & Sons.

Fisher, James M., and Kloiber, Lawrence A., (2006), "AISC Steel Design Guide 1: Base plate and anchor rod design." Second Edition, American Institute of Steel Construction, Chicago, IL.

Fouad, H. F., Sullivan, A., Calvert, E. A., and Hosch, I. E., (2009), "Design of overhead sign structures for fatigue loads." Project Number 930-680, Alabama Department of Transportation (ALDOT).

Garlich, Michael J, and Koonce, Jeremy W. (2011). "Anchor rod tightening for highmast light towers and cantilever sign structures." Transportation Research Board 90th Annual Meeting, Washington, D.C., January 23-27.

Garlich, Michael J., and Thorkildsen, Eric T., (2005), "Guidelines for the installation, inspection, maintenance and repair of structural supports for highway signs, luminaires, and traffic signals." FHWA Report NHI 05-036, Federal Highway Administration, Washington, D.C.

Hoisington, David, Hoffman, Jeff, and Hamel, Scott. (2014). "Measured anchor rod tightening of high-mast light poles in Alaska." *Transportation Research Record: Journal of the Transportation Research Board* 2431 (1), 67-72.

Hosch, I. (2013). "Experimental Validation of the AASHTO Natural Wind Fatigue Design Specifications for Cantilevered Sign Support Structure Anchor Bolts." *Practice Periodical on Structural Design and Construction* 04014020.

James, R. W., Keating, P. B., Bolton, R. W., Benson, F. C., Bray, D. E., Abraham, R. C., and Hodge, J. B., (1996), "Tightening procedure for large-diameter anchor bolts." FHWA/TX-98/1472-1F, Texas Department of Transportation, Austin, Texas.

Kaczinski, M. R., Dexter, R. J., and Dien, J. P. Van, (1998), "Fatigue-resistant design of cantileverd signal, sign and light supports." NCHRP Report 412, Transportation Research Board, National Research Council, Washington, D.C.

Lin, Zhibin, Petersen, Derek, Zhao, Jian, and Tian, Ying. (2011). "Simulation and design of exposed anchor bolts in shear." *International Journal of Theoretical and Applied Multiscale Mechanics* 2 (2), 111-129.

Liu, C. (2014). "Evaluation of anchor bolts with excessive standoff in cantilever sign and signal structures." *Practice Periodical on Structural Design and Construction* 19 (2), 04014002.

McBride, Kenton E., Cook, Ronald A., Prevatt, David O., and Potter, William. (2014). "Anchor Bolt Steel Strength in Annular Stand-Off Base Plate Connections." *Transportation Research Record: Journal of the Transportation Research Board* 2406 (1), 23-31.

McCormac, By Jack C., and Csernak, Stephen F. (2012). *Structural steel design*. Fifth Edition ed: Prentice Hall.

Pope, J. Edward. (1997). *Rules of thumb for mechanical engineers., a manual of quick, accurate solutions to everyday mechanical engineering problems. Houston: Gulf Pub. Co.*

Richards, K.L. (2012). *Design Engineer's Handbook*: CRC Press.

Scheer, J., Peil, U., and Nölle, P., (1987), "Schrauben mit planmäßiger Biegebeanspruchung (Screws under planned bending)." Report No. 6079, Institut für Stahlbau, Technischen Universität Braunschweig.

Till, R. D., and Lefke, N. A., (1994), "The relationship between torque, tension, and nut rotation of large diameter anchor bolts." MDOT Report R-1330, Michigan Department of Transportation, Lansing.

APPENDICES

Appendix A — Derivation of bending deflection for individual anchor bolt

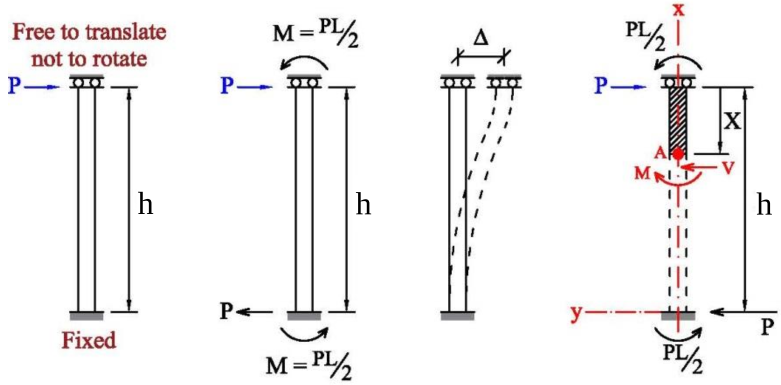

Bending Deflection of the Individual Anchor Bolt

$\sum M@A = 0$

$$M + \frac{Px}{2} - \frac{Ph}{2} = 0$$

$$M = \frac{Ph}{2} - Px$$

Elastic curve differential equation:

$$\frac{d^2y}{dx^2} = \frac{M}{EI} = \frac{Ph}{2EI} - \frac{Px}{EI}$$

Integrating: $\frac{dy}{dx} = \frac{Ph}{2EI}x - \frac{Px^2}{2EI} + C_1$ (1)

Integrating: $y = \frac{Ph}{4EI}x^2 - \frac{Px^3}{6EI} + C_1x + C_2$ (2)

Boundary conditions:

Slop $\left(\frac{dy}{dx}\right) = 0 \rightarrow x = 0$ (3)

Deflection $(y) = 0 \rightarrow x = h$ (4)

By substituting (3) in (1) $\rightarrow$ $C_1 = 0$

By substituting (4) in (3) $\rightarrow$ $0 = \frac{Ph}{4EI}h^2 - \frac{Ph^3}{6EI} + 0 + C_2$

$$C_2 = -\frac{Ph^3}{12EI}$$

$$y = \frac{Ph}{4EI}x^2 - \frac{Px^3}{6EI} - \frac{Ph^3}{12EI}$$

For $x = 0$ (Point of max deflection) $\rightarrow y = -\frac{Ph^3}{12EI} = \frac{Ph^3}{12EI} \rightarrow$

$$\Delta_b = \frac{Ph^3}{12EI}$$

Appendix B — Derivation of shear deflection for individual anchor bolt

$$\tau = \frac{P}{A} \tag{1}$$

where:
τ = shear stress
P = shear force
A = cross section area

$$G = \frac{\tau}{\gamma_s} \tag{2}$$

where:
G = modulus of rigidity
γ_s = shear strain

By substituting (1) in (2) → $G = \dfrac{P}{A\gamma_s}$

$$\gamma_s = \frac{P}{GA}$$

$$\gamma_s = \frac{\delta_s}{L} = \frac{P}{GA}$$ where: δ_s is the shear deflection

$$\delta_s = \frac{Ph}{GA} \tag{3}$$

By multiplying equation (3) by a factor k

$$\delta_s = k\frac{Ph}{GA}$$ where: k is the correction factor

Appendix C — Derivation of axial deflection for individual anchor bolt

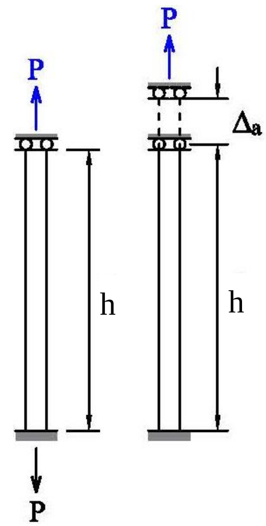

Axial Deflection of the Individual Anchor Bolt

$$\sigma_A = \frac{P}{A} \tag{1}$$

where:
σ_A = axial stress
P = axial force
A = cross section area

$$E = \frac{\sigma_A}{\varepsilon} \tag{2}$$

where:
σ_A = modulus of elasticity
ε = axial strain

By substituting (1) in (2) → $E = \frac{P}{A\varepsilon}$

$$\varepsilon = \frac{P}{EA}$$

$$\varepsilon = \frac{\Delta_a}{L} = \frac{P}{EA}$$

$$\Delta_a = \frac{PL}{EA}$$

Appendix D — Derivation of shear stresses on anchor bolts

$$\tau_i = \frac{F_{Ri} \cdot Q}{I \cdot t}$$

$$Q = A' \cdot y'$$

$$A' = \frac{A}{2} = \frac{\pi d^2}{8}$$

$$y' = \frac{4r}{3\pi} = \frac{2d}{3\pi}$$

$$Q = \frac{\pi d^2}{8} \cdot \frac{2d}{3\pi} = \frac{d^3}{12}$$

$$I = \frac{\pi d^4}{64}$$

$$t = d$$

$$\frac{Q}{I \cdot t} = \frac{d^3}{12} \cdot \frac{64}{\pi d^4} \cdot \frac{1}{d} = \frac{16}{3\pi d^2}$$

$$\tau_i = \frac{16}{3\pi d^2} F_{Ri}$$

Appendix E — Numerical model verification

1. Equations that used to calculate the normal stresses on the anchor bolts

Notation:

F_R = resultant force due to torsion on each anchor
T = torsional moment
r = radius of the anchor bolt group
J = polar moment of inertia of anchor bolt group
n = number of anchor bolts
F_{Rxi} = resultant force due to torsion on anchor *i* in *x*-direction
F_{Ryi} = resultant force due to torsion on anchor *i* in *y*-direction
θi = angle between horizontal and resultant forces due to torsion for anchor *i*
V_{xi} = force due to direct shear on anchor *i* in *x*-direction
V_{yi} = force due to direct shear on anchor *i* in *y*-direction
V_{tx} = total direct shear on anchor *i* in *x*-direction
V_{ty} = total direct shear on anchor *i* in *x*-direction
F_{xi} = total force on anchor *i* in *x*-direction
F_{yi} = total force on anchor *i* in *y*-direction
σ_{1xi} = bending stress on anchor *i* about *x*-direction
σ_{1yi} = bending stress on anchor *i* about *y*-direction
ℓ = stand-off distance
S = elastic section modulus
Σ_{Mi} = total bending stress on anchor *i*
$(M_{Group})_x$ = total group bending moment about *x*-axis
$(M_{Group})_y$ = total group bending moment about *y*-axis
σ_{2xi} = axial stress on anchor *i* due to moment about *x*-direction
σ_{2yi} = axial stress on anchor *i* due to moment about *y*-direction
x_i = distance between anchor *i* and the c.g of the anchor group *i* in *x*-direction
y_i = distance between anchor *i* and the c.g of the anchor group *i* in *y*-direction
A = cross section area
σ_{Ai} = total axial stress on anchor *i*
σ_{Ni} = normal stress on anchor *i*

Stresses due to torsion and direct shear

$$F_R = \frac{T\,r}{J}$$

$$J = n \cdot r^2$$

$$F_R = \frac{T}{n \cdot r}$$

$$F_{Rxi} = F_R cos\theta_i$$

$$F_{Ryi} = F_R sin\theta_i$$

$$V_{xi} = \frac{V_{tx}}{n}$$

$$V_{yi} = \frac{V_{ty}}{n}$$

$$F_{xi} = V_{xi} + F_{Rxi}$$

$$F_{yi} = V_{yi} + F_{Ryi}$$

$$\sigma_{1xi} = \frac{F_{yi} \cdot \ell/2}{S}$$

$$\sigma_{1yi} = \frac{F_{yi} \cdot \ell/2}{S}$$

$$\sigma_{bi} = \sigma_{1xi} + \sigma_{1yi}$$

Stresses due to moment group

$$\sigma_{2xi} = \frac{\left(M_{Group}\right)_x \cdot y_i}{I_y}$$

$$\sigma_{2yi} = \frac{\left(M_{Group}\right)_y \cdot x_i}{I_x}$$

$$I_x = \sum_{1}^{n} A_i \cdot y_i^2$$

$$I_y = \sum_{1}^{n} A_i \cdot x_i^2$$

$$\sigma_{Ai} = \sigma_{2xi} + \sigma_{2yi}$$

Total stresses

$$\sigma_{Ni} = \sigma_{bi} + \sigma_{Ai}$$

2. Properties

E = 29000 ksi	d = 1.5 in	A = 1.7671 in^2
		I = 0.2485 in^4
n = 8	r = 15 in	S = 0.3313 in^3

3. Stresses due to torsion and direct shear

T = 288 kip-in

V_{tx} = 0.75 kip

V_{ty} = 0.75 kip

$(M_{Group})_x$ = 240.75 kip-in

$(M_{Group})_y$ = 240.75 kip-in

Anchor #	*x*-in	*y*-in	*θ	cos θ	sin θ	F_{Rx}		F_{Ry}	
1	5.74	13.86	22.5	0.92	0.38	-2.22	←	0.92	↑
2	13.86	5.74	67.5	0.38	0.92	-0.92	←	2.22	↑
3	13.86	5.74	67.5	0.38	0.92	0.92	→	2.22	↑
4	5.74	13.86	22.5	0.92	0.38	2.22	→	0.92	↑
5	5.74	13.86	22.5	0.92	0.38	2.22	→	-0.92	↓
6	13.86	5.74	67.5	0.38	0.92	0.92	→	-2.22	↓
7	13.86	5.74	67.5	0.38	0.92	-0.92	←	-2.22	↓
8	5.74	13.86	22.5	0.92	0.38	-2.22	←	-0.92	↓

*$\theta = \tan^{-1}(x/y)$

Anchor #	F_{Rx}		F_{Ry}		V_x		V_y		F_x		F_y	
1	-2.22	←	0.92	↑	0.09	→	0.09	↑	-2.12	←	1.01	↑
2	-0.92	←	2.22	↑	0.09	→	0.09	↑	-0.82	←	2.31	↑
3	0.92	→	2.22	↑	0.09	→	0.09	↑	1.01	→	2.31	↑
4	2.22	→	0.92	↑	0.09	→	0.09	↑	2.31	→	1.01	↑
5	2.22	→	-0.92	↓	0.09	→	0.09	↑	2.31	→	-0.82	↓
6	0.92	→	-2.22	↓	0.09	→	0.09	↑	1.01	→	-2.12	↓
7	-0.92	←	-2.22	↓	0.09	→	0.09	↑	-0.82	←	-2.12	↓
8	-2.22	←	-0.92	↓	0.09	→	0.09	↑	-2.12	←	-0.82	↓

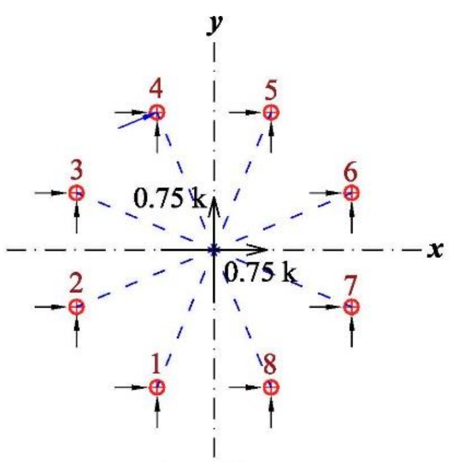

Direct Shear

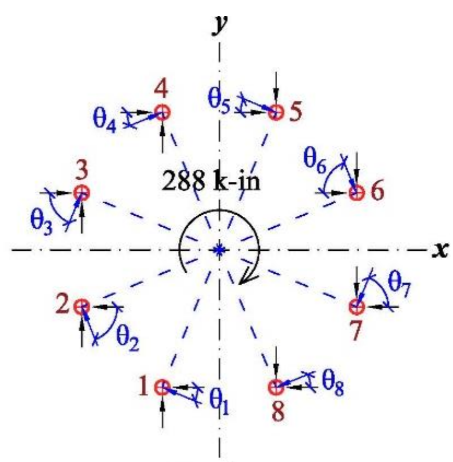

Torsion

Anchor #	ℓ-in	σ_{1x}	σ_{1y}	σ_b
1	1	1.53	3.20	4.73
2	1	3.49	1.24	4.73
3	1	3.49	1.53	5.01
4	1	1.53	3.49	5.01
5	1	1.24	3.49	4.73
6	1	3.20	1.53	4.73
7	1	3.20	1.24	4.45
8	1	1.24	3.20	4.45

In order to determine the max bending stresses, the stresses in x and y directions should be added together regardless of the sign.

4. Stresses due to moment group

Anchor #	x	y	x^2	y^2	$A\,x^2$	$A\,y^2$	σ_{2x}	σ_{2y}	σ_A
1	5.74	13.86	32.95	192.05	58.23	339.38	2.10	0.87	2.97
2	13.86	5.74	192.05	32.95	339.38	58.23	0.87	2.10	2.97
3	13.86	5.74	192.05	32.95	339.38	58.23	-0.87	2.10	1.23
4	5.74	13.86	32.95	192.05	58.23	339.38	-2.10	0.87	-1.23
5	5.74	13.86	32.95	192.05	58.23	339.38	-2.10	-0.87	-2.97
6	13.86	5.74	192.05	32.95	339.38	58.23	-0.87	-2.10	-2.97
7	13.86	5.74	192.05	32.95	339.38	58.23	0.87	-2.10	-1.23
8	5.74	13.86	32.95	192.05	58.23	339.38	2.10	-0.87	1.23
				$\Sigma =$	1590.44	1590.44			

5. Total stresses

Anchor #	σ_b	σ_A		σ_N	
1	4.73	2.97	T	7.70	T
2	4.73	2.97	T	7.70	T
3	5.01	1.23	T	6.24	T
4	5.01	1.23	C	6.24	C
5	4.73	2.97	C	7.70	C
6	4.73	2.97	C	7.70	C
7	4.45	1.23	C	5.68	C
8	4.45	1.23	T	5.68	T

Appendix F — Design example

Design with the Developed Analytical Equations

1. Properties

f_y = 55 ksi

E = 29000 ksi

μ [Poisson's ratio] = 0.3

G = 11153.85 ksi

d = 2 in

A = 3.1416 in^2

I = 0.7854 in^4

S = 0.7854 in^3

2. Loads

V_x = 0.75 kip $\rightarrow$

V_y = 0.75 kip $\uparrow$

$T[Pure\ torsion] = 288\ kip - in$ ↷

$(M_x)_{Group}$ = 240.75 kip-in ↞

$(M_y)_{Group}$ = 240.75 kip-in ↟

3. Layout of Anchor Bolts

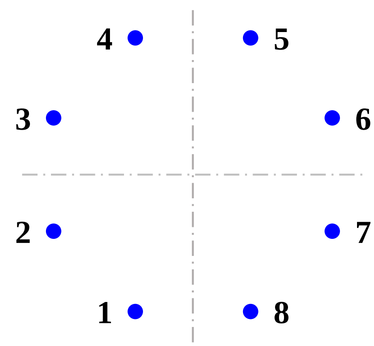

Anchor #	x	y	h-in
1	-5.74	-13.86	1
2	-13.86	-5.74	1.3844
3	-13.86	5.74	2.3123
4	-5.74	13.86	3.2403
5	5.74	13.86	3.6247
6	13.86	5.74	3.2403

Anchor #	*x*	*y*	*h*-in
7	13.86	-5.74	2.3123
8	5.74	-13.86	1.3844

4. Center of Rigidity (C.R.)

C.R. — *due to stiffness of bending and shear*

$$K_l = \left(\frac{h^3}{12EI} + \frac{10h}{9GA}\right)^{-1} \quad \textbf{(3-6)}$$

Calculations example of k_{li}

Anchor #1:

$$K_{l1} = \left(\frac{(1)^3}{12x29000x0.7854} + \frac{10x1}{9x3.1416x11153.85}\right)^{-1} = 28274.33\ kip - in$$

Anchor #2:

$$K_{l2} = \left(\frac{(1.3844)^3}{12x29000x0.7854} + \frac{10x1.3844}{9x3.1416x11153.85}\right)^{-1} = 18654.74\ kip - in$$

Summary of calculations

Anchor #	*h*-in	K_{li}
1	1	28274.33
2	1.3844	18654.74
3	2.3123	8434.93
4	3.2403	4400.96
5	3.6247	3458.11
6	3.2403	4400.96
7	2.3123	8434.93
8	5.74	18654.74
	Σ =	94713.72

Determination of C.R.

$$\bar{X}_l = \frac{\sum_{i=1}^{n} K_{li}\, x_i}{\sum_{i=1}^{n} K_{li}} \quad \textbf{(3-13)}$$

$$\bar{Y}_l = \frac{\sum_{i=1}^{n} K_{li}\, y_i}{\sum_{i=1}^{n} K_{li}} \quad \textbf{(3-14)}$$

$$\bar{X}_l = [-5.74x28274.33 + -13.86x18654.74 + -13.86x8434.93 + -5.74x4400.96 + 5.74x3458.11 + 13.86x4400.96 + 13.86x8434.93 + 5.74x18654.74]/94713.72 = -2.7257\ in$$

$$\bar{Y}_l = [-13.86x28274.33 + -5.74x18654.74 + 5.74x8434.93 + 13.86x4400.96 + 13.86x3458.11 + 5.74x4400.96 + -5.74x8434.93 + -13.86x18654.74]/94713.72 = -6.5805 \text{ in}$$

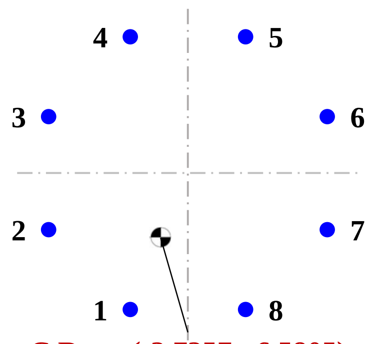

C.R. — *due to stiffness of axial*

$$K_a = \frac{EA}{h} \quad \textbf{(3-8)}$$

<u>Calculations example of k_{ai}</u>

Anchor #1:

$$K_{a1} = \frac{3.1416x29000}{1} = 91106.19 \; kip - in$$

Anchor #2:

$$K_{a2} = \frac{3.1416x29000}{1.3844} = 65809.15 \; kip - in$$

<u>Summary of calculations</u>

Anchor #	*h*-in	K_{ai}
1	1	91106.19
2	1.3844	65809.15
3	2.3123	39400.68
4	3.2403	28116.59
5	3.6247	25134.82
6	3.2403	28116.59
7	2.3123	39400.68
8	5.74	65809.15
	Σ =	382893.84

Determination of C.R.

$$\bar{X}_a = \frac{\sum_{i=1}^{n} K_{ai}\, x_i}{\sum_{i=1}^{n} K_{ai}} \quad \textbf{(3-15)}$$

$$\bar{Y}_a = \frac{\sum_{i=1}^{n} K_{ai}\, y_i}{\sum_{i=1}^{n} K_{ai}} \quad \textbf{(3-16)}$$

$$\bar{X}_a = [-5.74x91106.19 + -13.86x65809.15 + -13.86x39400.68 + -5.74x28116.59 + 5.74x25134.82 + 13.86x28116.59 + 13.86x39400.68 + 5.74x65809.15]/382893.84 = -1.7882\ in$$

$$\bar{Y}_a = [-13.86x91106.19 + -5.74x65809.15 + 5.74x39400.68 + 13.86x28116.59 + 13.86x25134.82 + 5.74x28116.59 + -5.74x39400.68 + -13.86x65809.15]/382893.84 = -4.31702\ in$$

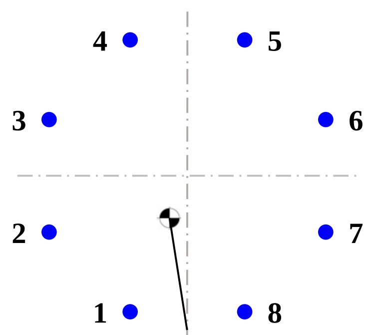

5. Shear Forces on the Anchor Bolts due to Direct Shear Loading

+ve directions

$$\rightarrow F_{1xi} = V_x \frac{K_{li}}{\sum_{i=1}^{n} K_{li}} \quad \textbf{(3-24)}$$

$$\uparrow F_{1yi} = V_y \frac{K_{li}}{\sum_{i=1}^{n} K_{li}} \quad \textbf{(3-25)}$$

given: V_x = 0.75 kip →

given: V_y = 0.75 kip ↑

<u>Calculations example of F_{1xi} and F_{1yi}</u>

Anchor #1:

$$F_{1x1} = 0.75x\frac{28274.33}{94713.72} = 0.22\ kip \rightarrow$$

$$F_{1y1} = 0.75x\frac{28274.33}{94713.72} = 0.22\ kip \uparrow$$

Anchor #2:

$$F_{1x2} = 0.75x\frac{18654.74}{94713.72} = 0.15\ kip \rightarrow$$

$$F_{1y2} = 0.75x\frac{18654.74}{94713.72} = 0.15\ kip \uparrow$$

Summary of calculations

Anchor #	K_{li}	F_{1xi}	F_{1yi}
1	28274.33	0.22→	0.22↑
2	18654.74	0.15→	0.15↑
3	8434.93	0.07→	0.07↑
4	4400.96	0.03→	0.03↑
5	3458.11	0.03→	0.03↑
6	4400.96	0.03→	0.03↑
7	8434.93	0.07→	0.07↑
8	18654.74	0.15→	0.15↑
Σ =	94713.72	0.75→	0.75↑

6. *Induced Torsional Moment on the Anchor Bolts due to Direct Shear Loading*

+ve rotation ↷

$$T' = \pm V_x \bar{X}_l \pm V_y \bar{Y}_l \quad \textbf{(3-27)}$$

given: V_x = 0.75 kip →

given: V_y = 0.75 kip ↑

$\bar{X}$ = 2.7257 in [–ve *x*-direction]

$\bar{Y}$ = 6.5805 in [–ve *y*-direction]

$T' = 0.75x6.5805 - 0.75x2.27257 = 2.891\ kip - in$ ↷

7. *Shear Forces due to Pure Torsion and the Induced Torsion from Direct Shear Loading*

+ve directions

$$\rightarrow F_{2xi} = T\frac{K_{li}\,y_i}{\sum_{i=1}^{n} K_{li}\,(x_i^2 + y_i^2)} \quad \textbf{(3-42)}$$

$$\uparrow F_{2yi} = T\frac{K_{li}\,x_i}{\sum_{i=1}^{n} K_{li}\,(x_i^2 + y_i^2)} \quad \textbf{(3-43)}$$

$T' = 2.891\ kip - in$ ↷

given: $T_2[Pure\ torsion] = 288\ kip - in$ ↷

$T = 2.891 + 288 = 290.891\ kip - in$ ↷

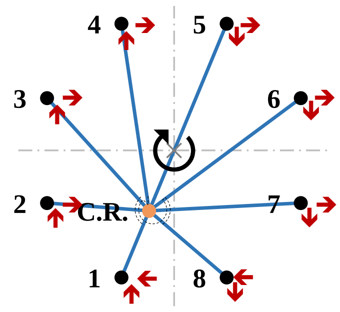

Calculations of x_i and y_i, with respect to the *C.R.* due to bending and shear

Anchor #1:

$x_1 = 5.74 - 2.73 = 3.01$

$y_1 = 13.86 - 6.58 = 7.28$

Anchor #2:

$x_2 = 13.86 - 2.73 = 11.13$

$y_2 = ABS(5.74 - 6.58) = 0.84$

Anchor #3:

$x_3 = 13.86 - 2.73 = 11.13$

$y_3 = 5.74 + 6.58 = 12.32$

Anchor #4:

$x_4 = 5.74 - 2.73 = 3.01$

$y_4 = 13.86 + 6.58 = 20.44$

Anchor #5:

$x_5 = 5.74 + 2.73 = 8.47$

$y_5 = 13.86 + 6.58 = 20.44$

Anchor #6:

$x_6 = 13.86 + 2.73 = 16.58$

$y_6 = 5.74 + 6.58 = 12.32$

Anchor #7:

$x_7 = 13.86 + 2.73 = 16.58$

$y_7 = ABS(5.74 - 6.58) = 0.84$

Anchor #8:

$x_8 = 5.74 + 2.73 = 8.47$

$y_8 = 13.86 - 6.58 = 7.28$

$$\sum_{1}^{n}(k_{it} \cdot x_i^2 + k_{it} \cdot y_i^2)$$

$$\begin{aligned} &= 28274.33[3.01^2 + 7.28^2] + 18654.74[11.13^2 + 0.84^2] \\ &+ 8434.93[11.13^2 + 12.32^2] + 4400.96[3.01^2 + 20.44^2] \\ &+ 3458.11[8.47^2 + 20.44^2] + 4400.96[16.58^2 + 12.32^2] \\ &+ 8434.93[16.58^2 + 0.84^2] + 18654.74[8.47^2 + 7.28^2] \\ &= 16505624.15 \end{aligned}$$

Calculations example of F_{2xi} and F_{2yi}

Anchor #1:

$$F_{2x1} = 290.891x\frac{28274.33x3.01}{16505624.15} = 3.63\ kip \leftarrow$$

$$F_{2y1} = 290.891x\frac{28274.33x7.28}{16505624.15} = 1.5\ kip \uparrow$$

Anchor #2:

$$F_{2x2} = 290.891x\frac{18654.74x11.13}{16505624.15} = 0.28\ kip \rightarrow$$

$$F_{2y2} = 290.891x\frac{18654.74x0.84}{16505624.15} = 1.5\ kip \uparrow$$

Summary of calculations

Anchor #	F_{2xi}	F_{2yi}
1	3.63←	1.50↑
2	0.28→	3.66↑
3	1.83→	1.65↑
4	1.59→	0.23↑
5	1.25→	0.52↓
6	0.96→	1.29↓
7	0.12→	2.47↓
8	2.39←	2.78↓
Σ =	0	0

8. *Group Moment Induced from the Shear forces on Anchors due to Direct Shear Loading and Torsion*

$$F_{txi} = F_{1xi} \pm F_{1xi}$$

$$F_{tyi} = F_{2yi} \pm F_{2yi}$$

Anchor #	F_{1xi}	F_{1yi}	F_{2xi}	F_{2yi}	F_{txi}	F_{tyi}
1	0.22→	0.22↑	3.63←	1.50↑	3.40←	1.73↑
2	0.15→	0.15↑	0.28→	3.66↑	0.42→	3.81↑
3	0.07→	0.07↑	1.83→	1.65↑	1.90→	1.72↑
4	0.03→	0.03↑	1.59→	0.23↑	1.62→	0.27↑
5	0.03→	0.03↑	1.25→	0.52↓	1.27→	0.49↓
6	0.03→	0.03↑	0.96→	1.29↓	0.99→	1.25↓
7	0.07→	0.07↑	0.12→	2.47↓	0.19→	2.40↓
8	0.15→	0.15↑	2.39←	2.78↓	2.24←	2.64↓

+ve directions

$$(M_{Group})_{1x} = \sum_{i=1}^{n} F_{tyi}\frac{h_i}{2} \qquad \textbf{(3-52)}$$

+ve directions —— ⊛ $$\left(M_{Group}\right)_{1y} = \sum_{i=1}^{n} F_{lxi}\,\frac{h_i}{2} \quad \textbf{(3-53)}$$

Anchor #	*h*-in	*F_{txi}	*F_{tyi}	**M_{xi}	**M_{yi}
1	1	-3.40	1.73	0.86	-1.70
2	1.3844	0.42	3.81	2.64	0.29
3	2.3123	1.90	1.72	1.99	2.19
4	3.2403	1.62	0.27	0.44	2.62
5	3.6247	1.27	-0.49	-0.89	2.31
6	3.2403	0.99	-1.25	-2.03	1.60
7	2.3123	0.19	-2.40	-2.77	0.22
8	5.74	-2.24	-2.64	-1.82	-1.55
			Σ =	-1.59	5.99

*The (-) and (+) signs represent the directions of the shear forces. The consideration of those signs was adopted because the summation of moments would be performed algebraically.

**Moments are applied at the anchor section below the leveling nuts. The sign (- or +) shown at the summation cell is ignored, and the true moment direction will be determined according to the assumed (+ve) moment directions, as demonstrated in the figures below.

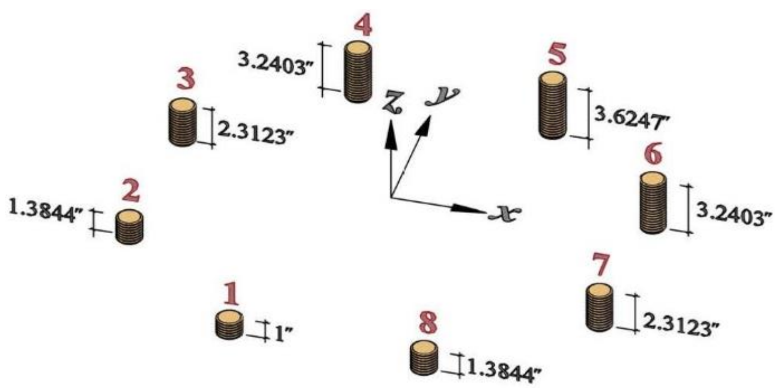

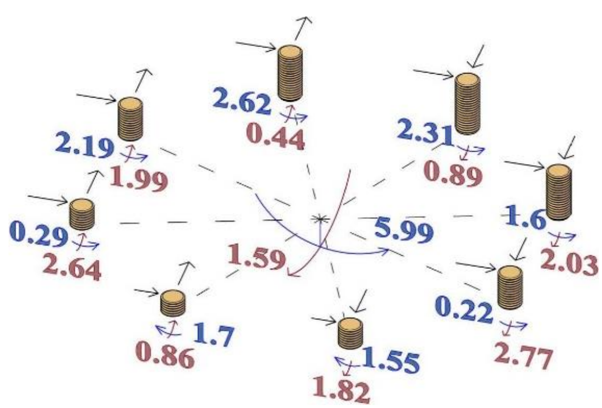

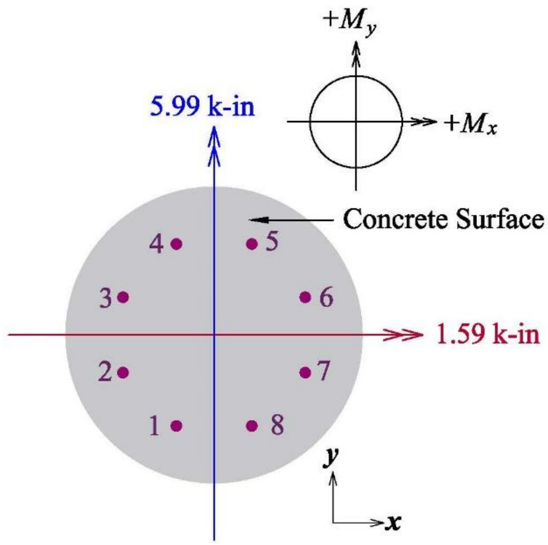

$\left(M_{Group}\right)_{1x} = 1.59\ kip - in\ \twoheadrightarrow$

$\left(M_{Group}\right)_{1y} = 5.99\ kip - in \Uparrow$

9. *Axial Forces on the Anchor Bolts due to Group Bending Moment*

$$N_{2i} = \left(M_{Group}\right)_{tx} \frac{K_{ai}\ y_i}{\sum_{i=1}^{n} K_{ai}\ y_i^2} \tag{3-73}$$

$$N_{3i} = \left(M_{Group}\right)_{ty} \frac{K_{ai}\ x_i}{\sum_{i=1}^{n} K_{ai}\ x_i^2} \tag{3-74}$$

$\left(M_{Group}\right)_{1x} = 1.59\ kip - in\ \twoheadrightarrow$

$\left(M_{Group}\right)_{1y} = 5.99\ kip - in \Uparrow$

given: $(M_{Group})_{2x}$ = 240.75 kip-in ↞

given: $(M_{Group})_{2y}$ = 240.75 kip-in ↟

$\left(M_{Group}\right)_{tx} = 240.75 - 1.59 = 239.16\ kip - in \twoheadleftarrow$

$\left(M_{Group}\right)_{ty} = 240.75 + 5.99 = 246.75\ kip - in \Uparrow$

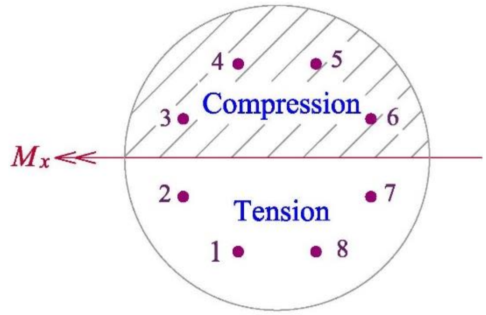

It can be inferred from the above figure that anchors: 1, 2, 7, and 8 are having tension; whereas anchors from 3 to 6 are having compression.

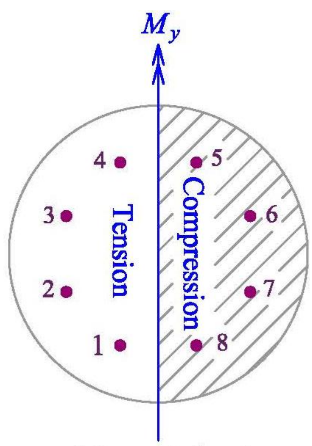

It can be inferred from the above figure that anchors from 1 to 4 are having tension; whereas anchors from 5 to 8 are having compression.

Calculations of x_i and y_i, with respect to the *C.R.* due to axial

Anchor #1:

$x_1 = 5.74 - 1.79 = 3.95$

$y_1 = 13.86 - 4.32 = 9.54$

Anchor #2:

$x_2 = 13.86 - 1.79 = 12.07$

$y_2 = 5.74 - 4.32 = 1.42$

Anchor #3:

$x_3 = 13.86 - 1.79 = 12.07$

$y_3 = 5.74 + 4.32 = 10.06$

Anchor #4:

$x_4 = 5.74 - 1.79 = 3.95$

$y_4 = 13.86 + 4.32 = 18.18$

Anchor #5:

$x_5 = 5.74 + 1.79 = 7.53$

$y_5 = 13.86 + 4.317 = 18.18$

Anchor #6:

$x_6 = 13.86 + 1.79 = 15.65$

$y_6 = 5.74 + 4.32 = 10.06$

Anchor #7:

$x_7 = 13.86 + 1.79 = 15.65$

$y_7 = 5.74 - 4.317 = 1.42$

Anchor #8:

$x_8 = 5.74 + 1.79 = 7.53$

$y_8 = 13.86 - 4.317 = 9.54$

Anchor #	K_{ai}	x_i	x_i^2	$K_{ai}\ x_i$	$K_{ai}\ x_i^2$	N_{2i}
1	91106.2	3.95	15.62	360063.36	1423016.7	5.34 T
2	65809.1	12.07	145.69	794318.31	9587444.7	0.58 T
3	39400.7	12.07	145.69	475567.30	5740110.9	2.44 C
4	28116.6	3.95	15.62	111120.38	439162.0	3.14 C
5	25134.8	7.53	56.68	189226.79	1424588.5	2.81 C
6	28116.6	15.65	244.81	439922.61	6883192.7	1.74 C
7	39400.7	15.65	244.81	616477.64	9645638.2	0.34 T
8	65809.1	7.53	56.68	495442.31	3729923.3	3.86 T
				Σ =	38873076.8	0

Anchor #	K_{ai}	y_i	y_i^2	$K_{ai}\ y_i$	$K_{ai}\ y_i^2$	N_{3i}
1	91106.2	9.54	91.03	869260.14	8293763.8	2.29 T
2	65809.1	1.42	2.03	93664.57	133310.5	5.04 T
3	39400.7	10.06	101.15	396265.39	3985369.5	3.02 T
4	28116.6	18.18	330.34	511025.33	9288000.0	0.71 T
5	25134.8	18.18	330.34	456831.01	8303006.1	1.20 C
6	28116.6	10.06	101.15	282777.66	2843986.7	2.79 C
7	39400.7	1.42	2.03	56078.03	79814.5	3.91 C
8	65809.1	9.54	91.03	627896.66	5990872.4	3.14 C
			Σ =		38918123.5	0

Summary of total axial forces

Anchor #	N_{2i}	N_{3i}	N_{ti}
1	5.34 T	2.29 T	7.63 T
2	0.58 T	5.04 T	5.62 T
3	2.44 C	3.02 T	0.58 T
4	3.14 C	0.71 T	2.44 C
5	2.81 C	1.20 C	4.01 C
6	1.74 C	2.79 C	4.53 C
7	0.34 T	3.91 C	3.57 C
8	3.86 T	3.14 C	0.71 T

10. Summary of Forces

Anchor #	F_{txi}	F_{tyi}	N_{ti}
1	3.40←	1.73↑	7.63 T
2	0.42→	3.81↑	5.62 T
3	1.90→	1.72↑	0.58 T
4	1.62→	0.27↑	2.44 C
5	1.27→	0.49↓	4.01 C
6	0.99→	1.25↓	4.53 C
7	0.19→	2.40↓	3.57 C
8	2.24←	2.64↓	0.71 T

11. Normal Stresses

$$\sigma_{Ni} = \pm \frac{N_{ti}}{A} \pm \frac{M_{xi} \cdot r}{I} \pm \frac{M_{yi} \cdot r}{I} \quad \textbf{(3-78)}$$

$$M_{xi} = \frac{F_{tyi} \cdot h}{2} \quad \textbf{(3-79)}$$

$$M_{yi} = \frac{F_{txi} \cdot h}{2} \quad \textbf{(3-80)}$$

r = 1 in

I = 0.7854 in^4

A = 3.1416 in^2

Anchor #	h-in	F_{txi}	F_{tyi}	N_{ti}	M_{xi}	M_{yi}
1	1	3.40	1.73	7.63 T	0.86	1.70
2	1.3844	0.42	3.81	5.62 T	2.64	0.29
3	2.3123	1.90	1.72	0.58 T	1.99	2.19
4	3.2403	1.62	0.27	2.44 C	0.44	2.62
5	3.6247	1.27	0.49	4.01 C	0.89	2.31
6	3.2403	0.99	1.25	4.53 C	2.03	1.60

Anchor #	*h*-in	F_{txi}	F_{tyi}	N_{ti}	M_{xi}	M_{yi}
7	2.3123	0.19	2.40	3.57 C	2.77	0.22
8	5.74	2.24	2.64	0.71 T	1.82	1.55

Anchor #	$\frac{M_{xi} \cdot r}{I}$	$\frac{M_{yi} \cdot r}{I}$	$\frac{N_{ti}}{A}$	σ_{Ni}
1	1.10	2.17	2.43 T	5.69 T
2	3.36	0.37	1.79 T	5.52 T
3	2.53	2.79	0.19 T	5.51 T
4	0.55	3.34	0.78 C	4.67 C
5	1.13	2.94	1.28 C	5.34 C
6	2.58	2.04	1.44 C	6.07 C
7	3.53	0.28	1.14 C	4.95 C
8	2.32	1.98	0.23 T	4.53 T

12. Shear Stresses

$$\tau_i = \frac{16}{3\pi d^2} F_{Ri} \qquad \textbf{(3-81)}$$

$$F_{Ri} = \sqrt{(F_{txi})^2 + \left(F_{tyi}\right)^2} \qquad \textbf{(3-82)}$$

d = 2 in

Anchor #	F_{txi}	F_{tyi}	F_{Ri}	τ_i
1	3.40	1.73	3.82	1.62
2	0.42	3.81	3.83	1.63
3	1.90	1.72	2.56	1.09
4	1.62	0.27	1.64	0.70
5	1.27	0.49	1.36	0.58
6	0.99	1.25	1.60	0.68
7	0.19	2.40	2.41	1.02
8	2.24	2.64	3.46	1.47

Design with *2013 Supports Specifications*

1. Properties

f_y = 55 ksi

E = 29000 ksi

μ [Poisson's ratio] = 0.3

G = 11153.85 ksi

d = 2 in

A = 3.1416 in^2

I = 0.7854 in^4

S = 0.7854 in^3

2. Loads

V_x = 0.75 kip ⟶

V_y = 0.75 kip ↑

$T[Pure\ torsion] = 288\ kip - in$ ↷

$(M_x)_{Group}$ = 240.75 kip-in ↞

$(M_y)_{Group}$ = 240.75 kip-in ↟

3. Layout of Anchor Bolts

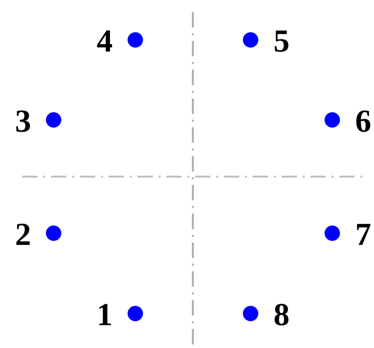

Anchor #	x	y	h-in
1	-5.74	-13.86	1
2	-13.86	-5.74	1.3844
3	-13.86	5.74	2.3123
4	-5.74	13.86	3.2403
5	5.74	13.86	3.6247
6	13.86	5.74	3.2403

Anchor #	x	y	h-in
7	13.86	-5.74	2.3123
8	5.74	-13.86	1.3844

4. *Shear Forces on the Anchor Bolts due to Direct Shear Loading*

$$V_{ix} = \frac{V_{xt}}{n}$$

$$V_{iy} = \frac{V_{yt}}{n}$$

given: V_x = 0.75 kip →

given: V_y = 0.75 kip ↑

n = 8

Anchor #	V_{ix}	V_{iy}
1	0.09→	0.09↑
2	0.09→	0.09↑
3	0.09→	0.09↑
4	0.09→	0.09↑
5	0.09→	0.09↑
6	0.09→	0.09↑
7	0.09→	0.09↑
8	0.09→	0.09↑

5. *Shear Forces due to Pure Torsion and the Induced Torsion from Direct Shear Loading*

$$F_{Ri} = \frac{T\ d}{\sum_{i=1}^{n}(x_i^2 + y_i^2)} \quad \textbf{(3-35)}$$

given: $T = 288\ kip - in$ ↷

Anchor #	x	y	d-in	x^2	y^2	F_{Ri}
1	-5.74	-13.86	15	32.95	192.10	2.4
2	-13.86	-5.74	15	192.10	32.95	2.4
3	-13.86	5.74	15	192.10	32.95	2.4
4	-5.74	13.86	15	32.95	192.10	2.4
5	5.74	13.86	15	32.95	192.10	2.4
6	13.86	5.74	15	192.10	32.95	2.4
7	13.86	-5.74	15	192.10	32.95	2.4
8	5.74	-13.86	15	32.95	192.10	2.4
			Σ =	900.1888	900.1888	

$$F_{Rxi} = F_{Ri}\, cos\theta_i$$

$$F_{Ryi} = F_{Ri}\, sin\theta_i$$

Anchor #	*θ_i	cos θ_i	sin θ_i	F_{Rxi}	F_{Ryi}
1	22.5	0.92	0.38	2.22←	0.92↑
2	67.5	0.38	0.92	0.92←	2.22↑
3	67.5	0.38	0.92	0.92→	2.22↑
4	22.5	0.92	0.38	2.22→	0.92↑
5	22.5	0.92	0.38	2.22→	0.92↓
6	67.5	0.38	0.92	0.92→	2.22↓
7	67.5	0.38	0.92	0.92←	2.22↓
8	22.5	0.92	0.38	2.22←	0.92↓
			Σ =	0	0

*θ = $\tan^{-1}(x/y)$

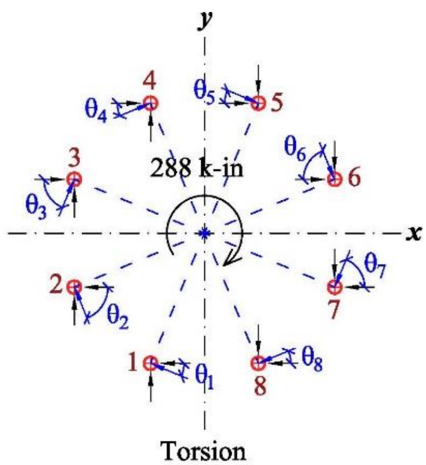

Total shear forces

Anchor #	V_{xi}	V_{yi}	F_{Rxi}	F_{Ryi}	F_{txi}	F_{tyi}
1	0.09→	0.09↑	2.22←	0.92↑	2.12←	1.01↑
2	0.09→	0.09↑	0.92←	2.22↑	0.82←	2.31↑
3	0.09→	0.09↑	0.92→	2.22↑	1.01→	2.31↑
4	0.09→	0.09↑	2.22→	0.92↑	2.31→	1.01↑
5	0.09→	0.09↑	2.22→	0.92↓	2.31→	0.82↓
6	0.09→	0.09↑	0.92→	2.22↓	1.01→	2.12↓
7	0.09→	0.09↑	0.92←	2.22↓	0.82←	2.12↓
8	0.09→	0.09↑	2.22←	0.92↓	2.12←	0.82↓

6. Axial Forces on the Anchor Bolts due to Group Bending Moment

$$N_{2i} = \left(M_{Group}\right)_{tx} \frac{y_i}{\sum_{i=1}^{n} y_i^2} \quad \textbf{(3-67)}$$

$$N_{3i} = \left(M_{Group}\right)_{ty} \frac{x_i}{\sum_{i=1}^{n} x_i^2} \quad \textbf{(3-68)}$$

given: $(M_{Group})_{tx}$ = 240.75 kip-in ↞

given: $(M_{Group})_{ty}$ = 240.75 kip-in ↟

Anchor #	x	y	x^2	y^2	$\frac{y_i}{\sum_{i=1}^{n} y_i^2}$	$\frac{x_i}{\sum_{i=1}^{n} x_i^2}$	N_{2i}	N_{3i}
1	5.74	13.86	32.95	192.05	0.00638	0.0154	3.71 T	1.54 T
2	13.86	5.74	192.05	32.95	0.01540	0.00638	1.54 T	3.71 T
3	13.86	5.74	192.05	32.95	0.01540	0.00638	1.54 C	3.71 T
4	5.74	13.86	32.95	192.05	0.00638	0.0154	3.71 C	1.54 T
5	5.74	13.86	32.95	192.05	0.00638	0.0154	3.71 C	1.54 C
6	13.86	5.74	192.05	32.95	0.01540	0.00638	1.54 C	3.71 C
7	13.86	5.74	192.05	32.95	0.01540	0.00638	1.54 T	3.71 C
8	5.74	13.86	32.95	192.05	0.00638	0.0154	3.71 T	1.54 C
		Σ =	1590.44	1590.44		Σ =	0	0

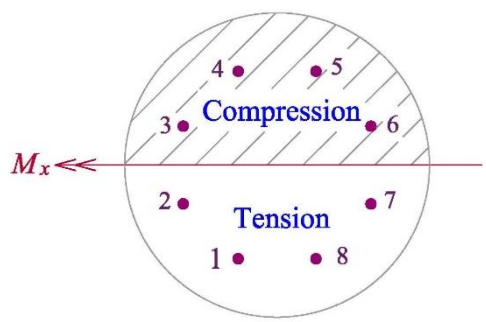

Moment about x-direction

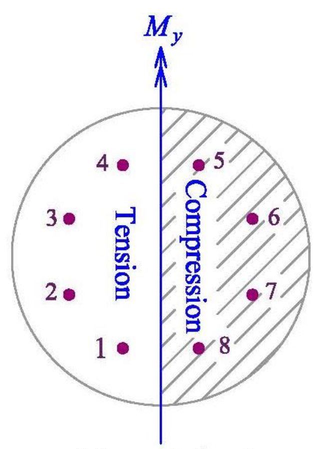

Moment about y-direction

Total axial forces

Anchor #	N_{2i}	N_{3i}	N_{ti}
1	3.71 T	1.54 T	5.24 T
2	1.54 T	3.71 T	5.24 T

3	1.54 C	3.71 T	2.17 T
4	3.71 C	1.54 T	2.17 C
5	3.71 C	1.54 C	5.24 C
6	1.54 C	3.71 C	5.24 C
7	1.54 T	3.71 C	2.17 C
8	3.71 T	1.54 C	2.17 T
Σ =	0	0	0

6. *Summary of Forces*

Anchor #	F_{Rxi}	F_{Ryi}	N_{ti}
1	2.12←	1.01↑	5.24 T
2	0.82←	2.31↑	5.24 T
3	1.01→	2.31↑	2.17 T
4	2.31→	1.01↑	2.17 C
5	2.31→	0.82↓	5.24 C
6	1.01→	2.12↓	5.24 C
7	0.82←	2.12↓	2.17 C
8	2.12←	0.82↓	2.17 T

7. *Normal Stresses*

$$\sigma_{Ni} = \pm\frac{N_{ti}}{A} \pm \frac{M_{xi} \cdot r}{I} \pm \frac{M_{yi} \cdot r}{I} \tag{3-78}$$

$$M_{xi} = \frac{F_{tyi} \cdot h}{2} \tag{3-79}$$

$$M_{yi} = \frac{F_{txi} \cdot h}{2} \tag{3-80}$$

r = 1 in

I = 0.7854 in^4

A = 3.1416 in^2

Anchor #	h-in	F_{txi}	F_{tyi}	N_{ti}	M_{xi}	M_{yi}
1	1	2.12	1.01	5.24 T	1.06	0.51
2	1.3844	0.82	2.31	5.24 T	0.57	1.60
3	2.3123	1.01	2.31	2.17 T	1.17	2.67
4	3.2403	2.31	1.01	2.17 C	3.74	1.64
5	3.6247	2.31	0.82	5.24 C	4.19	1.49
6	3.2403	1.01	2.12	5.24 C	1.64	3.44
7	2.3123	0.82	2.12	2.17 C	0.95	2.46
8	5.74	2.12	0.82	2.17 T	1.47	0.57

Anchor #	$\frac{M_{xi} \cdot r}{I}$	$\frac{M_{yi} \cdot r}{I}$	$\frac{N_{ti}}{A}$	σ_{Ni}
1	0.64	1.35	1.67 T	3.67 T
2	2.04	0.73	1.67 T	4.43 T
3	3.40	1.49	0.69 T	5.58 T
4	2.09	4.77	0.69 C	7.55 C
5	1.90	5.33	1.67 C	8.90 C
6	4.38	2.09	1.67 C	8.14 C
7	3.13	1.21	0.69 C	5.03 C
8	0.73	1.87	0.69 T	3.29 T

8. Shear Stresses

$$\tau_i = \frac{16}{3\pi d^2} F_{Ri} \quad \textbf{(3-81)}$$

$$F_{Ri} = \sqrt{(F_{txi})^2 + \left(F_{tyi}\right)^2} \quad \textbf{(3-82)}$$

d = 2 in

Anchor #	F_{txi}	F_{tyi}	F_{Ri}	τ_i
1	2.12	1.01	2.35	0.998
2	0.82	2.31	2.45	1.041
3	1.01	2.31	2.52	1.071
4	2.31	1.01	2.52	1.071
5	2.31	0.82	2.45	1.041
6	1.01	2.12	2.35	0.998
7	0.82	2.12	2.28	0.967
8	2.12	0.82	2.28	0.967

Summary of the Two Approaches

Anchor #	Analytical Equations		2013 Supports Specifications	
	σ_{Ni}	τ_i	σ_{Ni}	τ_i
1	5.69 T	1.62	3.67 T	0.998
2	5.52 T	1.63	4.43 T	1.041
3	5.51 T	1.09	5.58 T	1.071
4	4.67 C	0.70	7.55 C	1.071
5	5.34 C	0.58	8.90 C	1.041
6	6.07 C	0.68	8.14 C	0.998
7	4.95 C	1.02	5.03 C	0.967
8	4.53 T	1.47	3.29 T	0.967